Distribution Agreement

In presenting this dissertation as a partial fulfillment of the requirements for an advanced degree from Emory University, I hereby grant to Emory University and its agents the non-exclusive license to archive, make accessible, and display my dissertation in whole or in part in all forms of media, now or hereafter known, including display on the world wide web. I understand that I may select some access restrictions as part of the online submission of this dissertation. I retain all ownership rights to the copyright of the dissertation. I also retain the right to use in future works (such as articles or books) all or part of this dissertation.

Signature:

_____ _____

Nathan T. Mortimer Date

Drosophila archipelago regulates oxygen homeostasis via novel roles in tracheogenesis and the hypoxic response

By

Nathan T. Mortimer
Doctor of Philosophy

Graduate Division of Biological and Biomedical Science
Genetics and Molecular Biology

_____
Kenneth H. Moberg, Ph.D.
Advisor

_____
Victor Faundez, M.D., Ph.D.
Committee Member

_____
William G. Kelly, Ph.D.
Committee Member

_____
John C. Lucchesi, Ph.D.
Committee Member

_____
Iain Shepherd, Ph.D.
Committee Member

Accepted:

_____
Lisa A. Tedesco, Ph.D.
Dean of the Graduate School

_____
Date

Drosophila archipelago regulates oxygen homeostasis via novel roles in tracheogenesis and the hypoxic response

By

Nathan T. Mortimer

B.S., Emory University, 2000

Advisor: Kenneth H. Moberg, Ph.D.

An abstract of
A dissertation submitted to the Faculty of the Graduate School of Emory University
in partial fulfillment of the requirements for the degree of
Doctor of Philosophy
Graduate Division of Biological and Biomedical Science
Genetics and Molecular Biology
2009

Abstract

***Drosophila archipelago* regulates oxygen homeostasis via novel roles in tracheogenesis and the hypoxic response**

By Nathan T. Mortimer

The viability of complex organisms is dependent upon the maintenance of oxygen homeostasis. In *Drosophila* this is accomplished by the development of the tracheal system, a branched oxygen-conducting network, and by the ability of cells to sense and respond to conditions of lowered oxygen availability, or hypoxia. This hypoxic response is based on the transcriptional activity of the Hypoxia induced factor (HIF) which is conserved from *Drosophila* to humans. Here we describe novel functions of the *Drosophila* tumor suppressor homolog *archipelago* (*ago*) in regulating oxygen homeostasis via roles in tracheogenesis and in restricting the hypoxic response.

ago mutant embryos display defects in tracheal development due to deregulated activity of the Trachealess transcription factor, illustrating a key regulatory role for *ago* in the development of the oxygen delivery system. In addition to this developmental role, *ago* also controls the response to hypoxia in larval and adult *Drosophila* by regulating the activity of *Drosophila* HIF. Deregulation of dHIF in *ago* mutants uncouples activation of the hypoxic response from oxygen deprivation, leading to its ectopic induction in normoxia and altering the organismal response to oxygen deprivation. These findings identify *ago* as a member of a novel HIF regulatory pathway.

Drosophila archipelago regulates oxygen homeostasis via novel roles in tracheogenesis and the hypoxic response

By

Nathan T. Mortimer

B.S., Emory University, 2000

Advisor: Kenneth H. Moberg, Ph.D.

A dissertation submitted to the Faculty of the Graduate School of Emory University
in partial fulfillment of the requirements for the degree of
Doctor of Philosophy
Graduate Division of Biological and Biomedical Science
Genetics and Molecular Biology
2009

Acknowledgements

I would like to thank all of the members of the Moberg, Moses and Sanyal labs for their support and valued input over the years. I would especially like to thank Ken, a great mentor and role model, who taught me everything I know about being a good scientist and who even got me to do cell culture experiments (I'm not sure which was tougher), and Sharon for all her excellent help and for bailing me out when the flies wouldn't lay on my embryo collection plates. I also need to thank Victor, Bill, John and Iain for forming such a supportive and encouraging committee, along with Barry Yedvobnick and Guy Benian for giving me good guidance and mentorship since long before I began Grad school. Very special thanks go to my family, for everything else!!

I would like to thank the following for providing reagents/advice in my work: Debbie Andrew, Steve Crews, Mark Krasnow, Pablo Wappner, Alysia Vrailas Mortimer, Kevin Moses, Subhabrata Sanyal, Dan Marenda, Lazaro Centanin, Rheinallt Jones, Kerry Ross, Marie Csete, Lan Jiang, Sarah Bray, Tien Hsu, John Belote, Nick Tapon, Gisela D'Angelo, Samir Merabet and Gabriel Haddad.

Table of Contents

Index of Figures

Index of Tables

Table 4.4. Transcription of hypoxia inducible genes in normoxic *ago* larvae

Chapter One: Oxygen homeostasis

The development of oxygen-conducting organs and the tissue response to inadequate oxygen supply

1.A. Introduction

A fundamental requirement for all organisms is the ability to sense and respond to changing environmental conditions. Alterations in environmental factors such as atmospheric oxygen concentration, nutrient availability or temperature are reflected in changes within the organism's internal environment and can affect specific organs or tissues. Such changes are causes of organismal stress; for instance decreasing amounts of atmospheric oxygen can lead to an oxygen deficit in highly metabolic tissues. Specific responses must be triggered in order to survive these periods of stress and to maintain tissue homeostasis.

Environmental changes are sensed at the cellular level and the immediate responses are based on altered intracellular signaling. Metazoan cells share a conserved set of stress response pathways including the activation of stress-activated protein kinases and stress-induced transcription factors which combine to produce both cell autonomous and non-autonomous changes in metabolism, growth factor signaling and other cellular functions that allow the organism to adapt to its altered environmental conditions. These adaptive changes can range from a temporary increase in gene expression to long term anatomical or functional modifications that persist beyond the period of environmental stress.

One of the most intensely studied stress response pathways is the cellular response to an altered concentration of oxygen. Since the initial discovery of oxygen gas (O_2) and the demonstration of the detrimental effects of oxygen-deprivation (Priestley, 1775; Scheele, 1777), scientists have been aware of the necessity of oxygen for organismal survival. Oxygen is utilized in a variety of

cellular functions. The main requirement for oxygen is in the production of cellular energy via aerobic respiration in the mitochondria. Oxygen also serves as a required substrate for a wide range of enzymatic functions including oxidation, hydroxylation, isomerization and histone demethylation (Forneris et al., 2005; Hagen et al., 2003; Shen et al., 2003; Tu & Weissman, 2002). These non-mitochondrial functions can account for up to 30% of cellular oxygen consumption (reviewed in Denko, 2008; Herst & Berridge, 2007; Rosenfeld et al., 2002).

Due to this requirement for oxygen in the production of cellular energy and enzyme function, metazoan cells are especially sensitive to oxygen availability and changes in oxygen concentration. Complex organisms have evolved elaborate branched organs, such as our respiratory and cardiovascular systems, to ensure adequate oxygen delivery to internal tissues, along with sensitive sensors of cellular oxygen concentration. Metazoan cells sense and respond to conditions of hypoxia, or lowered oxygen concentration, via a highly conserved pathway. Central to this mechanism is the activity of the Hypoxia-inducible factor 1 (HIF-1), a heterodimeric stress induced transcription factor (Semenza & Wang, 1992; Wang et al., 1995; Wang & Semenza, 1995). HIF-1 transcriptional activity is required for cellular adaptation to hypoxic conditions.

Our knowledge of the mechanisms regulating both the elaboration of oxygen-conducting organs and the core hypoxic response pathway remain incomplete. Much of our understanding of the fundamental aspects of developmental biology has been derived from the study of genetic model

organisms, and model systems such as the mouse, the fruit fly *Drosophila melanogaster* and the nematode *Caenorhabditis elegans* are playing an increasingly important role in gaining insight into these aspects of oxygen-related biology. The high degree of conservation between both the development of the major oxygen-conducting networks and the hypoxic response mechanisms across metazoan species has enabled many important discoveries. Continued use of these models may help to further increase our understanding of the mechanisms of oxygen delivery and hypoxic response.

1.B. The *Drosophila* tracheal system: a conserved oxygen-conducting organ

Complex multi-cellular organisms have evolved elaborate branched organs to ensure adequate delivery of oxygen to their internal tissues. The elaboration of the main oxygen-conducting networks is accomplished by the process of tubular morphogenesis; the development of a branched, interconnected tubular network. The morphogenesis of oxygen-conducting networks typically involves multiple distinct stages; a preliminary stage involving cell specification and the formation of a rudimentary network and subsequent stages in which further branches are elaborated from this primary architecture. In mammalian lung development, tubular morphogenesis begins with a program of stereotyped branch budding and formation from the lung bud precursor. The structure is then further elaborated via interactions with surrounding tissue. This tubular network acts to carry oxygen-rich air through finer and finer branches in the alveoli where oxygen diffuses into the blood vessels for circulation to internal tissues (reviewed in Hogan, 1999). These blood vessels also arise through a program of tubular morphogenesis consisting of two distinct stages, vasculogenesis and angiogenesis. Formation of the vascular system begins with the process of vasculogenesis during embryonic development. In vasculogenesis, the endothelial precursor cells migrate into position and differentiate to form blood vessels. From this primary architecture, the process of angiogenesis further elaborates the branched blood vessels that make up the functional vascular system (reviewed in Flamme et al., 1997; Risau & Flamme, 1995). Additional

rounds of angiogenesis can lead to further vascular remodeling throughout the life of the organism.

Much of our understanding of the cell biological processes and genetic programs regulating these forms of tubular morphogenesis is based on studies into the development of the insect tracheal system, a simple oxygen-conducting network that is conserved across insect species (Locke, 1957; Manning & Krasnow, 1993; Wigglesworth, 1930). The *Drosophila* tracheal system is an interconnected branched network consisting of approximately 1600 polarized epithelial cells through which oxygen moves by diffusion (Manning & Krasnow, 1993). The tracheal system develops through a series of morphologically distinct steps from a placode of differentiated precursor cells to a highly branched network capable of conducting oxygen throughout the entire organism (reviewed in Ghabrial et al., 2003).

There are multiple stages in the life cycle of *Drosophila* and tracheal development mirrors the requirement for oxygen at each stage (Figure 1.1). Embryogenesis is characterized by gastrulation, segmental patterning, organ formation and other major morphogenetic events. The *Drosophila* embryo is small enough that its oxygen requirements can be met by passive diffusion; at this time the tracheal system is undergoing a developmental phase, driven by a genetically programmed pattern of gene expression. This embryonic-developmental phase is similar to the earliest stages of lung and vascular system morphogenesis, resulting in the production of a stereotyped primary architecture. Approximately twenty-four hours after egg laying (AEL) the embryo hatches,

beginning the larval stage of development. The larval stage lasts about five days and is characterized by two larval molts (at approximately forty-eight and seventy-two hours AEL) and a huge increase in size and subsequent increase in oxygen demand. The tracheal system undergoes a homeostatically-driven commensurate increase in growth and branching in response to signals generated by hypoxic tissues. This further elaboration of the terminal tracheal branches mirrors the secondary stages of lung and blood vessel branching. At approximately six days AEL, after the completion of larval development, the larva encloses itself in a protective pupal case, and undergoes a major remodeling of its tissues, including the tracheal system, during metamorphosis. Once this stage is complete, at ten to twelve days AEL, the adult fly ecloses from its pupal case. The tracheal system then undergoes an additional round of growth to supply oxygen to adult tissues. The most well-studied, and consequently most well understood stages of tracheal morphogenesis are the embryonic-developmental and larval-homeostatic phases (reviewed in Figure 1.2). These two phases are analogous to the stages of lung development and the vasculogenic and angiogenic phases of vascular system formation in mammals and provide a good model system in which to study these incompletely understood aspects of mammalian development.

In *Drosophila,* the pattern of embryonic tracheal branching is bilaterally symmetric, segmentally repeated and under fixed developmental control (Manning & Krasnow, 1993). A mature embryonic tracheal system (Figure 1.3) consists of two main anterior-posterior connections, the dorsal trunk (DT) and

lateral trunk (LT). These are connected via the transverse connective (TC). This primary branch framework also serves as the site for extension of specialized secondary branches, the ganglionic branches (GBs) and visceral branches (VBs), which carry oxygen to the central nervous system and viscera respectively, and the dorsal branches (DBs) which serve to connect the right and left sides of the embryo.

During *Drosophila* embryogenesis, the tracheal system is originally specified from ectodermal tissue in ten clusters of twenty cells on either side of the embryo approximately five hours AEL (Samakovlis et al., 1996a). Prior to tracheal morphogenesis, the cells divide twice and then exit the cell cycle. Subsequent morphogenesis takes place without further cell division or cell death (Samakovlis et al., 1996a).

The earliest marker of tracheal cell specification is the expression of the *trachealess* (*trh*) transcription factor in a segmentally-repeated pattern. *trh* is a member of the basic helix-loop-helix (bHLH)-PAS (PER-ARNT-SIM homology) domain containing family of transcription factors (Isaac & Andrew, 1996; Wilk et al., 1996). *trh* expression is induced in the presumptive tracheal cells by the activity of pattern formation genes including the JAK/STAT, *wingless* and *decapentaplegic* signaling pathways (Brown et al., 2001; Isaac & Andrew, 1996; Wilk et al., 1996) and is then maintained in specified tracheal cells by an auto-regulatory loop (Isaac & Andrew, 1996; Wilk et al., 1996). Trh protein heterodimerizes with a second bHLH-PAS family member Tango (Tgo,

Sonnenfeld et al., 1997). This dimerization is required for Trh function in tracheal morphogenesis (Ohshiro & Saigo, 1997; Sonnenfeld et al., 1997).

The earliest role for the Trh:Tgo dimeric transcription factor in tracheal development is in the invagination of the tracheal placodes. Tracheal invagination is a morphogenetic process in which the specified tracheal precursor cells fold inward from the surface of the embryo to occupy an internal position. This process requires signaling through the epidermal growth factor (EGF) pathway (Llimargas & Casanova, 1999). *trh* is required for expression of an EGF pathway mediator (*crossveinless-c*, Brodu & Casanova, 2006), and in *trh* mutant embryos, the cells that would normally form the trachea fail to invaginate and remain clustered at the site of their origin (Isaac & Andrew, 1996). This defect in *trh* mutants is not a defect in cell identity; the presumptive tracheal cells still express other tracheal-specific markers. Rather, the *trh* mutant phenotypes represent defects in the ability of the cells to undergo the normal process of invagination (Isaac & Andrew, 1996).

Once tracheal cells have invaginated, the branches are elaborated via multiple rounds of fibroblast growth factor (FGF) dependent cell migration. The FGF signaling pathway is activated when the FGF ligand binds to the FGF receptor tyrosine kinase (FGFR) triggering receptor dimerization and cross-phosphorylation of FGFR cytoplasmic domains. This FGFR activation leads to activation of a downstream kinase cascade which culminates with the dual phosphorylation and activation of the mitogen activated protein kinase (MAPK) family member ERK (extracellular signal-regulated kinase). Activated ERK (also

known as dually-phosphorylated or dpERK) phosphorylates and activates a variety of effector proteins, including multiple transcription factors (Cobb et al., 1994). It is the altered activity of these effector proteins that ultimately produces the cellular response triggered by the FGF signal (for a review of FGF/MAPK signaling see Mohammadi et al., 2005; Seger & Krebs, 1995; Thisse & Thisse, 2005).

The *Drosophila* genome encodes two FGFR homologs, *breathless* (*btl,* Glazer & Shilo, 1991; Klambt et al., 1992) and *heartless* (*htl*, Beiman et al., 1996; Gisselbrecht et al., 1996; Shishido et al., 1993) along with three putative FGF-like ligands, *branchless* (*bnl*, Sutherland et al., 1996), *pyramus* (*pyr*) and *thisbe* (*ths*, Stathopoulos et al., 2004). As the gene names suggest, *btl* and *bnl* are required for formation of the tracheal system, and *htl*, *pyr* and *ths* play essential roles in development of the mesoderm, including formation of the heart (Klambt et al., 1992; Reichman-Fried et al., 1994; Reichman-Fried & Shilo, 1995; Shishido et al., 1997; Stathopoulos et al., 2004). The *btl* receptor is specifically expressed in tracheal cells, and is required for the formation of the tracheal branches (Glazer & Shilo, 1991; Klambt et al., 1992). This role of *btl* is specific to branch cell migration, in *btl* mutant embryos the number of tracheal cells and their ability to complete invagination are not affected (Klambt et al., 1992). *trh* is required to initiate the expression of the *btl* receptor (Ohshiro & Saigo, 1997; Wilk et al., 1996) and is thus required for directed cell migration, along with its earlier role in invagination. After this initial *trh*-dependent activation, *btl* expression in tracheal cells is highly dynamic and subsequent transcription is mediated by an array of

transcriptional activators and repressors, many of which are regulated by a Btl-dependent positive feedback loop (Kuhnlein & Schuh, 1996; Ohshiro et al., 2002; Ohshiro & Saigo, 1997; Zelzer & Shilo, 2000). The role of the FGF signaling pathway in regulating tubular morphogenesis in the *Drosophila* tracheal system is conserved in development of the mammalian lung (Min et al., 1998) and vascular system (reviewed in Poole et al., 2001).

A loss of branch formation is also seen in embryos mutant for *bnl*, the ligand of the Btl receptor (Sutherland et al., 1996). *bnl* is expressed in clusters of non-tracheal cells in a developmentally controlled, dynamic pattern, such that it is able to provide directional cues to the migrating tracheal branch cells (Sutherland et al., 1996). Once it receives the Bnl signal, the Btl receptor tyrosine kinase activates the conserved MAPK pathway via an FGF specific adaptor protein encoded by the *downstream of FGF* gene (also known as *stumps* or *heartbroken*, Imam et al., 1999; Michelson et al., 1998 Nov; Vincent et al., 1998). Pathway activity leads to the activation of ERK and downstream effector proteins including the transcription factors *grainy head* and *pointed* (Hemphala et al., 2003; Samakovlis et al., 1996a). These effector proteins are required for specification of specialized tracheal cells (including the fusion and terminal cells, see below), lumen growth control and regulation of *btl* transcription (see Figures 1.4 and 1.5 for an overview of Btl/FGF signaling in tracheal development).

The pattern of Btl receptor activity can be visualized by using antisera that recognizes the active form of ERK (dpERK). Experiments using the dpERK antibody demonstrate that after an initial placode-wide ERK activation, pathway

activity is confined to the lead cells of migrating branches (Gabay et al., 1997). These lead migratory cells are a class of specialized tracheal cells known as fusion cells (Figure 1.6). Fusion cells are induced prior to branch migration, and are specified one per branch by *Notch* mediated lateral inhibition (Figure 1.6A; reviewed in Artavanis-Tsakonas et al., 1995). One cell receives a higher level of FGF signal than its neighbors; this cell then begins expressing the *Notch* ligand *Delta* and signals via Notch expressed in surrounding tracheal cells, repressing their ability to become fusion cells (Ikeya & Hayashi, 1999; Llimargas, 1999; Steneberg et al., 1999). *btl* is then transcriptionally down-regulated in the non-fusion cells by the activity of the transcriptional repressors *spalt* and *anterior open* (Figure 1.6B; Kuhnlein & Schuh, 1996; Ohshiro et al., 2002; Ohshiro & Saigo, 1997; Zelzer & Shilo, 2000). The newly specified fusion cell is thus the only branch cell competent to respond to the *bnl* signal and will act as the lead migratory cell (Figure 1.6C).

Beyond this function in branch migration, fusion cells play a required role in mediating the fusion between cells of migrating DT and LT branches from adjacent placodes, and between DBs from opposing placodes (Samakovlis et al., 1996b; Tanaka-Matakatsu et al., 1996). This function of the fusion cells is dependent on the expression of the transcription factor *escargot* (*esg*, Tanaka-Matakatsu et al., 1996). Among other targets, *esg* drives transcription of the bHLH-PAS transcription factor *dysfusion* (*dys*, Jiang & Crews, 2003; Jiang & Crews, 2006). Dys dimerizes with Tgo and the Dys:Tgo complex drives transcription of multiple genes required for interplacode fusion (Jiang & Crews,

2006; Jiang & Crews, 2007). Dys:Tgo targets include the adhesion proteins *shotgun* and *CG13196* and an unknown target that is required for the down-regulation of Trh protein levels in fusion cells (Jiang & Crews, 2006). Lack of Dys:Tgo function in *dys* mutant embryos leads to defects in branch fusion (Jiang & Crews, 2003; Jiang & Crews, 2006).

Following completion of branch fusion, tracheal cells undergo a conserved cell biological process of lumen formation (Tsarouhas et al., 2007). Throughout tracheal development, the fusion cells retain their unique identity and are involved in regulating cuticle molting and growth control during larval development when they are commonly known as node cells (Locke, 1958; Samakovlis et al., 1996a).

Negative regulators of the Btl/FGF signaling pathway play an important role in embryonic tracheal development. The refining of *btl* expression to a single fusion cell is required for directed branch migration. Ectopic pathway activity, either by loss of the *spalt*-mediated repression of *btl* transcription, or transgenic over-expression of *btl* in non-fusion cells, prevents branch migration by obscuring the gradient of Bnl signal (Ghabrial & Krasnow, 2006; Kuhnlein & Schuh, 1996). Prior to interplacode fusion, FGF signaling is down-regulated in fusion cells (Figure 1.6D), both by repression of *btl* transcription (Ohshiro et al., 2002; Ohshiro & Saigo, 1997), and via Btl receptor endocytosis and degradation mediated by *abnormal wing discs* (*awd*, Dammai et al., 2003). Ectopic Btl activity in *awd* mutants leads to defects in branch fusion (Dammai et al., 2003),

suggesting that down-regulation of FGF signaling in fusion cells is required for interplacode fusion to occur.

The existence of multiple regulators of the Btl/FGF signaling pathway throughout tracheal morphogenesis suggests that strict spatial and temporal regulation of the pathway is essential for proper development. This idea is supported by the tracheal morphogenetic defects seen following transgenic over-expression of the *bnl* ligand (Sutherland et al., 1996) or a constitutively active form of the *btl* receptor (λ*btl*, Lee et al., 1996a). All primary branch growth was arrested in embryos expressing ubiquitously high levels of *bnl* (Sutherland et al., 1996). A variety of defects were observed in embryos in which λ*btl* was transgenically expressed in tracheal cells, ranging from migration defects of primary branches to secondary branch duplication and ectopic branching (Lee et al., 1996a). Clearly, negative regulators of the Btl/FGF signaling pathway play an important role in the tubular morphogenesis of the embryonic *Drosophila* tracheal system.

The second phase of tracheal morphogenesis is the homeostatically-regulated branching that occurs during the larval stages. After hatching, the oxygen demand of a *Drosophila* larva is too great to be fulfilled by the passive diffusion of oxygen to its internal tissues. Therefore the tracheal system, elaborated during the embryonic stages, becomes the functional oxygen-conducting organ of the larva. At the end of embryogenesis, formation of the tracheal lumen is complete and it becomes filled with air (Tsarouhas et al., 2007). After hatching, larval tracheal development begins with the budding of

specialized terminal cells in response to homeostatically-driven migration cues (Manning & Krasnow, 1993). In contrast to the thick, multi-cellular, cuticle-lined primary and secondary branches, these terminal branches are formed by cytoplasmic extensions of a single terminal cell, and serve as the site of gas exchange between the trachea and the internal tissues (Guillemin et al., 1996; Manning & Krasnow, 1993; Wigglesworth, 1983). This larval tracheal growth and branching requires reiterative use of the Btl/FGF signaling pathway (Figure 1.7; Centanin et al., 2008; Jarecki et al., 1999). During this stage the transcription of *btl* in tracheal cells is dependent on hypoxia, and the expression of *bnl* outside the tracheal system is triggered specifically in hypoxic tissue. This dependence on hypoxia suggests the involvement of the conserved oxygen sensing/hypoxic response pathway.

Figure 1.1 The *Drosophila* life cycle and tracheal development.

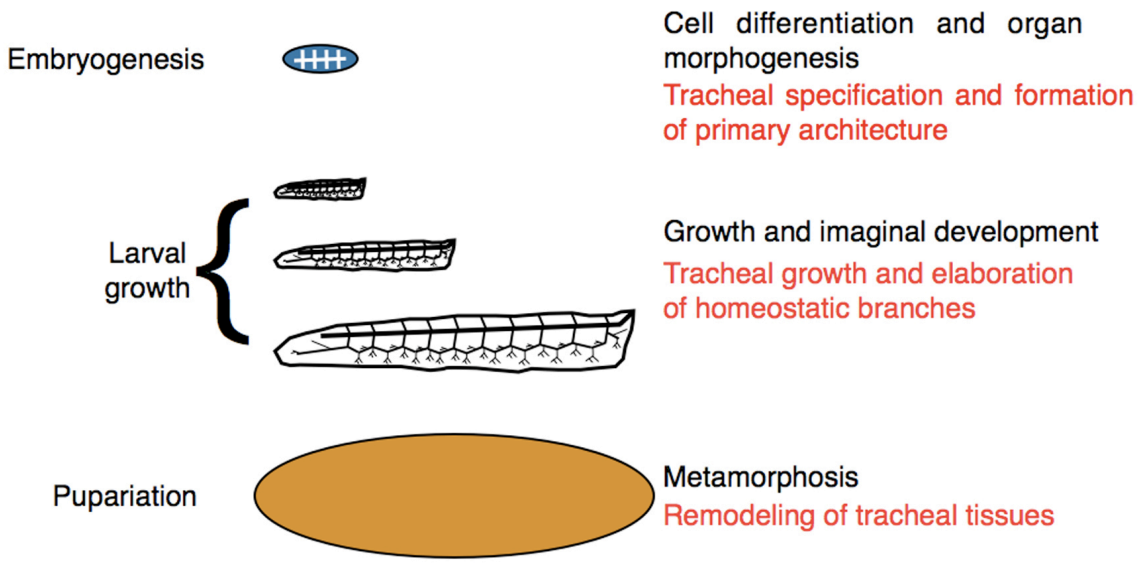

Tracheal development mirrors organismal development throughout the *Drosophila* life cycle. Pictured are embryonic through pupal stages, with major developmental (black text) and tracheogenic (red text) events listed for each.

Figure 1.2. Tracheal branch growth.

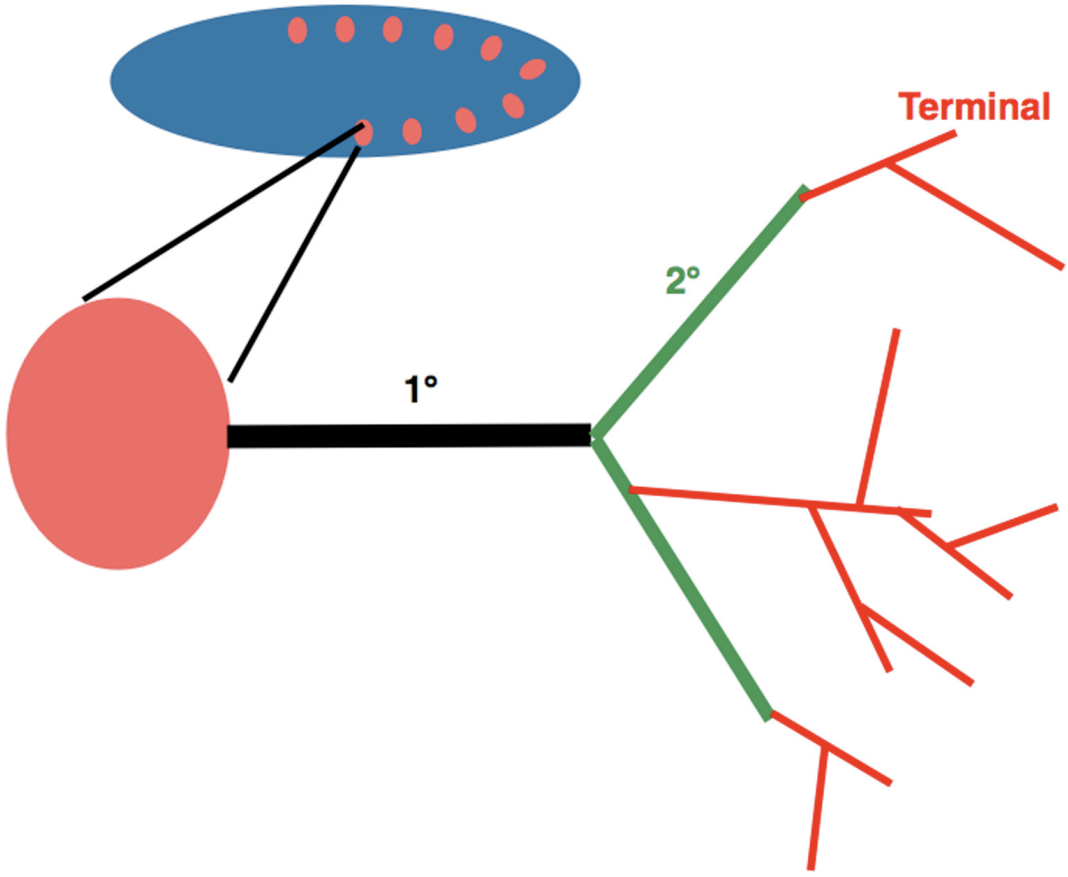

Tracheal development begins with the specification of tracheal placodes during embryonic stage 8, which subsequently elaborate a branched network. Primary (1°, black) and secondary (2°, green) branches are are extended during the embryonic-developmental period of tracheal growth. Terminal branches (red) are then elaborated during larval-homeostatic tracheogenesis.

Figure 1.3. The embryonic tracheal system.

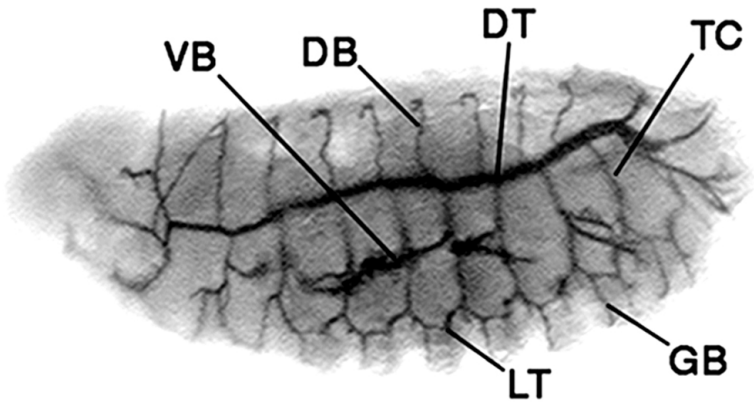

Architecture of the *Drosophila* embryonic tracheal system. Pictured is a late stage *Drosophila* embryo immunostained with a marker of the tracheal lumen, with anterior to the left and dorsal to the top. The main primary and secondary branches are indicated: DT, dorsal trunk; TC, transverse connective; LT, lateral trunk; DB, dorsal branch; GB, ganglionic branch; VB, visceral branch.

Figure 1.4. The *breathless*/FGF signaling pathway.

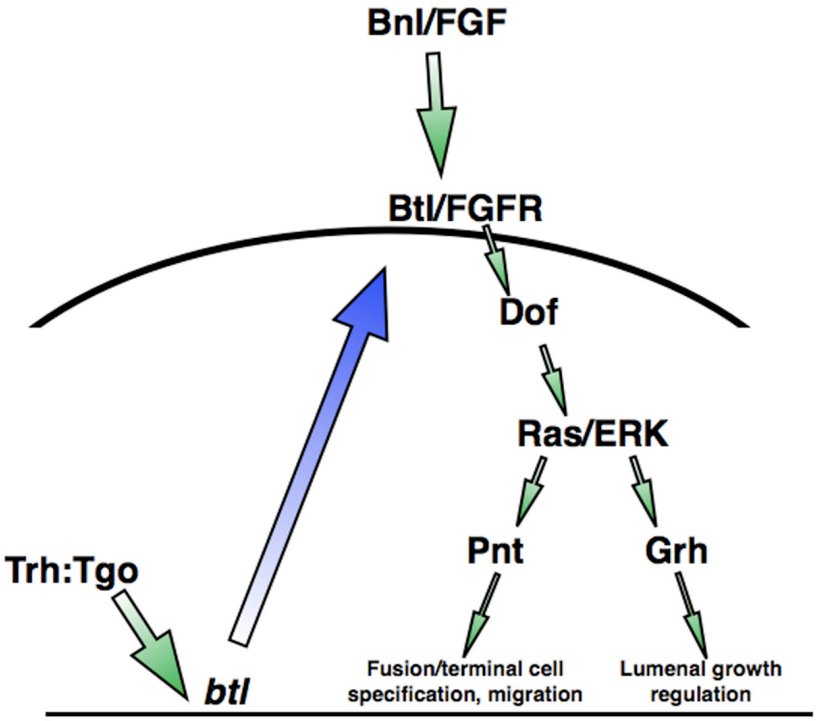

The Btl/FGF signaling pathway within an embryonic tracheal cell. Trh, Trachealess; Tgo, Tango; Btl/FGFR, Breathless FGF receptor; Bnl/FGF, Branchless FGF ligand; Dof, Downstream of FGF; ERK, Extracellular signal-regulated kinase; Pnt, Pointed; Grh, Grainyhead.

Figure 1.5. The Btl/FGF pathway regulates developmental tracheal branching.

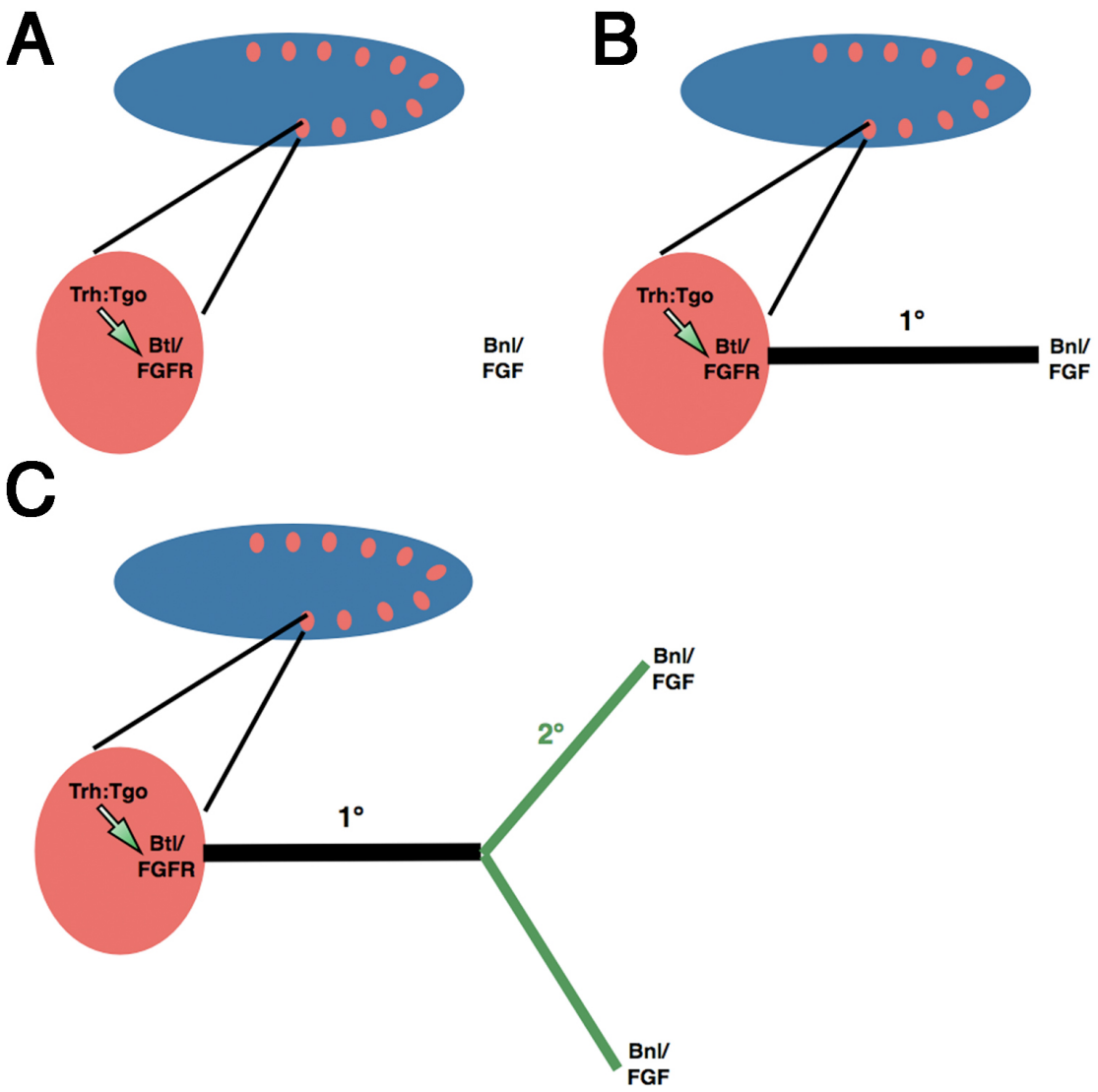

(A) In tracheal cells, the Trh:Tgo transcription factor drives expression of the FGF receptor (FGFR) Btl. Surrounding tissue begins to express the FGF ligand Bnl. (B) 1° tracheal branches grow towards this initial round of Bnl expression. (C) Following 1° branching, the initial round of Bnl expression ceases and a second round is initiated. This second round of expression leads to the elaboration of 2° tracheal branches.

Figure 1.6. Specification and function of tracheal fusion cells.

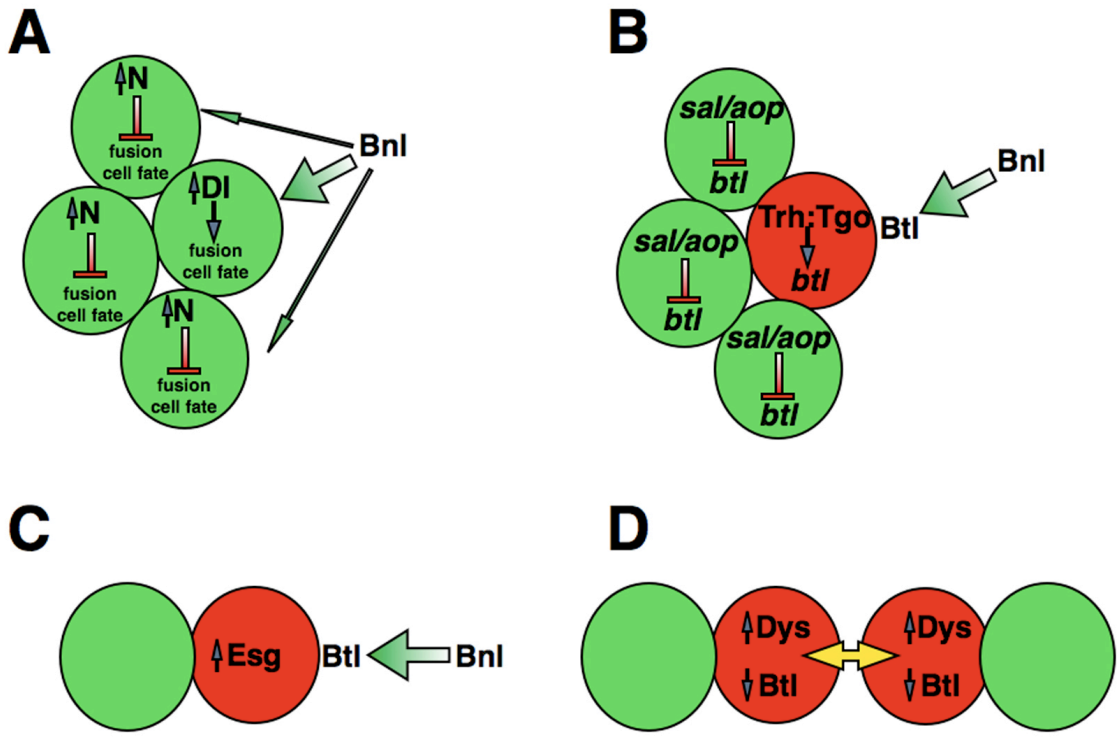

(A) Within an equivalent group of tracheal cells, one cell will stochastically receive a higher level of Bnl signal. This causes an up-regulation of the Notch (N) ligand Delta (Dl) which promotes the fusion cell fate. Dl signals to N expressed in surrounding cells, this N signal suppresses the fusion cell fate. (B) The transcription factors *spalt* (*sal*) and *anterior open* (*aop*) repress *btl* transcription in non-fusion cells (green); the fusion cell (red) is therefore the only cell competent to respond to the Bnl signal. (C) Because of this, the fusion cell (red) becomes the lead migratory cell and begins expressing the pro-fusion transcription factor *escargot* (*esg*). (D) For inter-placode fusion to occur (yellow arrows) the fusion cells up-regulate levels of the pro-fusion transcription factor *dysfusion* (*dys*) and down-regulate levels of Btl.

Figure 1.7. The Btl/FGF pathway regulates homeostatic tracheal branching.

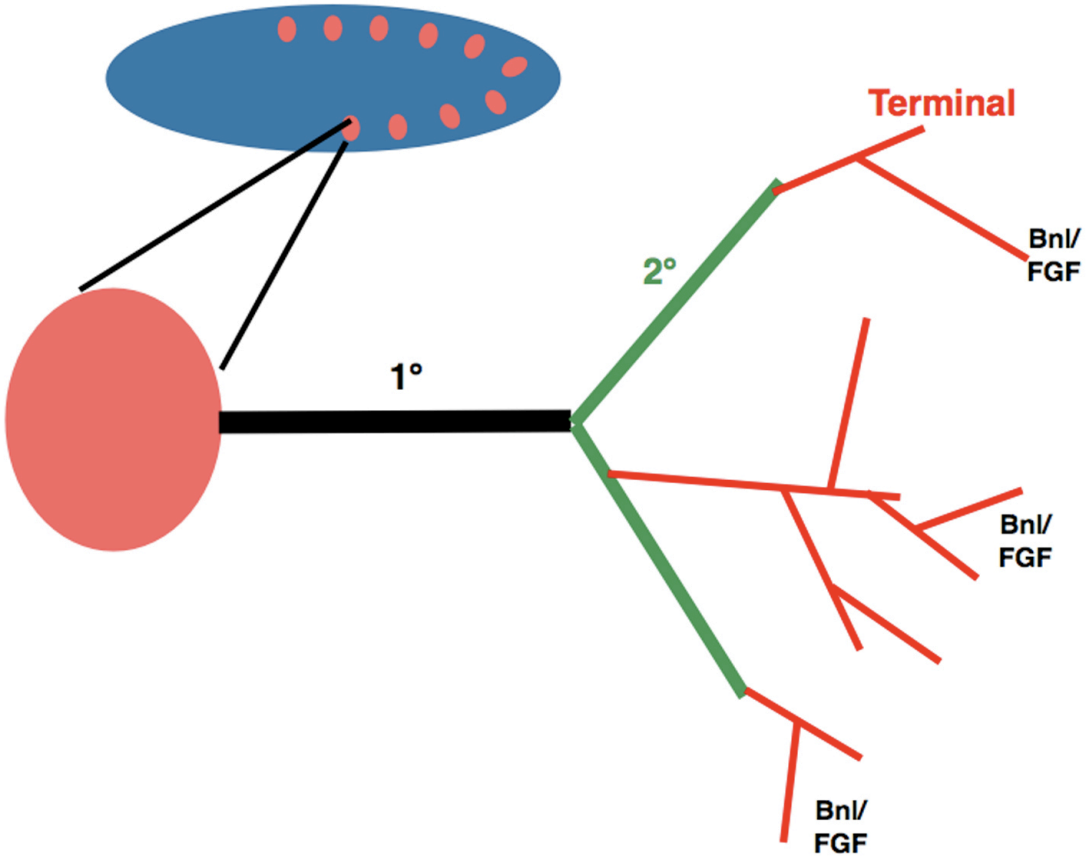

Terminal branches (red) are elaborated during the larval-homeostatic stage of tracheogenesis in response to hypoxia-induced Bnl expression in tracheal target tissues.

1.C. A conserved mechanism for sensing and responding to hypoxia

The stress induced transcription factor HIF-1 is composed of an oxygen-sensitive α subunit and a constitutively stable β subunit; HIF-1 activity is regulated both by stability of the α subunit and its ability to interact with transcriptional co-activators (reviewed in Fong & Takeda, 2008; Kaelin & Ratcliffe, 2008; Lisy & Peet, 2008; Weidemann & Johnson, 2008). Both the HIF-1α and HIF-1β (also known as ARNT) subunits are members of the bHLH-PAS domain containing family of transcription factors (Wang et al., 1995). HIF-1α and HIF-1β form a heterodimer and this dimerization allows HIF-1 transport into the nucleus, where it is competent to drive transcription of genes required for the hypoxic response (Jiang et al., 1996a). Since the original identification of HIF-1α, two other HIFα subunits, HIF-2α and HIF-3α, have been discovered (see Figure 1.8; Gu et al., 1998; Tian et al., 1997). Both HIF-1α and HIF-2α promote transcription of a partially overlapping set of hypoxia-induced genes, while the role of HIF-3α is not clearly understood and will not be discussed further; from this point HIF will be used to refer to shared properties and functions of complexes including either HIF-1α or HIF-2α. The HIFα subunits are constitutively expressed and specific proline residues in their oxygen-dependent degradation (ODD) domains are hydroxylated by members of the Egl9/HIF prolyl-hydroxylase (HPH) 2-oxoglutarate/iron(II)-dependent prolyl-4-hydroxylase family in an oxygen dependent manner (Bruick & McKnight, 2001; Epstein et al., 2001; Ivan et al., 2001; Jaakkola et al., 2001). This enzymatic dependence on the presence of oxygen allows the HPH family of prolyl-hydroxylases to act as oxygen-sensors.

Prolyl-hydroxylated HIFα is recognized and targeted for proteosomal degradation by an E3 ubiquitin ligase complex containing the von Hippel Lindau (VHL) tumor suppressor protein and is thus only stable in hypoxic conditions (Cockman et al., 2000; Iwai et al., 1999; Lisztwan et al., 1999; Maxwell et al., 1999; Ohh et al., 2000). The VHL protein acts as the substrate specificity factor for this ubiquitin ligase complex, which also includes Rbx, cullin2 and the elongins B and C (Kamura et al., 1999; Kibel et al., 1995; Pause et al., 1997; Stebbins et al., 1999). Loss of function mutations in VHL lead to accumulation of HIFα in normoxia and subsequent induction of an ectopic hypoxic response (reviewed in Kapitsinou & Haase, 2008).

The activity of HIF is further regulated by oxygen-dependent hydroxylation of the HIFα subunits by Factor inhibiting HIF (FIH), a 2-oxoglutarate/iron(II)-dependent asparaginyl-hydroxylase (reviewed in Kaelin & Ratcliffe, 2008; Lisy & Peet, 2008). FIH activity is also dependent on oxygen availability and thus acts as a second oxygen sensor by hydroxylation of a conserved asparagine residue in the C-terminal transactivation domain (CTAD) of HIFα. This prevents CTAD association with the CBP/p300 transcriptional co-activators, while the N-terminal transactivation domain (NTAD) is insensitive to FIH activity (Hewitson et al., 2002; Lando et al., 2002a; Lando et al., 2002b; Mahon et al., 2001). This CTAD hydroxylation therefore reduces the transcriptional potential of HIF. The activity of FIH is more hypoxia-tolerant than that of HPH, accordingly HIF transcriptional activity is regulated at oxygen concentrations at which HIFα is VHL-insensitive (Dayan et al., 2006; Koivunen et al., 2004). Additionally, HIF-1α is more sensitive

to the activity of FIH than HIF-2α (Bracken et al., 2006; Yan et al., 2007). These properties of FIH allow for a gradient of HIF activity; transcriptional targets will be differentially expressed at changing oxygen concentrations based both on their dependence on the function of the CTAD (as opposed to the NTAD) and on their requirement for HIF-1α (relative to HIF-2α) activity (reviewed in Kaelin & Ratcliffe, 2008). This highly regulated HIF transcriptional activity targets a wide range of genes required for organismal adaptation to hypoxia (see Figure 1.9 for an overview of HIFα regulation).

The core oxygen sensing/hypoxic response pathway is conserved in *Drosophila* (reviewed in Gorr et al., 2006; Romero et al., 2007). The first functional evidence supporting the conservation of the hypoxic response between mammals and *Drosophila* was the demonstration that extracts from *Drosophila* cells can form hypoxia-inducible complexes on the enhancers of mammalian hypoxia-induced genes (Nagao et al., 1996). This was followed by the observation that expression of human HIF-1α can induce gene expression in *Drosophila* (Zelzer et al., 1997). The *Drosophila* HIF (dHIF) α and β subunits are encoded by the *similar* (*sima*) and *tgo* genes respectively (Figure 1.8; Bacon et al., 1998; Ma & Haddad, 1999; Nambu et al., 1996; Sonnenfeld et al., 1997). *sima* is required for survival in hypoxia (Centanin et al., 2005) and like mammalian HIFα, its stability is dependent on an ODD domain (Arquier et al., 2006; Bacon et al., 1998). The Sima ODD domain is hydroxylated in an oxygen-dependent manner by the HPH family member *fatiga* (*fga*, Arquier et al., 2006; Centanin et al., 2008; Centanin et al., 2005). Furthermore, the biochemical

function of the *Drosophila* homolog of VHL (*dVHL*) is highly conserved; dVHL can bind and direct polyubiquitination of human HIF-1α (Aso et al., 2000). However, the *in vivo* functions of *dVHL* are only beginning to be explored and are not yet completely understood (Adryan et al., 2000; Arquier et al., 2006). The *Drosophila* genome also encodes a putative FIH homolog (*CG13902*, Klose et al., 2006); however the CTAD asparagine residue targeted by FIH in other organisms is not conserved in *sima*, suggesting that this gene may not function to regulate oxygen sensing in *Drosophila*. The mechanisms regulating the mammalian hypoxic response may be better understood through further study of the conserved Fga/ dVHL/Sima hypoxic response pathway in *Drosophila*.

Figure 1.8. The HIF family of bHLH-PAS transcription factors.

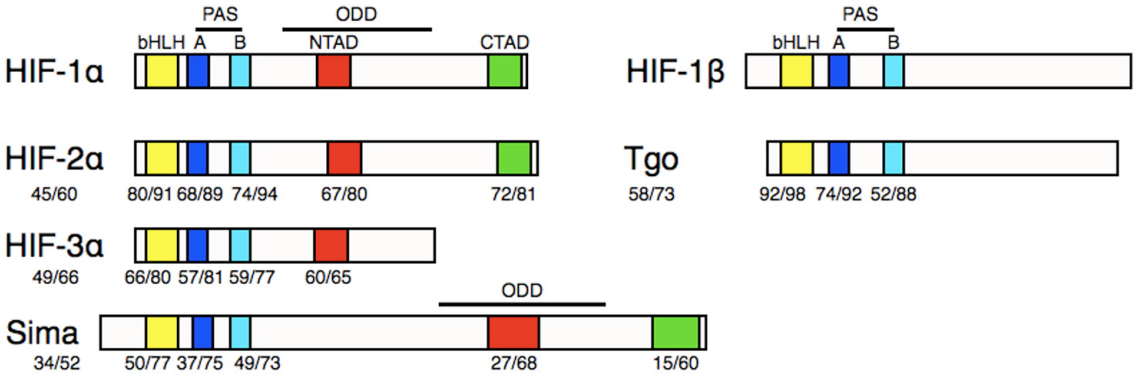

Domain structure of the human and *Drosophila* HIFα and β family members. Numbers represent % identity/similarity between each family member with its founding member (HIF-1α or HIF-1β) for the entire protein (under protein name) or each domain (under domain). Domain abbreviations: bHLH, basic helix-loop-helix; PAS, Per/Arnt/Sim homology domain; NTAD, N-terminal transactivation domain; CTAD, C-terminal transactivation domain; ODD, oxygen dependent degradation domain.

Figure 1.9. HIF regulatory mechanisms.

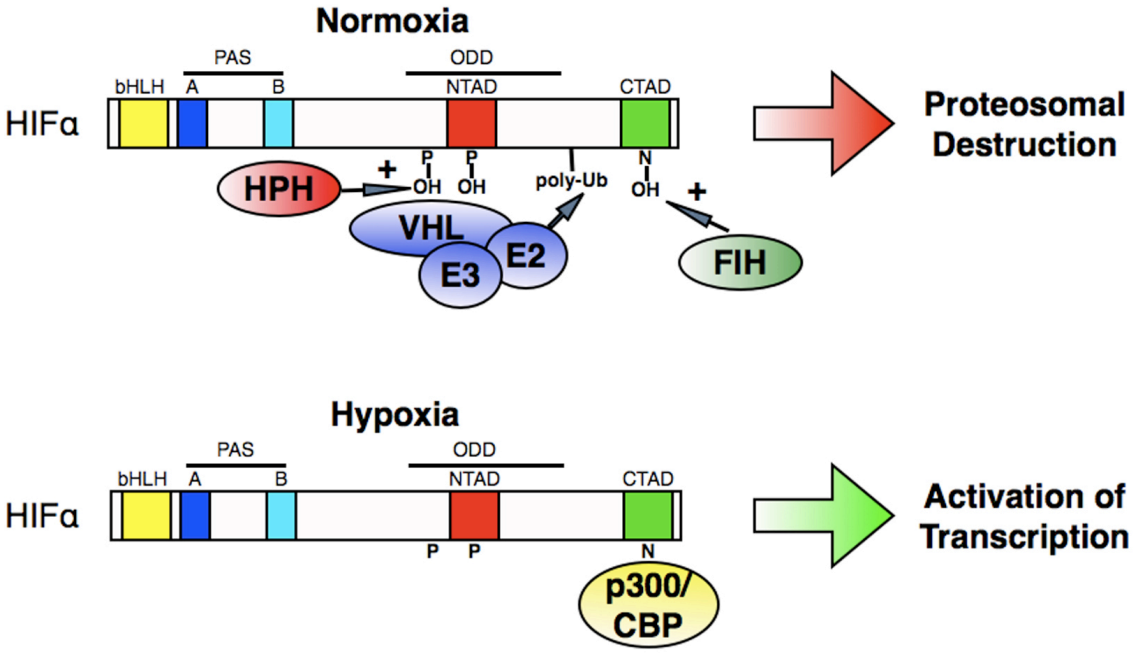

In normoxia (top), HIFα is prolyl-hydroxylated by HPH family members in the ODD domain. This allows the VHL ubiquitin ligase (VHL along with other E3 ligase components) to bind to the ODD, poly-ubiquitinating HIFα to target it for degradation. HIFα is also asparaginyl-hydroxylated by FIH in the CTAD, preventing association of HIFα with transcriptional co-activators. In hypoxia (bottom) neither of these hydroxylases are active, stabilizing HIFα and allowing it to associate with the p300/CBP transcriptional co-activators leading to transcription of HIF targets.

1.D. Hypoxia and HIF signaling in oxygen homeostasis, development and disease

Organisms encounter periods of hypoxia both environmentally and in an internally localized manner. The reasons for exposure to a hypoxic environment vary across species. While *Drosophila* larvae are commonly found in the hypoxic micro-environment of the decaying fruit on which they live and feed (Romero et al., 2007), we will most commonly encounter environmental hypoxia when traveling to regions of increased elevation (and thus decreased atmospheric oxygen concentration). Indeed, the study of the hypoxic response began when the physiological response to increased altitude was first observed in 1890 (Viault, 1890). Since that time, the responses allowing an organism to adapt to its altered surroundings have been intensely studied (reviewed in Smith et al., 2008). In addition to this environmental hypoxia, low levels of oxygen occur in a variety of tissues, both naturally throughout development (Centanin et al., 2008; Lee et al., 2001), and in response to pathological states (reviewed in Semenza, 2001; Semenza et al., 2000). This localized hypoxia and the subsequent HIF-mediated hypoxic response play important roles both in the morphogenesis of the *Drosophila* tracheal system and mammalian heart, vasculature and nervous system (reviewed in Covello & Simon, 2004; Ghabrial et al., 2003; Kaelin & Ratcliffe, 2008; Simon & Keith, 2008), and in the progression of disease states including tumor growth, pulmonary hypertension and myocardial or cerebral ischemic disease (reviewed in Maxwell, 2005; Rankin & Giaccia, 2008; Ratan et al., 2007; Semenza, 2001; Semenza, 2003; Semenza et al., 2000).

HIF transcriptional activity targets a wide range of genes required for organismal adaptation to hypoxia. This adaptation includes an increase in the capacity of the oxygen-conducting organs and changes in metabolic oxygen consumption (reviewed in Hoogewijs et al., 2007; Weidemann & Johnson, 2008). The hypoxic response acts to increase the oxygen delivery capacity of the oxygen-conducting organs via three distinct mechanisms; erythropoiesis, modulation of vascular tone and angiogenesis. Erythropoiesis is accomplished by the increased production of erythropoietin (EPO). EPO was the first identified target of HIF-1 (Semenza & Wang, 1992) and acts as a hematopoietic growth factor, leading to production of red blood cells (reviewed in Tabbara & Robinson, 1991). This HIF-mediated increase in EPO results in an increased capacity for blood oxygen transport (reviewed in Scholz et al., 1990).

The hypoxic response can also trigger morphological changes to the vascular system which lead to an increase in oxygen carrying capacity. Hypoxia signaling leads to vasodilation; the relaxation of the smooth muscle lining the blood vessels. This leads to a widening of the vascular lumen and thus an increase in the flow of blood through the vessels (reviewed in Paffett & Walker, 2007). Additional vascular remodeling comes from the further elaboration of blood vessels from the existing vasculature via the re-activation of the angiogenic program (reviewed in Richard et al., 1999). This role for the hypoxic response in angiogenesis is largely due to the ability of HIF to transcriptionally up-regulate signaling via the vascular endothelial growth factor (VEGF) pathway (reviewed in Kliche & Waltenberger, 2001). HIF has been demonstrated to up-regulate levels

of both the VEGF ligand and VEGF receptor (Forsythe et al., 1996; Gerber et al., 1997; Shweiki et al., 1992). Up-regulation of VEGF leads to an increase in endothelial cell proliferation and migration (Ferrara & Davis-Smyth, 1997), resulting in increased vascularization of (and therefore oxygen delivery to) the hypoxic tissue.

This function of the oxygen sensing/hypoxic response pathway is conserved in the homeostatically-driven tracheal morphogenesis that occurs during *Drosophila* larval development. Similar to the increase in oxygen carrying capacity stimulated by hypoxia in mammals, an increase in both the diameter of primary tubes and the degree of growth and branching of the terminal branches has been observed when larval tissues become hypoxic, either by disrupting the tracheal network or by placing the organism in an oxygen-poor environment (Henry & Harrison, 2004; Jarecki et al., 1999; Locke, 1958; Wigglesworth, 1954). This angiogenic-like phase of tracheal development makes reiterative use of the Btl/FGF signaling pathway (Figure 1.10). In hypoxic conditions, *sima* signaling is activated, first in tracheal cells, and later in surrounding non-tracheal tissue (Centanin et al., 2008; Lavista-Llanos et al., 2002). Stabilization of Sima in larval tracheal cells, either in hypoxia or *fga* mutants, leads to an up-regulation of *btl* transcription (Centanin et al., 2008). This *btl* up-regulation initiates an 'active searching' mode, increasing the sensitivity of terminal tracheal cells to *bnl* signals from surrounding tissues. Hypoxic non-tracheal tissues respond by a *sima*-mediated elevation of Bnl levels, which in turn leads to the attraction of an increased number of terminal branches (Centanin et al., 2008; Jarecki et al.,

1999). Indeed, this function of FGF signaling is conserved in mammals, where, along with VEGF, FGF is a potent inducer of angiogenesis in hypoxic tissues (Folkman & Klagsbrun, 1987; Presta et al., 2005).

Along with increased capacity of oxygen-conducting tissues, the hypoxic response triggers alterations in cellular metabolism. In a series of landmark discoveries, the essential role for oxygen in the generation of energy via aerobic cellular respiration has been elucidated (Friedkin & Lehninger, 1949; Krebs & Johnson, 1937; Meyerhof, 1920a; Meyerhof, 1920b; Meyerhof, 1920c; Mitchell, 1961). Cellular respiration begins with the uptake of glucose, the initial substrate for energy production. The first stage of cellular respiration is glycolysis, which converts glucose to pyruvate and produces two molecules of ATP, the cellular energy currency. In the presence of oxygen (aerobic respiration), the pyruvate products of glycolysis are converted to acetyl-CoA, which enters the Krebs cycle and is further metabolized leading to production of additional ATP and NADH molecules. In the main ATP-producing step of aerobic respiration, this NADH is oxidized by the electronic transport chain in the process of oxidative phosphorylation. In the absence of oxygen (anaerobic respiration), the cell is incapable of activating the Krebs cycle or oxidative phosphorylation and the pyruvate produced by glycolysis is broken down by the process of fermentation, a less efficient means of producing ATP.

The goal of the hypoxia-induced metabolic adaptations in mammalian tissues is to maintain energy production in spite of decreased oxygen levels. This energy-compensation strategy is based on the activation of the Pasteur effect, a

switch to high-flux glycolytic carbohydrate consumption (Hoogewijs et al., 2007; Krebs, 1972). The main basis of this metabolic switch is the transcriptional up-regulation of genes involved the glycolytic pathway (reviewed in Denko, 2008). This leads to increases in glucose uptake and in the total amount of ATP generated from the metabolism of glucose to pyruvate (Gleadle & Ratcliffe, 1997; Ouiddir et al., 1999; Seagroves et al., 2001; Webster, 1987; Webster, 2003). HIF activity also contributes to the shift toward anaerobic respiration by decreasing the conversion of pyruvate into acetyl-CoA thereby preventing activation of the Krebs cycle and leading to lowered mitochondrial function (Kim et al., 2006a; Papandreou et al., 2006). These adaptations allow hypoxic cells to adapt to brief periods of hypoxia by continuing to produce ATP (albeit less efficiently) while limiting the requirement for oxygen. After a short period of time however, this activated Pasteur effect will deplete substrate stores and lead to a build-up of toxic by-products (Hoogewijs et al., 2007). Cells using this metabolic response can therefore only survive brief periods of severe oxygen deprivation and are termed hypoxia-sensitive. If the hypoxic conditions are too severe or last for extended periods of time, the cells will die, either through apoptotic or necrotic cell death pathways (Hoogewijs et al., 2007).

Similar to the mammalian hypoxic response, the transcriptional output of the hypoxic response in *Drosophila* includes genes involved in altered metabolism (Liu et al., 2006; Zhou et al., 2008). The transcriptional profile of *Drosophila* exposed to hypoxic conditions differs with oxygen concentration and length of hypoxic exposure (Liu et al., 2006). Unlike hypoxia-sensitive

mammalian tissues, most insects, including *Drosophila*, are hypoxia-tolerant. The basis of this tolerance is the utilization of energy-conserving, along with energy-compensating, metabolic strategies (reviewed in Gorr et al., 2006; Hoogewijs et al., 2007). There is evidence that these hypoxia-tolerant insects can employ two distinct metabolic responses to altered oxygen concentration, under moderate hypoxia they can activate the high-flux glycolysis employed by mammalian cells, while a more severe hypoxic response in these hypoxia-tolerant organisms can also trigger entry into a hypometabolic state in which ATP demand is decreased to balance the ATP production from anaerobic respiration (Boutilier, 2001; Hochachka et al., 1996). This hypometabolic state is characterized by a down-regulation of most cellular functions including protein synthesis, ion-motive ATPases and gluconeogenesis (reviewed in Grieshaber et al., 1994; Hoogewijs et al., 2007). These adaptations allow *Drosophila* to survive extended periods of severe oxygen-deprivation.

Hypoxia-triggered physiological adaptations, including increased capacity of oxygen-conducting organs and altered metabolism, are required for organisms to maintain oxygen homeostasis. However, deregulation of the hypoxic response can have pathological consequences. This deregulation can include either a failure to induce the hypoxic response when required or an ectopic hypoxic response due to the inappropriate stabilization or activity of HIFα.

The consequences of an inability to induce the hypoxic response are clearly evident in genetic models of HIF loss of function. In *Drosophila*, *sima* mutants are sensitive to decreases in atmospheric oxygen that are easily

tolerated by wild type animals (Centanin et al., 2005). The requirement for HIF in responding to localized hypoxia during normal embryonic development has been intensely studied in loss of function mouse models of HIF-1α and HIF-2α (reviewed in Patel & Simon, 2008; Weidemann & Johnson, 2008). HIF-1α knockout mice have defects in vascular development, and immune system and cardiac function (Cramer et al., 2003; Huang et al., 2004; Peyssonnaux et al., 2007; Ryan et al., 1998), along with defects in limb and skeletal development (Provot et al., 2007; Wang et al., 2007). Loss of function mouse models of HIF-2α have revealed an additional set of processes regulated by HIF signaling. This includes the regulation of heart rate, fat metabolism, catecholamine synthesis and response to oxidative stress (Scortegagna et al., 2003; Tian et al., 1998). Additionally, the ability to increase stabilization of HIF has been shown to be beneficial in the prevention and treatment of many ischemic vascular diseases (reviewed in Kaelin & Ratcliffe, 2008) including stroke and myocardial infarction (Ratan et al., 2007; Shohet & Garcia, 2007).

Conversely, the inappropriate stabilization of HIFα subunits plays a major role in the development of many human diseases including rheumatoid and osteoarthritis (Cramer et al., 2003; Pfander et al., 2006), pulmonary hypertension (Semenza, 2000), preeclampsia (Genbacev et al., 1996; Genbacev et al., 1997), and, most prominently, cancer (reviewed in Covello & Simon, 2004; Hoogewijs et al., 2007; Kaelin & Ratcliffe, 2008; Rankin & Giaccia, 2008). HIF stabilization is observed in tumors from a wide variety of cancers, including breast, glial, renal, ovarian and pancreatic (Talks et al., 2000). In fact, it has been estimated that

approximately 50-60% of all solid tumors display stabilization of the HIFα subunits (Vaupel & Mayer, 2007).

HIF accumulation in tumor cells is either a result of localized hypoxia occurring in solid tumors, or a result of lesions in pathways that normally act to repress HIF stabilization. As solid tumors grow, the availability of oxygen is limited in cells that are beyond the oxygen diffusion distance (50-230μm from a blood vessel), leading to an imbalance between oxygen supply and use in the proliferating tumor tissue, thus inhibiting HPH function and causing HIFα stabilization (Carmeliet & Jain, 2000; Tannock, 1968; Tannock, 1972; Vaupel & Mayer, 2007). Stabilization of HIF can also result from defects in the HPH/VHL pathway, which normally serves to target HIFα subunits for proteosome-mediated degradation. Heritable mutant alleles of VHL lead to the development of the von Hippel Lindau cancer syndrome, characterized by highly vascularized tumors in multiple tissues including clear cell-renal cell carcinomas (CC-RCC), hemangioblastomas of the central nervous system and pheochromocytomas (reviewed in Lonser et al., 2003). Mutations in VHL are also seen in a variety of sporadic cancers, most notably CC-RCC (Gnarra et al., 1994).

Regardless of the cause, this increased HIF signaling in tumor cells contributes to tumorigenesis and to the development of common hallmarks of cancer (reviewed in Hanahan & Weinberg, 2000; Kroemer & Pouyssegur, 2008) including sustained angiogenesis, tissue invasion/metastasis and the altered metabolism that is characteristic of tumor cells. Due to the previously mentioned limit on oxygen diffusion, tumors must attract blood vessels and develop their

own vasculature in order to grow beyond the diffusion-imposed limit (Bouck et al., 1996; Folkman, 1971; Hanahan & Folkman, 1996). This is accomplished by re-activation of the HIF-mediated angiogenic program associated with the hypoxic response as discussed previously (reviewed in Richard et al., 1999). Sustained angiogenesis is required for the continuous proliferation seen in developing tumors (Folkman, 1971). Recent studies have shown that anti-angiogenic therapies, mediated by VEGF-blocking antibodies, are a promising new treatment of cancer (reviewed in Gasparini et al., 2005).

Along with this role in triggering tumor angiogenesis, HIF signaling also promotes tissue invasion and metastasis (reviewed in Brahimi-Horn & Pouyssegur, 2006; Chaudary & Hill, 2007; Gort et al., 2008). These related processes result in the formation of secondary tumors which form from cancer cells migrating from the primary tumor (reviewed in Hanahan & Weinberg, 2000), and are the major cause of death in cancer patients (Sporn, 1996). Clearly, treatments inhibiting this activity of HIF would be of great benefit in treating disease.

As first observed by Otto Warburg in the 1920s, cancer cells are characterized by metabolic changes (Warburg, 1956). In what is now known as the Warburg effect, cancer cells preferentially metabolize glucose via glycolysis even in the presence of sufficient levels of oxygen for aerobic respiration. This aerobic glycolysis is accomplished by activating the metabolic changes characteristic of the hypoxic response in hypoxia-sensitive mammalian cells; increased function of the glycolytic pathway and inhibition of mitochondrial

function. This induction of aerobic glycolysis is a common occurrence in cancers, suggesting that it may confer an advantage to tumor cells (reviewed in Denko, 2008).

In severe conditions, cancer cells can switch to utilizing an energy-conserving metabolic strategy similar to that of hypoxia-tolerant organisms to survive in near anoxic conditions (Ebbesen et al., 2004; Giaccia, 1996). These tumor cells then remain in a hypometabolic state until angiogenic vascular growth allows for tissue re-oxygenation. In the human body, this hypoxia-tolerant switch is unique to cancer cells; gaining a better understanding of the initiation of this hypometabolic state in hypoxia-tolerant organisms may prove beneficial in targeting this tumor-specific metabolic strategy in treating cancer (Hoogewijs et al., 2007).

Figure 1.10. Homeostatic tracheogenesis is dependent on *sima* and the Btl/ FGF signaling pathway and increases tracheal oxygen-conducting capacity.

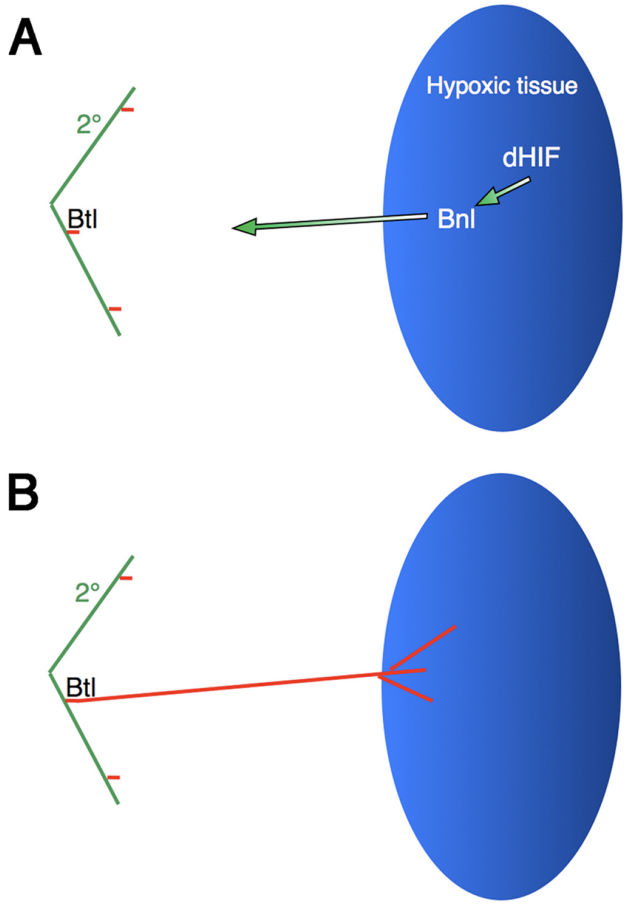

(A) The dHIF (Sima:Tgo) transcription factor is stabilized by hypoxia, driving expression of Btl in tracheal cells and Bnl in hypoxic non-tracheal tissue. This activates Btl/FGF signaling leading to elaboration of tracheal terminal branches (B). These terminal branches oxygenate the tissue causing a destabilization of dHIF and cessation of Btl/FGF signaling.

1.E. Non-canonical regulation of HIF signaling by tumor suppressor proteins

Consistent with its vital roles in oxygen homeostasis, development and disease progression, HIF signaling is subject to a high degree of regulation; along with the conserved HPH/VHL and FIH oxygen-dependent regulatory mechanisms, HIF activity is also regulated by the phosphatidylinositol 3-kinase (PI3K)-AKT-PTEN kinase pathway (reviewed in Jiang & Liu, 2008a; Jiang & Liu, 2008b).

There is evidence that HIFα stability can also be regulated by a variety of VHL-independent pathways in hypoxic conditions or rapidly proliferating cells. HIFα stability is regulated under hypoxic conditions via a GSK-3β-dependent pathway and by a negative feedback loop initiated by HIF transcriptional activity (Demidenko et al., 2005; Flugel et al., 2007). In actively proliferating cells, HIFα stability is regulated by its association with Hypoxia-Associated Factor, an E3-ubiquitin ligase subunit that can act to suppress tumorigenesis in mouse xenograft models (Koh et al., 2008). The exact mechanisms of these pathways remain to be elucidated but may explain the accumulation of HIFα in cells with intact HPH/VHL function, for instance cells from glioblastoma and ovarian cancer lines (Imai et al., 2003; Skuli et al., 2006; Zagzag et al., 2000).

Hyper-accumulation of HIFα and activation of HIF signaling due to deficiency in these regulatory networks leads to organismal lethality. In *Drosophila*, mutations in *fga* lead to pupal lethality in a *sima*-dependent manner (Centanin et al., 2005). Similarly, mice lacking function of either the HPH family member *PHD2* or *VHL* die during embryogenesis with defects in vascular

development (Gnarra et al., 1997; Takeda et al., 2006). Loss of function mouse models of the recently discovered tumor suppressor gene *archipelago* (*ago*, also known as *Fbw7*, *Fbxw7*, *sel-10* and *cdc4*; Moberg et al., 2001; Strohmaier et al., 2001), are embryonic lethal due to a combination of defects in hematopoiesis and vascular development and remodeling (Tetzlaff et al., 2004; Tsunematsu et al., 2004). This data reveals a previously unappreciated role for *ago*/*Fbw7* in the tubular morphogenesis of branched oxygen-conducting networks. The similarity of the defects seen in *ago*/*Fbw7* and *PHD2*-*VHL* loss of function models may also suggest a role for *ago* in regulating the hypoxic response.

The *ago* locus encodes a protein containing an F-box domain and seven tandem WD (tryptophan-aspartic acid) repeats in the C-terminal half of the protein (Koepp et al., 2001; Moberg et al., 2001; Strohmaier et al., 2001). Based on this domain structure, Ago is thought to function as a specificity factor for an SCF (Skp-Cullin-F-box) type ubiquitin ligase (Figure 1.11; Skowyra et al., 1997). Ago interacts with the ubiquitination machinery via its F-box domain, while the WD repeats form a β-propeller structure through which Ago interacts with its specific substrates, recruiting them to the assembled ubiquitin ligase where they are poly-ubiquitinated and targeted for proteosomal degradation. Mutations in *ago* were first isolated in a forward genetic screen for mutations displaying increased cell proliferation in the developing *Drosophila* eye (Moberg et al., 2001). *Drosophila ago* has been shown to coordinately regulate cell cycle progression and growth in proliferating cells. *ago* mutant tissues show elevated levels of CycE (Moberg et al., 2001) and dMyc proteins (Moberg et al., 2004),

leading to ectopic cell divisions and increased tissue growth respectively. These functions are conserved in vertebrate *ago* homologs; mouse and human Fbw7 have been shown to regulate levels of both CycE (Koepp et al., 2001; Strohmaier et al., 2001) and c-Myc (Welcker et al., 2004a). Fbw7 has also been shown to regulate levels of a variety of other proteins including Notch (Tetzlaff et al., 2004; Tsunematsu et al., 2004), c-Jun (Nateri et al., 2004), PGC-1α (Olson et al., 2008), SRC-3 (Wu et al., 2007), Presenilin 1 (Li et al., 2002) and SREBP (Sundqvist et al., 2005).

Ectopic expression of many of these *ago*/*Fbw7* targets can contribute to tumorigenesis, and not surprisingly *Fbw7* has been identified as a tumor suppressor gene in mouse models (Mao et al., 2004; Maser et al., 2007; Onoyama et al., 2007) and in human disease (reviewed in Tan et al., 2008; Welcker & Clurman, 2008). Loss of *Fbw7* function is associated with an ever-increasing variety of human cancers including T-cell and B-cell acute lymphocytic leukemias (Malyukova et al., 2007; O'Neil et al., 2007; Song et al., 2008; Thompson et al., 2007; Van Vlierberghe et al., 2008), glioblastoma (Gu et al., 2007; Hagedorn et al., 2007), and prostate (Koh et al., 2006), ovarian (Kwak et al., 2005), endometrial (Cassia et al., 2003; Spruck et al., 2002), and pancreatic (Calhoun et al., 2003) tumors. Gaining further insight into the putative novel role of Ago/Fbw7 in the regulation of oxygen-homeostatic biology, including both the development of the oxygen-conducting organs and the hypoxic response, may be important in understanding the tumorigenic role of the loss of *ago*/*Fbw7*.

Figure 1.11. The SCFAgo ubiquitin ligase.

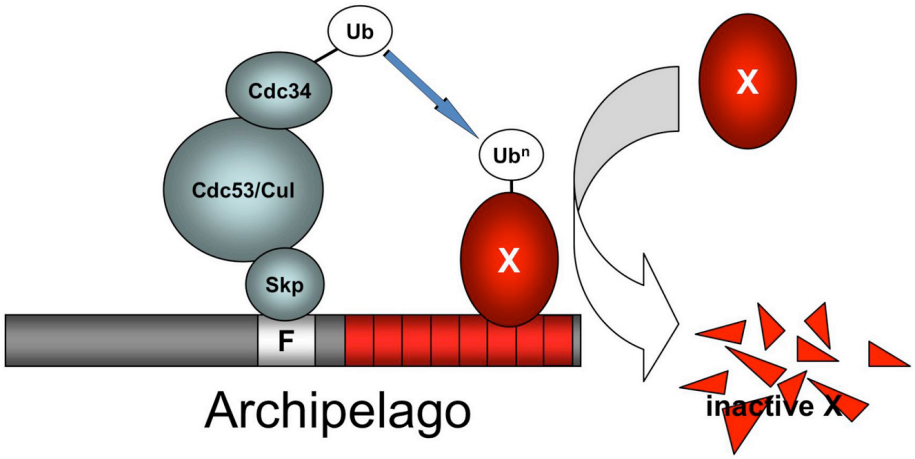

The Ago protein interacts with the ubiquitination machinery via its F-box ('F') domain and binds to substrates ('X') via the WD-repeat domain (red). Substrates are thereby recruited into the SCF complex where they are ubiquitinated and targeted for proteosomal degradation.

1.F. Purpose

Clearly, regulation of the oxygen homeostatic machinery is a fundamental aspect of organismal development. Based on the previously discussed data, I hypothesize that *ago* plays a vital role in the regulation of oxygen homeostasis, firstly in the development of the oxygen-conducting organs and secondly in the restriction of the transcriptional response to oxygen deprivation. In this project I will use the development of the *Drosophila* tracheal system to explore this interesting and potentially clinically relevant aspect of *ago* biology.

Firstly, defects in the development of the oxygen-conducting organs can result in an insufficient oxygen supply to internal tissues, leading to widespread hypoxia. The *ago*/*Fbw7* knockout mouse model displays embryonic lethality due to such defects in vascular morphogenesis. It is my hypothesis that this apparent function in tubular morphogenesis is conserved across species. I would therefore predict that loss of *ago* in *Drosophila* would cause defects in the embryonic-developmental stage of tracheogenesis. I will test this prediction by conducting a phenotypic examination of tracheal development in *ago* mutant embryos.

Secondly, a tightly-regulated response to environmental or localized oxygen deprivation is essential; an insufficient response can result in hypoxia-mediated organismal lethality, while ectopic hypoxic signaling is linked to the development of a wide range of pathologies, most notably playing a required role in tumorigenesis. This regulation of the hypoxic response is based on the ability to regulate HIF stability and activity. Recent findings demonstrate that the HPH/VHL and FIH pathways alone are not sufficient to provide an adequate degree of

sensitivity in the regulation of HIF. Novel regulators have been identified that may act in specific cell types or conditions, but a second HIF regulatory pathway is incompletely understood. I hypothesize that *ago* is an important member of this second pathway. I would predict that loss of *ago* would therefore lead to an ectopic hypoxic response reflected in excess terminal branching during the larval-homeostatic stage of tracheogenesis. This prediction will be tested by examination of terminal branching in normoxic *ago* mutant larvae. I would further predict that loss of *ago* would alter the response to oxygen deprivation, which will be assayed throughout *Drosophila* development.

If this hypothesis is true it would represent an important advance in understanding the control of oxygen homeostasis. The mechanisms regulating this basic biological phenomenon are incompletely understood and data linking the regulation of both tubular morphogenesis and the hypoxic response to a second protein degradative pathway would be a novel finding. In particular, discovery of a secondary HIF regulatory mechanism would be a major advance in our understanding of this stress response pathway. Since HIF deregulation is intimately associated with a wide range of pathologies, a more thorough understanding of the regulatory mechanisms may have important clinical implications.

Chapter Two: The *Drosophila* F-box protein Archipelago controls levels of the Trachealess transcription factor in the embryonic tracheal system[1]

2.A. Introduction

The morphogenesis of branched networks of cells with a single, fused lumen plays an important role in the development of many metazoan organs, including the vertebrate lungs, vasculature, kidneys, and mammary glands. The cellular architecture of these mammalian organs is quite similar to tubular structures in simpler metazoans, suggesting that the molecular and cellular mechanisms underlying the process of branching morphogenesis are conserved. In the fruit fly *Drosophila melanogaster*, tubular morphogenesis underlies formation of the tracheal system, a network of interconnected tubes that duct air throughout the developing organism. The complete embryonic tracheal network is composed of approximately 1600 polarized epithelial cells that originate in early embryogenesis as 20 ectodermal placodes distributed along either side of the embryo (Samakovlis et al., 1996a). Each tracheal placode contains approximately 20 cells, which undergo two rounds of cell division, exit the cell cycle, and complete the subsequent stages of invagination and tracheal development without further cell division or cell death. Following invagination, primary branches bud from the tracheal sac and form a continuous lumen within each placode (Lubarsky & Krasnow, 2003). The pattern of placode branching is segmentally repeated and under fixed genetic control (Samakovlis et al., 1996a). Budded branches extend toward their target tissues by a process of cell migration and cell extension, and subsequent fusion between adjacent tracheal metameres at later stages of embryogenesis produces a continuous, open tubular system.

Forward genetic screens for mutations that disrupt tracheal development have revealed a central role for fibroblast growth factor (FGF) signaling in promoting the post-mitotic cell migration and extension of the embryonic tracheal arbor (reviewed in Metzger & Krasnow, 1999). The central components of the *Drosophila* FGF pathway are encoded by the *breathless* (*btl*, Klambt et al., 1992) and *branchless* (*bnl*, Sutherland et al., 1996) genes, which encode an FGF-like receptor and an FGF-like secreted ligand respectively. The role of this receptor/ligand pair in controlling tracheal outgrowth is based upon a simple model in which the restricted expression of *bnl* in cells outside the tracheal placode represents a directional cue for the migration of *btl*-expressing cells within the tracheal placode. Initial induction of *btl* transcription within tracheal cells depends upon the *trachealess* (*trh*) gene, which encodes a basic helix-loop-helix Per/Arnt/Sim (bHLH-PAS) domain transcription factor (Isaac & Andrew, 1996; Kuo et al., 1996; Ohshiro & Saigo, 1997; Wilk et al., 1996) most closely homologous to the mammalian NPAS1 and NPAS3 proteins (Brunskill et al., 1999; Zhou et al., 1997). Mutation of any one of these core components - *btl*, *bnl* or *trh* - produces a failure of tracheal branching. Phenotypic analysis of these and other tracheal development genes has shown that Btl/FGF signaling is used to promote successive rounds of primary and secondary tracheal branching during embryonic *Drosophila* development (reviewed in Ghabrial et al., 2003). A similar role has been proposed for the FGF pathway in controlling the branching morphogenesis of tubes in the mammalian lung (Min et al., 1998).

In addition to a positive role in tracheal outgrowth, experimental evidence indicates that inappropriately timed Btl/FGF signaling can also impair tracheal development. First, in the course of normal development *btl* expression is not constant in tracheal cells, but oscillates: initially *btl* mRNA rises in all placode cells at stages 10-12 preceding primary branch formation, subsequently falls during late stage 12/early stage 13, and is re-initiated in a restricted set of cells that define sites of secondary branching at late stage 13/early stage 14. Unlike early *btl* expression, this second wave is dependent upon a *bnl*-dependent feedback loop (Ohshiro et al., 2002; Ohshiro & Saigo, 1997). Second, ectopic activation of Btl, either by mutational inactivation of the *btl* inhibitor *abnormal wing disc* (*awd*, Dammai et al., 2003), or by constitutive expression of *bnl* (Sutherland et al., 1996) or *btl* (this study and Lee et al., 1996a), interferes with directed cell migration in the trachea. Similarly, expression of activated *Ras* or *btl* perturbs the ability of tracheal cells to form proper branching patterns in larval development (Cabernard & Affolter, 2005). These observations have led to the hypothesis that spatial and quantitative restriction of Btl activity is necessary to permit normal patterns of tracheal cell migration and fusion (Lee et al., 1996a). While many genes that modulate Btl/FGF signaling have been identified, it is likely that other as yet unrecognized mechanisms are required to restrict Btl/FGF signaling to specific times and places in the developing organism.

Here we identify *archipelago* (*ago*), a gene known primarily for its role in cell proliferation control, as a component of the genetic circuitry that patterns the post-mitotic development of the embryonic tracheal system. *ago* encodes an F-

box/WD-repeat protein that recruits target proteins to an SCF-type E3 Ub-ligase for subsequent poly-ubiquitination and proteolytic destruction. *ago* limits the division and growth of *Drosophila* eye epithelial cells by targeting the G1/S regulator Cyclin E and dMyc, the fruit fly ortholog of the human c-Myc proto-oncogene, for proteosome mediated-degradation (Moberg et al., 2001; Moberg et al., 2004). A highly conserved mammalian *ago* ortholog (variously termed *Fbw7*, *Fbxw7*, *hAgo*, *hCDC4* or *hSel-10*) also targets Cyclin E and c-Myc and is a mutational target in a rapidly expanding array of human cancers (Balakrishnan et al., 2007; Bredel et al., 2005; Calhoun et al., 2003; Hagedorn et al., 2007; Malyukova et al., 2007; Mao et al., 2004; Maser et al., 2007; Minella et al., 2005; O'Neil et al., 2007; Rajagopalan et al., 2004; Thompson et al., 2007). Our current data indicate that *ago* is required for tracheal morphogenesis via a previously unrecognized target, the Trh transcription factor. We find that *ago* mutant embryos contain excess Trh protein and ectopically express the *btl* gene, a known Trh target. Alleles of *ago* exhibit strong genetic interactions with *trh* and other known tracheal development genes, and the Ago protein is able to bind the Trh protein and regulate its proteosomal turnover via a mechanism that involves a third factor, the bHLH-PAS protein Dysfusion (Dys, Jiang & Crews, 2003). Collectively, these data reveal a previously unappreciated developmental function for the *ago* tumor suppressor in the embryonic tracheal system, and identify the Trh transcription factor as a target of Ago in this process.

2.B. *ago* has a role in embryonic tracheal development

Analysis of the growth restrictive role of *ago* in proliferating larval imaginal disc cells has provided an excellent model to understand the tumor suppressive properties of *ago* mammalian orthologs. However, the Ago protein is widely expressed in the early embryo (Figure 2.1) and mutations that disrupt it lead to embryonic death (Moberg et al., 2001). Intercrossing the ago^{1} or ago^{3} alleles (respectively encoding a C-terminal truncation in the WD-repeat/substrate-binding domain and a G1131E missense mutation in the 4th WD repeat; Moberg et al., 2001) produces *trans*-heterozygous mutant embryos that develop through all embryonic stages but fail to hatch as L1 larvae, suggesting lethality occurs during late embryogenesis. The severity of this and other phenotypes (see below) in homozygous or heteroallelic mutant animals is indistinguishable from those carrying either allele in *trans* to a chromosomal deficiency that removes the *ago* locus (Table 2.1; *Df(3L)Exel9000*), indicating that ago^{1} and ago^{3} are either null or strong loss-of-function alleles. Considered together, these observations indicate that *ago* may have as yet unappreciated roles in early development.

The earliest morphological defects in *ago* zygotic mutant embryos are observed in the developing trachea visualized with the anti-lumen antibody mAb2A12 (Figure 2.2C-F). This analysis reveals two major defects in tracheal branching patterns of *ago* embryos when compared to control wild type (*WT*) embryos. The first of these is interruptions, or ‘breaks’, in the continuity of the tracheal lumen (Figure 2.2C-E). The breaks occur throughout the tracheal system and are prominent in the dorsal trunk (DT; Figure 2.2C,D, arrowheads), the

lateral truck (LT; Figure 2.2C, arrows), and between dorsal branches of opposing tracheal placodes (DB; Figure 2.2E, arrow). What appears to be a misrouting phenotype is also observed in the dorsal branches (Figure 2.2E, arrowhead) and ganglionic branches. Approximately 70% of all *ago* mutant embryos show combinations of these break or misrouting effects. The second prominent tracheal phenotype (occurring in ~25% of all *ago* mutant embryos) is excess lumen convolution throughout the primary and secondary branches (Figure 2.2F). This combined spectrum of breaks, apparent misrouting, and convolution indicates that *ago* is required for normal development of the tracheal system. Moreover, the absence of any accompanying defects in the major morphogenetic events of embryogenesis suggests that these phenotypes reflect a requirement for *ago* in the trachea, rather than as a secondary effect of a more general developmental role outside this tissue.

The DT break phenotype occurs in almost half of all *ago* mutant embryos (46% [n=85]) with an average of 1.2 ± 0.09 breaks among those that show the phenotype (n=39). On a per fusion event basis, this corresponds to a greater than 15-fold increase in the rate of defective interplacode fusion events in *ago* mutants compared to control embryos (Table 2.2). Due to the prevalence of this phenotype, DT morphogenesis was selected as a system in which to characterize the role of *ago* in the developing tracheal system. To investigate the cellular architecture of DT breaks in *ago* mutant embryos, the *1-eve-1* enhancer trap line, which carries a *lacZ* insertion in the *trh* gene and expresses β-galactosidase (β-gal) in every tracheal cell (Perrimon et al., 1991; Wilk et al.,

1996), was placed in the wild type and *ago* mutant backgrounds (Figure 2.2B,D). Anti-β-gal staining of these embryos reveals that lumenal gaps detected with the mAb2A12 antibody reflect physical gaps between cells of adjacent tracheal placodes (Figure 2.2D, arrowhead). Interplacode fusion along the DT is normally dependent upon specialized 'fusion cells', which are specified 2 per placode by a *Notch*-dependent process (Ikeya & Hayashi, 1999). At the appropriate stage, one migrates anteriorly and the other posteriorly to meet with fusion cells coming from adjacent placodes. Thus, the gaps between adjacent DT placodes in *ago* mutant embryos suggest either that *ago* is necessary for proper fusion cell specification, or that *ago* mutations impair fusion cell migration and/or fusion. To test these hypotheses, DT fusion cells were visualized in wild type and *ago* mutant stage 15 embryos (Figure 2.3) using the fusion cell-specific enhancer trap *escargot* (*esg)-lacZ* (Tanaka-Matakatsu et al., 1996). Analysis of wild type embryos in which the process of DT fusion is complete shows *esg-lacZ* expression (purple nuclei; Figure 2.3A) in a pair of adjacent fusion cell nuclei. In *ago* mutant embryos, pairs of *esg-lacZ* positive fusion cells flank regions of DT breaks (Figure 2.3B; arrows mark fusion cell nuclei; arrowhead marks gap in DT). Analysis of a second fusion cell marker, the Dys protein (Jiang & Crews, 2003), gives similar results. Thus *ago* DT breaks are not associated with altered fusion cell numbers but rather a failure of *ago* mutant DT fusion cells to fuse with adjacent placodes. This differs significantly from tracheal phenotypes elicited by *btl-Gal4* driven over-expression the putative Ago target Notch (Fryer et al., 2004; Gupta-Rossi et al., 2001; Oberg et al., 2001; Tsunematsu et al., 2004; Wu et al., 2001), which results in a

complete loss of fusion cells (Ikeya & Hayashi, 1999). The lack of an effect on fusion cell number also contrasts with *ago* proliferative phenotypes in imaginal discs (Moberg et al., 2001; Moberg et al., 2004). To further confirm this, we measured total cell number in wild type and *ago* mutant DTs using an anti-Tango antiserum (Sonnenfeld et al., 1997). This analysis shows that these genotypes have approximately equal numbers of nuclei per DT segment (*WT* = 16.7 ± 0.4 [n=6]; *ago* = 17.0 ± 0.7 [n=9]). Thus the primary effect of *ago* loss in the DT is not on cell number, but rather on the ability of cells to follow the normal developmental program of cell migration and fusion.

Because Ago protein is expressed uniformly in tracheal and non-tracheal cells (Figure 2.4), the requirement for *ago* in the DT could be indicative of a cell-autonomous role for *ago* in tracheal cells or it might reflect a non-cell autonomous role for *ago* outside the developing placode in, for example, the mesodermal 'bridge cells' necessary for DT fusion (Wolf & Schuh, 2000). To determine the site of *ago* action, a wild type *UAS-ago* transgene and a dominant-negative *UAS-agoΔF* transgene were expressed specifically in the developing tracheal system using the *btl-Gal4* driver (Shiga et al., 1996). *btl-Gal4* driven expression of wild type *ago* in an ago^{1}/ago^{3} mutant background significantly reduces the frequency of DT breaks (Figure 2.5E; compare yellow and blue bars) and the other observed tracheal phenotypes in *ago* mutant embryos. Moreover, *btl-Gal4* driven expression of the *agoΔF* dominant-negative transgene in otherwise wild type tracheal cells is sufficient to produce DT breaks at similar penetrance as zygotic deficiency for *ago* (Table 2.3 and Figure 2.5A,D). The

agoΔF allele carries an internal deletion of the core F-box domain (Moberg et al., 2004), and is defective in ubiquitin-dependent protein degradation. While these data do not rule out a secondary role for *ago* in non-tracheal cells, they do argue that *ago* plays a required role in a protein degradation pathway that is active in embryonic tracheal cells.

Figure 2.1. Ago is widely expressed during embryogenesis.

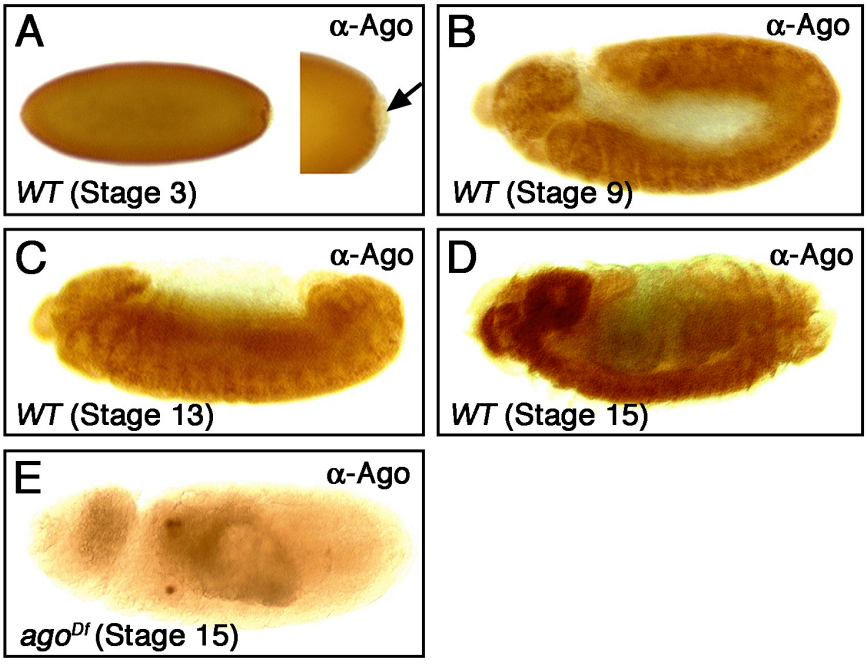

Lateral views of *WT* control embryos stained with Ago-specific antiserum. Ago expression is detected uniformly during the cellularization (A), and germ-band extended (B) and retracted (C) stages, but is not detectable in pole cells (arrow in A). Ago is concentrated in the CNS during late embryogenesis (D). In this and all further figures, embryos are shown anterior left and dorsal up (unless indicated). Anti-Ago staining in an embryo homozygous for the *Df(3L)Exel9000* deletion, which removes the *ago* gene (E).

Figure 2.2. *ago* is required for tracheal development.

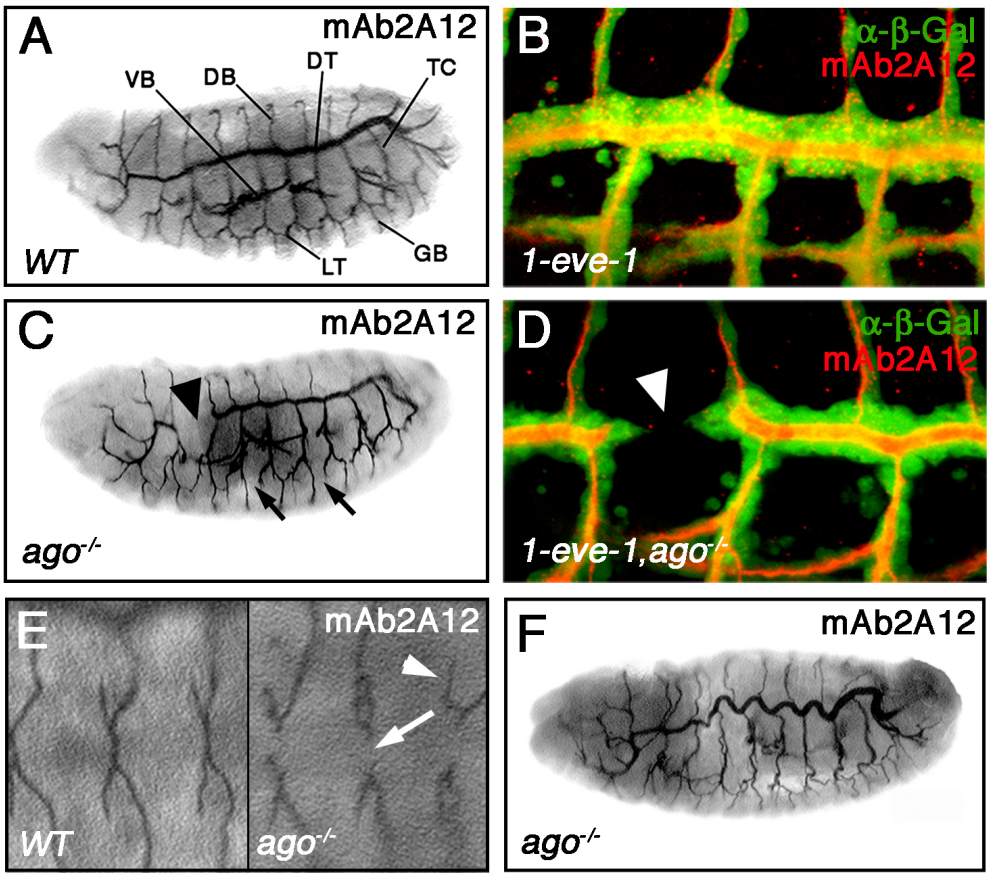

Lateral views of *WT* (A) or *ago* embryos (C,F) stained with mAb2A12 to visualize the tracheal lumen. *ago* mutants display interruptions in the lumen of the DT (arrowhead in C) and LT (arrows in C). *1-eve-1* (B) or *1-eve-1*, *ago* (D) embryos stained with anti-β-Gal (green) and mAb2A12 (red) to mark the tracheal cells and lumen respectively. The DT lumen interruptions in *ago* mutant embryos correspond to physical breaks in the DT (arrowhead in D). (E) Dorsal views of *WT* (left) and *ago* (right) embryos stained with mAb2A12. *ago* mutant embryos show defects in DB fusion (arrow) as well as DB misrouting (arrowhead). The DT lumens in *ago* mutant embryos display a convolution defect (F). Panels B and D are reconstructions of serial sections.

Figure 2.3 Fusion cell specification in *ago* mutant embryos.

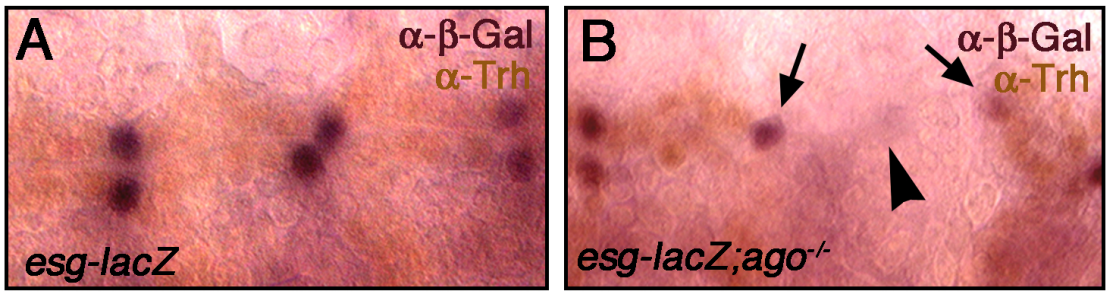

Staining of *esg-lacZ* (A) and *esg-lacZ;ago* (B) embryos with anti-Trh (brown) and anti-β-Gal (purple). Arrows in B mark fusion cells in adjacent placodes. Arrowhead indicates a break in the dorsal trunk.

Figure 2.4. Ago is expressed in both tracheal and non-tracheal cells.

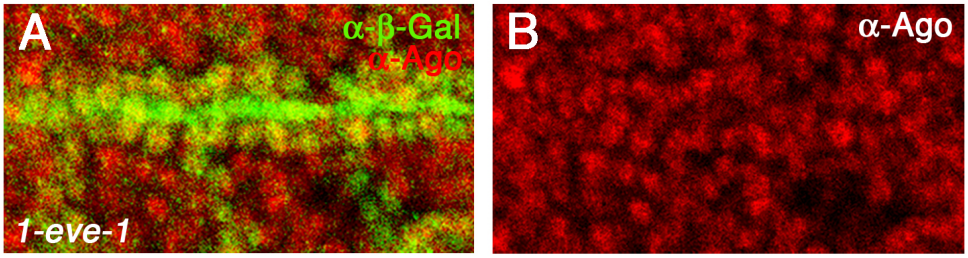

Stage 15 *1-eve-1* embryos stained with anti-β-Gal (green) to show tracheal cells and anti-Ago (red) showing nuclear *ago* expression in all cells in the field.

Figure 2.5. *ago* acts within tracheal cells and interacts with Btl/FGF signaling components.

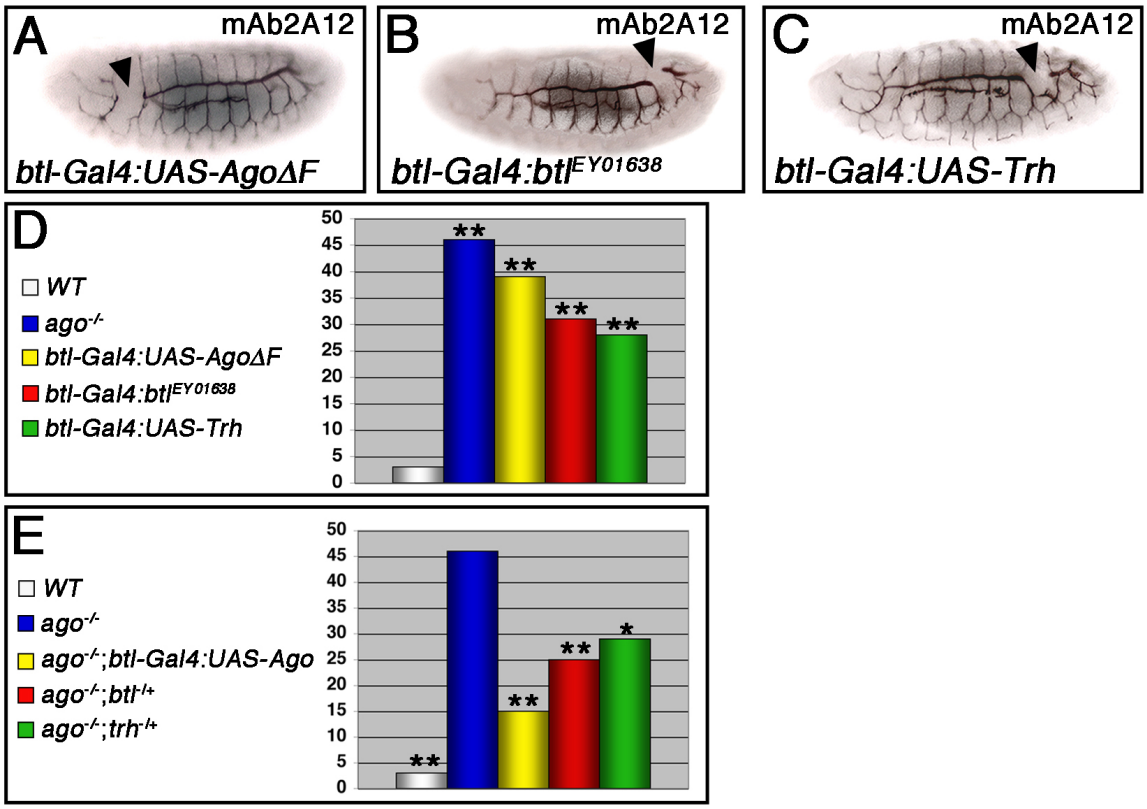

mAb2A12 staining of stage 15 embryos (A-C). *btl-Gal4* driven expression of *agoΔF* (A), *btl* (B) or *trh* (C) phenocopies the *ago* DT break phenotype (arrowheads). (D,E) Quantitative summary of the DT break phenotype in stage 15 embryos of the indicated genotypes. (D) *btl-Gal4* driven expression of *agoΔF* (yellow), *btl* (red) or *trh* (green) phenocopies *ago* mutations (blue). (E) The *ago* mutant phenotype is suppressed by expression of wild type *ago* in the *btl-Gal4* domain (yellow), or by reducing the genetic dosage of either *btl* (red) or *trh* (green). * $p<0.05$ and ** $p<0.01$ compared to *WT* (D) or *ago* (E).

Table 2.1. *ago*^{1} and *ago*^{3} behave as null alleles in tracheal development

Genotype	DT Breaks (%)	n=
WT	3**	61
ago^{1}/*ago*^{3}	46	85
ago^{1}/*Exel9000*	39	57
ago^{3}/*Exel9000*	38	42

The penetrance of indicated tracheal phenotypes in stage 15 embryos of the indicated genotypes. ** $p < 0.01$ compared to *ago*.

Table 2.2. Quantitation of the penetrance of *ago* and *ago;awd* DT 'breaks' per fusion event

Genotype	Frequency of defective DT fusion events		P value	n=
WT	0.2±0.1%	(.03/18)	-	61
ago^{1}/ago^{3}	3.4±0.4%	(.61/18)	$5.5x10^{-8}$	85
$awd^{j2A4}/+$	2.4±1.3%	(.43/18)	$4.1x10^{-2}$	42
$ago^{3},awd^{j2A4}/+$	15.5±5.4%	(2.8/18)	$2.2x10^{-4}$	33
$ago^{3},awd^{j2A4}/ago^{1}$	26.8±4.6%	(4.8/18)	$7.1x10^{-9}$	52

Penetrance of indicated tracheal phenotypes in stage 15 embryos of the indicated genotypes.

Table 2.3. *ago* is phenocopied by ectopic expression of FGF pathway members, but not known Ago targets

Genotype	DT Breaks (%)	n=
WT	3**	61
ago^{1}/ago^{3}	46	85
btl-Gal4:UAS-agoΔF	39	56
btl-Gal4:UAS-trh	28	56
btl-Gal4:btl^{EY01638}	31	53
btl-Gal4:UAS-CycE	18**	64
btl-Gal4:UAS-dMyc	3**	66

Penetrance of indicated tracheal phenotypes in stage 15 embryos of the indicated genotypes. ** $p < 0.01$ compared to *ago*.

2.C. *ago* acts upstream of *trachealess* and *breathless*

Because loss of *ago* leads to excess activity of proteins normally regulated by Ago-dependent degradation (Moberg et al., 2001; Moberg et al., 2004), known Ago target proteins were tested for their ability to reproduce *ago* mutant tracheal phenotypes when expressed in the *btl-Gal4* domain. Expression of *cycE* and *dMyc*, two targets of Ago in imaginal disc cells, do not reproduce the *ago* mutant tracheal phenotype (Table 2.3), suggesting that *ago* controls tracheal morphogenesis via a novel target. Significantly, *btl-Gal4* driven expression of either *trh* or its downstream target *btl* produces DT breaks of similar penetrance and expressivity as *ago* mutations (Figure 2.5B-D), and also leads to lumen convolution (see Figure 3.6B). Moreover, loss-of-function alleles of *trh* (*trh*^{10512}, Isaac & Andrew, 1996) or *btl* (*btl*^{dev1}, Kennison & Tamkun, 1988) are each able to dominantly suppress *ago* tracheal phenotypes (Figure 2.5E, green and red bars respectively, Table 2.4). The sensitivity of *ago* phenotypes to the genetic dosage of *trh* and *btl* suggests that *ago* may inhibit Trh in the developing trachea. To test the effect of *ago* mutations on Trh protein levels, wild type and *ago* mutant embryos were stained with a Trh-specific antiserum (Figure 2.6). Compared to control embryos, *ago* mutant embryos contain significantly higher levels of Trh in all tracheal cells (Figure 2.6A,B). This effect is also evident in immunoblot analysis of Trh levels in *ago* and control embryos (Figure 2.6C). Trh protein is normally detected in the nuclei of all tracheal cells, but is specifically eliminated from fusion cells, including those of the dorsal trunk, by a mechanism that requires fusion-cell specific expression of the Dys bHLH-PAS domain

transcription factor (Figure 2.7; Jiang & Crews, 2003). In addition to limiting the steady-state levels of Trh in all tracheal cells, *ago* is also required for the Dys-stimulated elimination of Trh that occurs specifically in fusion cells (Figure 2.6D,E). Expression of Dys occurs normally in *ago* embryos (see middle panel, Figure 2.6E), but in these same cells Trh levels do not decline, and DT fusion cells with high levels of both Dys and Trh are readily observed (Figures 2.6E and 2.7). Thus, the antagonistic genetic interaction between *ago* and *trh* in the tracheal system appears to have its basis in a requirement for *ago* in limiting the steady-state levels of Trh in all tracheal cells, and in the specific elimination of Trh from fusion cells.

The effect of *ago* alleles on Trh levels, and the genetic interaction between *ago* and the Trh target gene *btl*, indicates that ectopic Trh-driven transcription of *btl* may contribute to the *ago* phenotype. The developmental regulation of the *btl* promoter is complex and involves inputs from a number of factors other than Trh, including the transcriptional activators *pointed* (Klambt, 1993; Ohshiro et al., 2002) and *ventral veinless* (Anderson et al., 1996), and the transcriptional repressors *anterior open* (Ohshiro et al., 2002) and *spalt* (Kuhnlein & Schuh, 1996). To test whether the failure to down-regulate Trh in *ago* mutant cells is sufficient to cause misexpression of *btl*, RNA *in situ* hybridization analysis was performed using a *btl*-specific anti-sense RNA probe. In stage 15 control embryos, levels of *btl* mRNA expression in the DT do not rise above the background signal obtained with *btl* anti-sense (Figure 2.8A) or sense probes. In contrast, pairs of *btl*-positive cells are evident along the DT of all *ago* mutant

embryos (Figure 2.8B; see arrows). The location and pattern of this ectopic *btl* expression suggest that these paired cells correspond to fusion cells, and that failure to eliminate Trh in these cells leads to ectopic *btl* transcription. The lack of a similar effect in the remaining *ago* mutant tracheal cells suggests that excess Trh that must collaborate with fusion-cell specific factors in order to drive ectopic *btl* transcription.

In view of the requirement for *btl* in the *ago* phenotype (see Table 2.4 and Figure 2.5B) and the finding that excess Btl activity disrupts DT architecture (see Figure 2.5B and Dammai et al., 2003; Lee et al., 1996a; Ohshiro et al., 2002), the effect of *ago* on *btl* suggests that Trh-driven transcriptional deregulation of *btl* is an important element of *ago* DT phenotype. However, while the molecular effect of *ago* inactivation on Trh and *btl* is fully penetrant, the resultant morphological defects in tracheal structure are not. This might be expected if the elevated levels of Trh and *btl* reach a threshold that is sufficient to perturb tracheal development in a portion of embryos, but that other pathways acting redundantly to *ago* are able to enforce the developmental down-regulation of the Btl pathway. If so, then *ago* mutations might be predicted to sensitize the tracheal system to other mutations that increase Btl activity by non-transcriptional mechanisms. To test this, a loss-of-function allele of the *abnormal wing discs* gene (*awd*^{j2A4}, Spradling et al., 1999), which encodes a factor that promotes the endocytic down-regulation of the Btl receptor in embryonic tracheal cells (Dammai et al., 2003), was assayed for its ability to enhance the *ago* tracheal phenotype (Figure 2.8C,D). Reducing *awd* gene dosage by half in *ago* mutant animals strongly

enhances both the penetrance (from 46% of embryos to greater than 80% of embryos; see Figure 2.8D and Table 2.5) of the DT break phenotype and its expressivity among affected embryos (from 1.2 ± 0.09 breaks/embryo [n=39] to 6.1 ± 0.95 breaks/embryo [n=41], see also Table 2.2). These *ago/ago,awd/+* embryos also show a much more severe disruption of the entire tracheal system than do *ago* mutants alone (compare Figure 2.8C to 2.2C). Moreover, a significant fraction of *ago/+,awd/+ trans*-heterozygous embryos show DT breaks. In view of the data indicating that *ago* and *awd* are both upstream of *btl* via transcriptional and endocytic mechanisms respectively, these strong synthetic effects suggest that *ago* and *awd* mutations collaborate to deregulate Btl in the developing tracheal system.

Figure 2.6. *ago* regulates Trh levels and is required for Trh elimination in tracheal fusion cells.

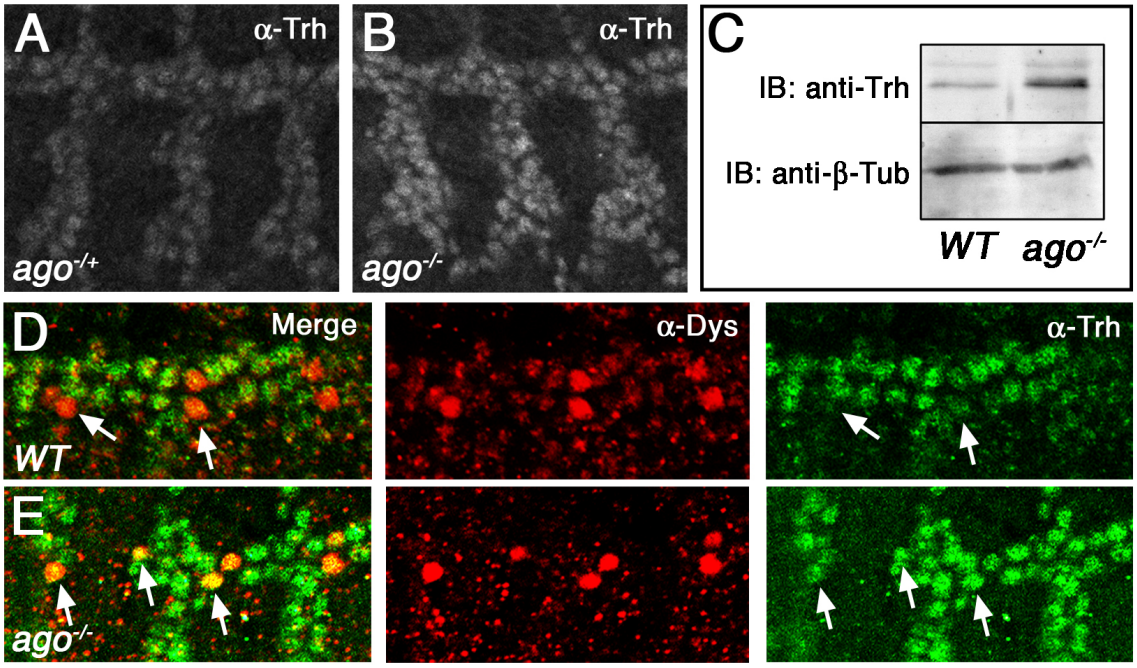

Anti-Trh staining in *ago/TM6B, P{iab-2(1.7)lacZ}6B, Tb*[1] (A) and *ago*[1]*/ago*[3] (B) embryos. (C) Anti-Trh (top) and anti-β-tub (bottom; loading control) Western blot analysis of stage 13/14 control and *ago* mutant embryos (10 embryos/lane). *WT* (D) and *ago* (E) embryos stained with anti-Trh (green, right panel) and anti-Dys (red, center panel) to mark fusion cells. Trh levels are reduced in Dys-positive wild type fusion cells (arrows in D), but not in Dys-positive *ago* mutant fusion cells (arrows in E).

Figure 2.7. Relationship between Trh and Dys levels in tracheal fusion cells.

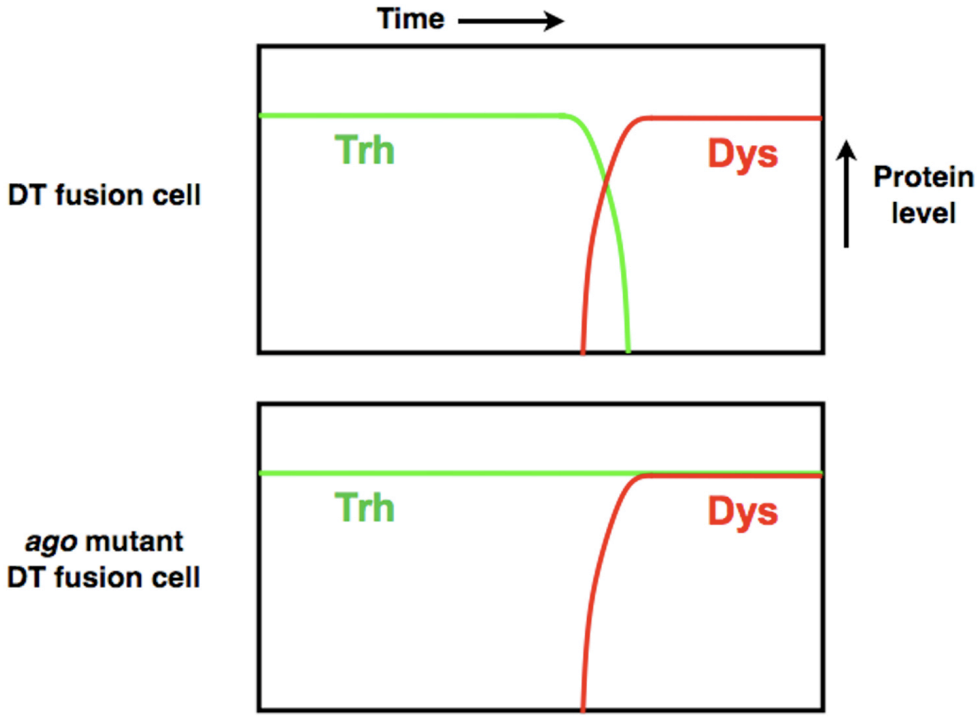

In a DT fusion cell (top), an increased level of Dys corresponds to a decrease in Trh levels. However, in *ago* mutant cells (bottom) the levels of Trh are uncoupled from the increase in Dys expression.

Figure 2.8. *btl* transcription is deregulated in *ago* mutant embryos.

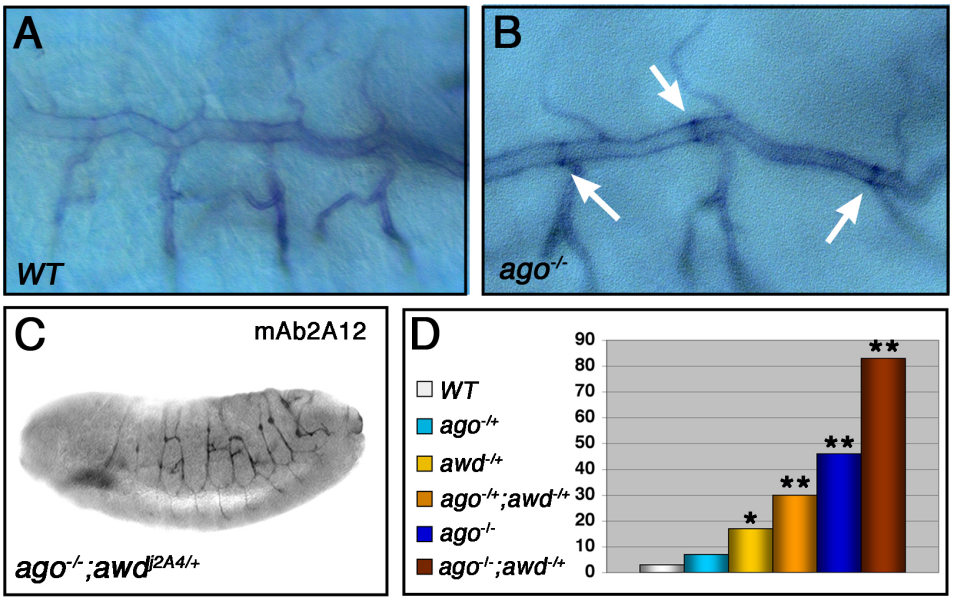

RNA in situ hybridization of *WT* (A) and *ago* (B) stage 16 embryos with *btl* anti-sense probe. Arrows in B denote *btl*-expressing cells. (C) Lateral view of a stage 15 *ago*;*awd*$^{-/+}$embryo stained with mAb2A12 showing enhanced expressivity of the *ago* mutant phenotype. (D) Quantitative summary of the DT break phenotype in stage 15 embryos of the indicated genotypes showing interactions between *ago* and *awd*.

Table 2.4. The *ago* phenotype is dominantly suppressed by alleles of FGF pathway members, and is rescued by tracheal cell specific expression of Ago

Genotype	DT Breaks (%)	n=
WT	3**	61
ago^1/ago^3	46	85
ago^1/ago^3;btl-Gal4:UAS-ago	15**	73
$ago^1/ago^3;trh^{10512}/+$	31*	135
$ago^1/ago^3;bt^{ldev1}/+$	26**	99

Penetrance of indicated phenotypes in stage 15 embryos of the indicated genotypes. * $p < 0.05$ and ** $p < 0.01$ compared to *ago*.

Table 2.5. *ago* dominantly interacts with an allele of the Btl antagonist *awd*

Genotype	DT Breaks (%)	n=
WT	3	61
$ago^{3}/+$	7	56
$awd^{j2A4}/+$	17*	42
$ago^{3},awd^{j2A4}/+$	30**	33
$ago^{3},awd^{j2A4}/ago^{1}$	83**	52

Penetrance of indicated phenotypes in stage 15 embryos of the indicated genotypes. * $p < 0.05$ and ** $p < 0.01$ compared to *WT*.

2.D. Ago binds Trh and restricts Trh levels in cells

The ability of *ago* mutations to elevate Trh levels *in vivo* and to uncouple Trh levels from the rise in Dys indicates that Ago acts downstream of Dys as part of the mechanism that eliminates Trh protein in fusion cells (Figure 2.7). To examine interactions between Ago and Trh more closely, epitope tagged versions of these proteins were co-expressed in S2 cells (Figure 2.9A,B). Analysis shows that while Trh accumulates to high levels when expressed in S2 cells, co-expression of Ago results in a subtle but reproducible reduction (~20% by density quantitation; Photoshop) in Trh levels (Figure 2.9A, top panel, lanes 1-2). This effect appears to parallel the negative effect *ago* has on Trh levels in non-fusion cells that do not normally express Dys (see Figure 2.6B). However, when Ago and Trh are co-expressed with Dys, the *in vivo* trigger of Trh down-regulation, Trh levels drop dramatically (Figure 2.9A, top panel, lane 3) in much the same way Trh levels drop in response to Dys expression *in vivo* (see Figures 2.6D, 2.7 and Jiang & Crews, 2003). The parallel decline in the level of Ago is consistent with findings that other F-box proteins are destabilized by reductions in the level of their substrates (Li et al., 2004) and mimics the relationship between dMyc and Ago stability in S2 cells (Moberg et al., 2004). Examination of the effect of Dys on Trh reveals that expression of *dys* is sufficient to decrease Trh levels in the absence of exogenous Ago (Figure 2.9B, lane 3). However, as is observed in embryonic tracheal cells (Figure 2.6E), this effect of Dys in S2 cells still requires endogenous Ago since RNAi-knockdown of *ago* is sufficient to block it (Figure 2.9B, lane 4). Addition of the proteasome inhibitor MG132 also blocks the Ago/

Dys-stimulated decline in Trh levels in S2 cells (Figure 2.9B, lane 5). In parallel to these *in vitro* effects, *btl-Gal4* mediated expression of dominant-negative alleles of the proteasome subunits *Pros26* and *Prosβ2* (Belote & Fortier, 2002) is sufficient to phenocopy *ago* alleles and block down-regulation of Trh in embryonic fusion cells (Figure 2.9C). From these data, it appears that Trh is a target of a proteosomal degradation pathway in embryonic tracheal cells and in cultured S2 cells, and that in both cases the mechanism underlying this effect requires *ago* and can be greatly potentiated by co-expression of *dys*.

The genetic and functional interactions between *ago* and *trh* suggest that their encoded products may physically interact in cells. To test this hypothesis, Flag-tagged Trh and HA-tagged versions of either wild type Ago, the AgoΔF dominant negative protein, or the truncated Ago^{1} protein (lacking an intact WD domain) were expressed in S2 cells and analyzed by co-immunoprecipitation (Figure 2.10). Wild type Ago, Ago^{1}, and AgoΔF are all recovered in anti-Flag immunoprecipitates (Figure 2.10A, lanes 2-4) and reciprocally, Flag-Trh is readily detected in anti-HA immunoprecipitates from cells expressing HA-AgoΔF (Figure 2.10B). Thus, in the absence of exogenous Dys, Trh is able to interact with all three forms of Ago in S2 cells, including the Ago^{1} WD-truncation mutant that is defective in Trh regulation *in vivo*. Co-expression of Dys with these combinations of Ago and Trh, and simultaneously blocking proteosome function so as to stabilize the Ago-Trh complex, induces a significant change in the nature of the Ago-Trh interaction (Figure 2.10C). The form of Trh protein that accumulates in MG132-treated, Dys-expressing cells remains competent to bind wild type Ago

but fails to interact with the WD-truncation mutant Ago^{1} (Figure 2.10C, top panel, compare lanes 3 and 5). Thus, an *ago* mutation that deregulates Trh levels *in vivo* is defective in binding to the form of Trh normally targeted for proteosome-dependent elimination in Dys-expressing fusion cells. Considered together, these data show that Ago and Trh can bind specifically to one another, and that this interaction is required to limit Trh levels *in vivo*.

Figure 2.9. Ago regulates Trh levels in S2 cells and during embryogenesis.

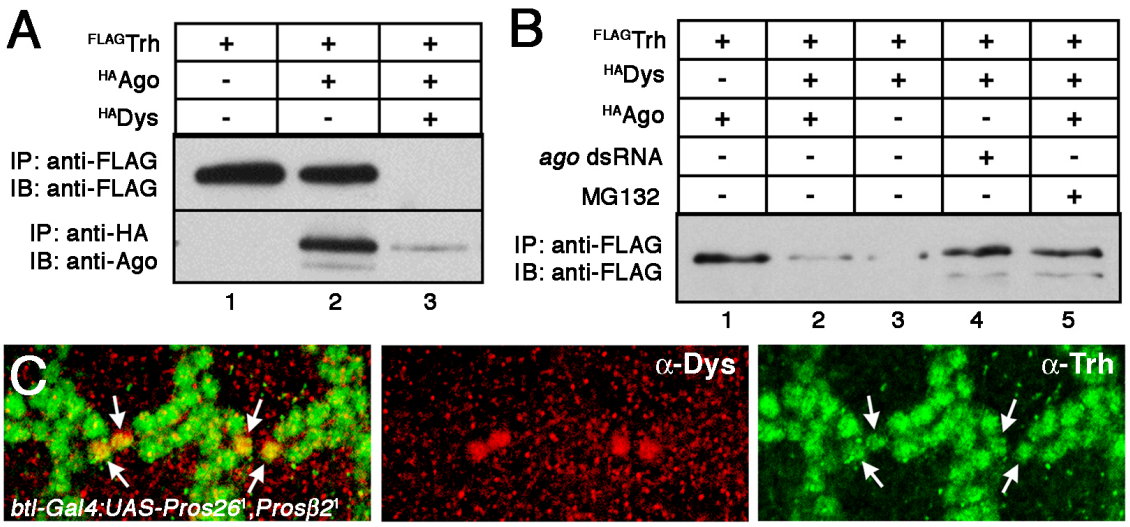

Quantification of the steady-state levels of either Trh and Ago by immunoprecipitation-immunoblot (IP/IB) from S2 cells transfected with the indicated plasmids. (A) Trh accumulates to detectable levels in S2 cells (lane 1), is slightly reduced in the presence of Ago (lane 2), and is greatly reduced after co-expression of Ago and Dys (lane 3). (B) The Dys-mediated reduction in Trh levels occurs in the absence of transfected Ago (lane 3) but is blocked by *ago* dsRNA treatment (lane 4) or by blocking proteasome function with MG-132 (lane 5). (C) Inhibition of proteasome function also stabilizes Trh levels *in vivo*. *btl-Gal4:UAS-Pros26¹,UAS-Prosβ2¹* embryos stained with anti-Trh (green, right panel) and anti-Dys (red, center panel) show a failure to down-regulate Trh levels in fusion cells (arrows).

Figure 2.10. Physical interaction between Ago and Trh.

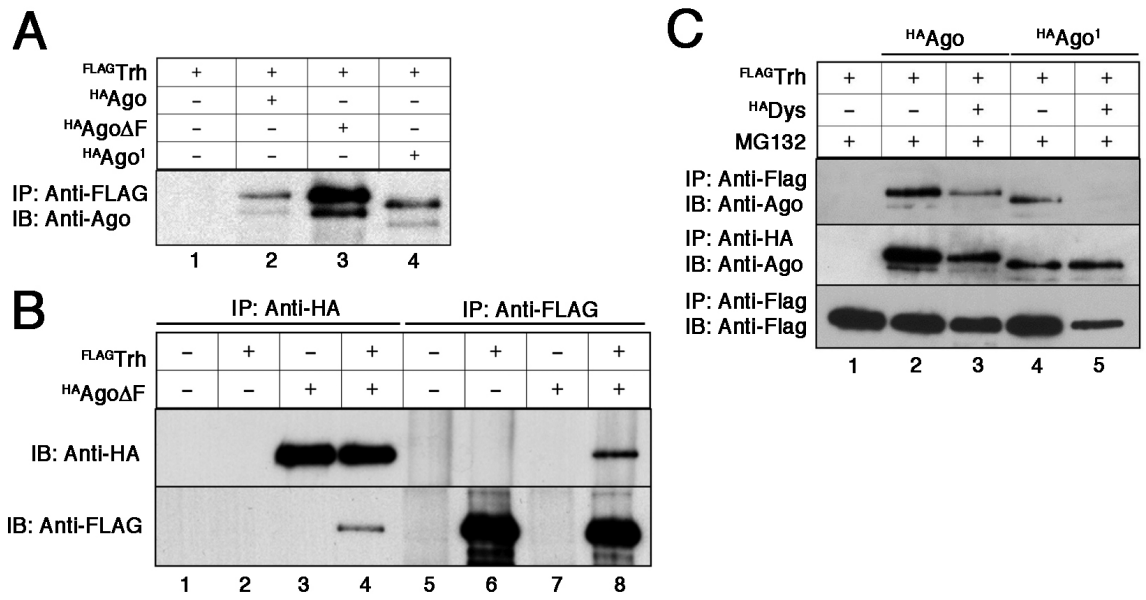

IP/IB analysis from S2 cells expressing the indicated cDNAs shows that wild type Ago, AgoΔF, and Ago^{1} are recovered in anti-Flag precipitates (A) and that Trh is reciprocally recovered in anti-HA precipitates from cells expressing AgoΔF (B). IP/IB analysis of MG132-treated cells expressing the indicated cDNAs (C) shows that Trh is bound equally well by Ago (top panel, lane 2) and Ago^{1} (top panel, lane 4) in the absence of Dys, but that in Dys-positive cells Trh is bound only by wild type Ago (top panel, lane 3) but not the Ago^{1} mutant (top panel, lane 5) that is defective in Trh regulation in vivo. Levels of Ago (middle panel) and Trh (bottom panel) are shown.

2.E. Discussion of results

The biological properties of individual F-box proteins are to a large degree determined by their repertoire of target proteins. In the case of the *Drosophila* Ago F-box protein, failure to degrade these targets promotes excess proliferation of imaginal disc cells. This observation has led to the identification of Cyclin E and Myc proteins as *ago* targets (Moberg et al., 2001; Moberg et al., 2004). However the broad pattern of Ago expression in the embryo suggests that it might regulate distinct processes and targets in other cell types. In view of the rapidly growing body of work showing that inactivation of human *ago*/*Fbw7* is a common event in a variety of cancers (e.g. Malyukova et al., 2007; O'Neil et al., 2007; Thompson et al., 2007), identification of these targets may provide important insight into the biology of cancers lacking *ago* function.

Here we show that *Drosophila* Ago is required for the post-mitotic morphogenesis of the embryonic tracheal system and that this requirement is due, at least in part, to the ability of Ago to bind directly to a previously unrecognized target, the Trh transcription factor, and stimulate its proteosomal degradation (Figure 2.11). This *ago* degradation mechanism appears to fulfill different regulatory roles in different populations of tracheal cells. In non-fusion tracheal cells, *ago* is required to limit overall levels of Trh, which is normally expressed at moderate levels throughout the tracheal system. In tracheal fusion cells the *ago* degradation mechanism appears to be strongly potentiated by an unidentified signal generated by Dys, such that Trh is completely eliminated from Dys-expressing cells. At a genetic level, the dependence of *ago* tracheal

phenotypes on *trh* gene dosage argues that elevated Trh levels are primarily responsible for branching defects that occur in *ago* zygotic mutant embryos. In support of this, persistent Trh expression is also observed in *ago* mutant fusion cells in other tracheal branches. This novel role for Ago in tracheal development is supported by the independent finding that homozygosity for a genomic deletion containing the *ago* locus is associated with cell migration defects in embryonic tracheal metameres (Myat et al., 2005).

Many important developmental events are controlled by multiple mechanisms that collaborate to regulate a key step in the process. This somewhat redundant control insulates the process from defects in any single pathway, such that major defects only occur when multiple control mechanisms are blocked. The observation that the effect of *ago* mutations on Trh and *btl* levels is completely penetrant, but the resulting morphological defects are not, suggests that another pathway acts redundantly to *ago* to control tracheal development. The strong, dominant enhancement of the *ago* phenotype by a mutation in the *awd* gene fits very well into a model in which multiple pathways are responsible for the precisely timed down-regulation of the Breathless/FGF pathway (Figure 2.11): *ago* attenuates *btl* transcription by degrading Trh, *awd* lowers levels of Btl protein on the cell surface by promoting its endocytic internalization (Dammai et al., 2003), and other pathways act independently to control expression of the FGF ligand *branchless* in non-tracheal cells (Merabet et al., 2005; Sutherland et al., 1996). Thus, the incomplete penetrance of the *ago* phenotype is not indicative of an insignificant role for the gene in tracheal

development, but rather may indicate that the tracheal system uses multiple mechanisms to redundantly control a key step in its development.

The Ago WD repeat region binds Cyclin E and dMyc, and the current work demonstrates that it also binds Trh. Broadly, the Ago-Trh interaction is quite similar to interactions with Cyclin E and dMyc: it is required for the down-regulation of substrate levels *in vivo*, and its disruption elevates levels of substrate that then drive downstream phenotypes. For substrates like Myc, site-specific phosphorylation generates a motif that binds to the Ago WD-region and stimulates rapid, SCF-mediated protein turnover of the target protein (reviewed in Minella & Clurman, 2005). In contrast, the data here suggest that Trh can physically interact with Ago in two distinct configurations: one that does not require an intact WD-domain and a second WD-dependent mode of binding. The observation that the Ago^{1} allele can participate in the first complex but not the second and is defective in Trh regulation *in vivo*, suggests that like other Ago targets, WD-dependent binding is associated with rapid Trh turnover. Expression of Dys appears to shift the balance in favor of this second mode of binding. Combined with the genetic and phenotypic data implicating *ago* as an *in vivo* regulator of Trh activity, these molecular data support a model in which Ago can bind to Trh in the absence of Dys and inefficiently stimulate Trh turnover by a WD-dependent mechanism. This inefficient mechanism may be responsible for the fairly mild increase in Trh levels observed in all *ago* mutant dorsal trunk cells. However, in the presence of Dys, the efficiency of Trh turnover in DT fusion cells is enhanced to the degree that the entire pool of Trh is rapidly eliminated.

Interestingly, the correlate of this hypothesis, that ectopic expression of *dys* in non-fusion cells should be sufficient to trigger down-regulation of endogenous Trh, was confirmed in a recent study (Jiang & Crews, 2006).

The nature of the Dys-generated signal responsible for this effect is not currently known. Precedent with other Ago targets suggests that it may involve Trh phosphorylation (Fryer et al., 2004; Koepp et al., 2001; Nateri et al., 2004; Sundqvist et al., 2005; Wei et al., 2005; Welcker et al., 2004a; Welcker et al., 2003; Yada et al., 2004; Ye et al., 2004). Recent work on the mammalian *ago* ortholog *Fbw7* has shown that interactions with substrates can also be modulated by interaction with accessory factors (Punga et al., 2006), or by conformational changes in the substrate driven by the isomerization of proline residues within the Ago/Fbw7 binding motif (Drogen et al., 2006). Proline isomerization has been implicated in the degradation of mammalian c-Myc (Yeh et al., 2004), but such mechanisms are not currently known to play a role in the degradation of either Myc or bHLH-PAS proteins in *Drosophila*. An important goal of future studies will be to determine if any of these types of mechanisms are involved in Dys-induced Trh degradation in tracheal cells.

The requirement for *ago* in tracheal cells suggests that the consequences of *ago* loss vary considerably depending on the proliferative state of the cells, their location within the organism, and their developmental stage. *ago* mutant clones in the mitotically active larval eye disc show no evidence of excessive Trh levels or deregulated Btl/FGF signaling and conversely, *ago* zygotic mutant trachea do not display ‘extra cell’ defects similar to those observed in the eye.

The origins of this tissue specificity are currently not clear, although it might simply reflect the differential expression patterns of Ago targets in various mitotic and post-mitotic cell populations. These findings confirm the hypothesis that *ago* plays a conserved role in the development of oxygen-conducting organs, demonstrating that *ago* functions to regulate oxygen homeostasis. Further work will be required to investigate other oxygen-homeostatic roles of *ago*.

[1] Mortimer, N. T. and Moberg, K. H. (2007). The Drosophila F-box protein Archipelago controls levels of the Trachealess transcription factor in the embryonic tracheal system. *Dev Biol, 312*(2), 560–571.

Figure 2.11. Model for Ago function in embryonic tracheal development.

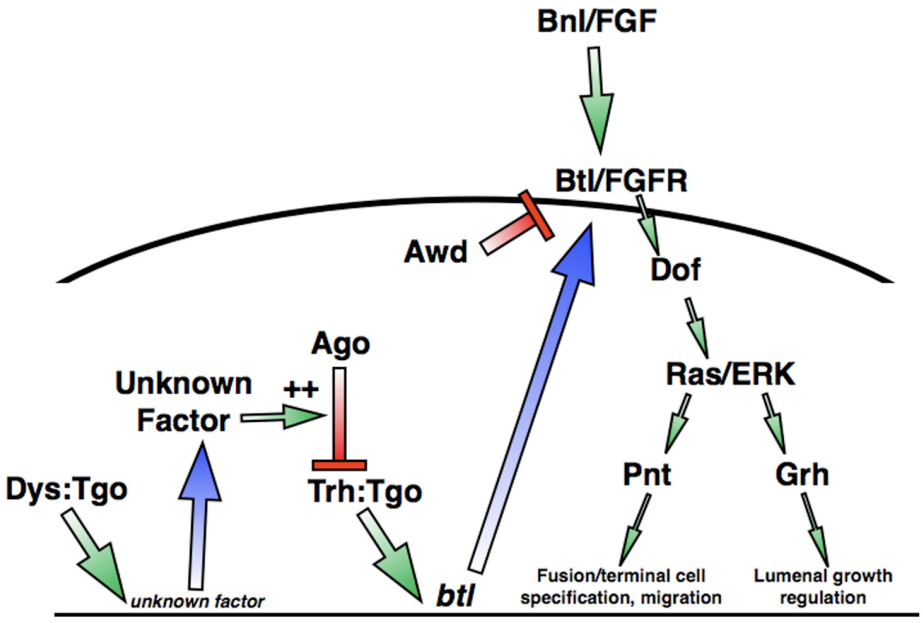

Ago acts to restrict Btl/FGF signaling via down-regulation of Trh, inhibiting Trh:Tgo-mediated transcription of *btl*. This activity of Ago is enhanced by the Dys:Tgo-mediated transcription of an unknown Trh-degradation enhancing factor, and complemented by the Awd-mediated internalization and degradation of the Btl/FGFR protein.

Chapter Three: Regulation of *Drosophila* embryonic tracheogenesis by *dVHL* and hypoxia[2]

3.A. Introduction

The development and survival of an organism are dependent on its ability to adapt to changing environmental conditions. Responses to some environmental changes, for example in nutrient availability, temperature, or oxygen concentration, involve alterations in patterns of gene expression that allow the organism to survive periods of environmental stress. In metazoan cells, the cellular response to reduced oxygen is mediated primarily by the HIF (hypoxia inducible factor) family of transcription factors, which are heterodimers composed of α and β subunits belonging to the bHLH Per-ARNT-Sim (bHLH-PAS) protein family (reviewed in Kaelin & Ratcliffe, 2008). The HIF-1 αβ heterodimer is the primary oxygen-responsive HIF in mammalian cells and binds to a specific DNA sequence termed hypoxia response element (HRE) present in the promoters of target genes involved in energy metabolism, angiogenesis, erythropoiesis, and autophagy (Manalo et al., 2005). HIF-1 activity is inhibited under normoxic conditions by two hydroxylase enzymes that use dioxygen as a substrate for catalysis to hydroxylate specific proline or aspartate residues in the HIF-1α subunit (reviewed in Kaelin & Ratcliffe, 2008). These modifications limit HIF-1 activity by either reducing HIF-1α levels or inhibiting its ability to activate HRE-containing target promoters. One of these inhibitory mechanisms involves the 2-oxoglutarate/Fe(II)-dependent HIF-1 prolyl hydroxylase (HPH), which attaches a hydroxyl group onto each of two conserved proline residues in the oxygen-dependent degradation domain (ODD) of mammalian HIF-1α. These modifications create a binding site in the HIF-1α ODD for the Von Hippel-Lindau

(VHL) protein, the substrate adaptor component of a ubiquitin ligase that subsequently polyubiquitinates HIF-1α and targets it for degradation by the proteasome (reviewed in Kaelin, 2005). This degradation mechanism operates constitutively in normoxia and is epistatic to otherwise wide spread expression of HIF-1α mRNA. HIF-1α protein is also modified by a second oxygen-dependent hydroxylase termed Factor Inhibiting HIF (FIH) that hydroxylates an asparagine residue in the HIF-1α C-terminal activation domain (reviewed in Kaelin, 2005). This blocks interaction with the CBP/p300 transcriptional co-factor and thus further restricts expression of HIF-1 responsive genes. These parallel oxygen-dependent hydroxylation mechanisms by HPH and FIH ensure that HIF-1α levels and activity remain low in normoxic conditions. However as oxygen levels become limiting in the cellular environment, rates of hydroxylation decline and HIF-1α is rapidly stabilized in a form that dimerizes with HIF-1β, translocates to the nucleus, and promotes transcription of HRE-containing target genes.

Evidence suggests that invertebrate homologs of HIF-1 are also regulated in response to changes in oxygen availability (reviewed in Gorr et al., 2006). In the fruit fly *Drosophila melanogaster*, the HPH homolog *fatiga* (*fga*) has been shown to genetically antagonize the HIF-1α homolog *similar* (*sima*) during development (Centanin et al., 2005). The *Drosophila* VHL protein (dVHL) has also been shown to be capable of binding to human HIF-1α and stimulating the proteosomal turnover in vitro (Aso et al., 2000). In addition, the *Drosophila* genome encodes a well-characterized HIF-1β homolog *tango* (*tgo*, Sonnenfeld et al., 1997), and two potential FIH homologs (*CG13902* and *CG10133*; Berkeley

Drosophila Genome Project) that have yet to be analyzed functionally. Spatiotemporal analysis of *sima* activation using *sima*-dependent hypoxia-reporter transgenes has shown that exposure to an acute hypoxic stress induces Sima most strongly in cells of the larval and embryonic tracheal system (Arquier et al., 2006; Lavista-Llanos et al., 2002), while induction of reporter activity in other tissues requires more chronic exposure to low oxygen (Lavista-Llanos et al., 2002). The larval tracheal system is composed of an interconnected network of polarized, epithelial tubes that duct gases through the organism (reviewed in Ghabrial et al., 2003). As the trachea acts as the primary gas-exchange organ in the larva, it is thus a logical site of hypoxia sensitivity. During larval stages, specific cells within the tracheal system called 'terminal cells' respond to hypoxia by initiating new branching and growth that results in the extension of fine, unicellular, gas-filled tubes toward hypoxic tissues in a manner somewhat analogous to mammalian angiogenesis (Guillemin et al., 1996; Jarecki et al., 1999). Studies have shown that *sima* and its upstream antagonist *fga* function within terminal cells to regulate this process (Centanin et al., 2008). *sima* is necessary for terminal cell branching in hypoxia and its ectopic activation, by either transgenic overexpression or loss of *fga*, is sufficient to induce excess branching even in normoxia. These phenotypes have been linked to the ability of *sima* to promote expression of the *breathless* (*btl*) gene (Centanin et al., 2008), which encodes an FGF receptor (Klambt et al., 1992) that is activated by the *branchless* (*bnl*) FGF ligand (Sutherland et al., 1996). This receptor/ligand pair is known to act via a downstream MAP-kinase signaling cascade to promote cell

motility and tubular morphogenesis in a variety of systems (reviewed in Lubarsky & Krasnow, 2003). Excessive activation of this pathway within tracheal cells by transgenic expression of *btl* is sufficient to drive excess branching (Chapter 2 and Lee et al., 1996a). Reciprocally, misexpression of the *bnl* ligand in certain peripheral tissues is sufficient to attract excess terminal cell branching (Jarecki et al., 1999). Indeed production of secreted factors such as Bnl may be a significant part of the physiologic mechanism by which hypoxic cells attract new tracheal growth. Sima-driven induction of *btl* in conditions of hypoxia thus allows larval terminal cells to enter what has been termed an 'active searching' mode (Centanin et al., 2008) in which they are hyper-sensitized to signals emanating from nearby hypoxic non-tracheal cells.

The role of the *btl/bnl* pathway in tracheal development is not restricted to hypoxia-induced branching of larval terminal cells. It also plays a critical, earlier role in the initial development of the embryonic tracheal system from the tracheal placodes, groups of post-mitotic ectodermal cells distributed along either side of the embryo that undergo a process of invagination, polarization, directed migration, and fusion to create a network of primary and secondary tracheal branches (reviewed in Ghabrial et al., 2003). *btl* and *bnl* are each required for this process via a mechanism in which restricted expression of *bnl* in cells outside the tracheal placode represents a directional cue for the migration of *btl*-expressing cells within the placode. Accordingly, *btl* expression is normally highest in pre-migratory and migratory embryonic fusion cells (Ohshiro & Saigo, 1997). In contrast to the larval hypoxic response, *sima* does not appear to be required for

morphogenesis of the embryonic tracheal system (Ohshiro & Saigo, 1997). Rather, developmentally programmed signals in the embryo dictate a stereotyped pattern of *btl* and *bnl* expression that leads to a similarly stereotyped pattern of primary and secondary tracheal branches (Centanin et al., 2008). The *btl/bnl* pathway thus responds to developmental signals to drive a fixed pattern of branching in the embryo, while in the subsequent larval stage it responds to hypoxia-dependent *sima* activity to facilitate the homeostatic growth of larval terminal cells and tracheal remodeling.

Under normal circumstances, developing *Drosophila* tissues do not begin to experience hypoxia until the first larval stage, when organismal growth and movement begin to consume more oxygen than can be provided by passive diffusion alone (Romero et al., 2007). As a consequence, the first hypoxic challenge normally occurs after the *btl/bnl*-dependent elaboration of the primary and secondary embryonic branches is complete. Thus, the ability of the larval tracheal system to drive new branching and remodeling via *sima* and *btl* represents the response of a developed 'mature' tracheal system to reduced oxygen availability. By contrast the effect of hypoxia on embryonic tracheal development, which requires tight spatiotemporal control of Btl signaling to pattern the tracheal network, is not as well understood. Given that the trachea does not function as a gas exchange organ until after fluid is cleared from the tubes at embryonic stage 17 (Tsarouhas et al., 2007), it may be that the transcriptional response of embryonic tracheal cells to hypoxia (Lavista-Llanos et al., 2002) leads to mainly metabolic changes rather than to a *btl*-driven program

of tubulogenesis and remodeling. However, if the embryonic tracheal system does utilize the *sima* pathway to induce hypoxia-dependent changes in *btl* gene transcription, then hypoxic exposure of embryos might be predicted to produce a situation of competing developmental and homeostatic inputs that converge on the *btl/bnl* pathway. The ability of tracheal cells to integrate such signals may then determine whether or not the embryonic tracheal system is able to adapt to oxygen stress, or whether embryonic tracheal development represents a sensitive period during which the organism's ability to respond to changes in oxygen levels is inherently limited by a pre-programmed pattern of developmental gene expression.

Here we show that the embryonic tracheal system utilizes the *dVHL/sima* pathway to respond to hypoxia, but that the type and severity of resulting phenotypes depend on the developmental stage of exposure. Hypoxic challenge while embryonic tracheal cells are responding to developmentally programmed *btl/bnl* migration signals disrupts tracheal development and results in fragmented and unfused tracheal metameres. In contrast, hypoxic challenge at a somewhat later embryonic stage after fusion is complete results in overgrowth of the primary tracheal branches and the production of extra secondary branches. Interestingly, we find that the threshold of hypoxia required to induce tracheal phenotypes in the early embryo is higher than that required to induce excess branching phenotypes in later embryonic stages, indicating that tracheal patterning events in the embryo are relatively resistant to hypoxia. Genetic analysis indicates that both types of hypoxic tracheal phenotypes – stunting and

overgrowth – require *sima* and can be phenocopied in normoxia by reducing expression of the HIF-1α ubiquitin ligase gene *dVHL* specifically within tracheal cells. Moreover, we find that reduced *dVHL* expression in the larval trachea leads to excess terminal cell branching in a manner quite similar to that observed in *fga* mutants. Molecular and genetic data indicate that excess *btl* transcription is a major cause of hypoxia-induced tracheal phenotypes. Consistent with this, mutations in the *archipelago* (*ago*) gene, which antagonizes *btl* transcription in tracheal fusion cells, synergize strongly with *dVHL* inactivation to disrupt tracheal migration and branching. Interestingly, *ago* mutations also lower the threshold of hypoxia required to elicit tracheal phenotypes in the 'early' embryo, suggesting that the relative activity of the *btl* promoter can affect hypoxic sensitivity. These findings show that the *dVHL/sima* pathway plays an important role in tracheal development, and identify two distinct phases of embryonic development that show different phenotypic outcomes of activating this pathway: an early phase during which *sima* activity conflicts with developmental control of tracheal branching and migration, and a later phase during which the tracheal system uses the *dVHL/sima/btl* pathway to adapt to hypoxia by increasing its future capacity to deliver oxygen to target tissues.

3.B. Stage-specific effects of hypoxia on embryonic tracheogenesis

To determine how the embryonic tracheal system responds to hypoxia, wild type embryos were placed in a reduced oxygen environment according to the scheme depicted in Figure 3.1A. Two different hypoxic treatments were used: 0.5% O_2 for 5 hours, or 1% O_2 for 4 hours. In one set of embryos (denoted 'early'), hypoxic treatment was initiated at stage 11 (6-8 hrs after egg laying; AEL) when dorsal trunk (DT) branches are actively migrating, and in the other (denoted 'late') it was initiated at stage 15 (13-15 hrs AEL) when DT fusion is complete. Following these treatments, embryos were returned to normoxia (21% O_2) and allowed to develop to embryonic stage 16, at which time tracheal architecture was visualized with the mAb2A12 tracheal lumen antibody (Figure 3.1B-F). As has been described elsewhere (DiGregorio et al., 2001; Douglas et al., 2001), embryonic development was arrested by the stronger 0.5% O_2 treatment but resumed upon re-exposure to normoxia. The weaker hypoxic treatment only led to a slight delay in embryonic development. With very high penetrance (Figure 3.1G and Tables 3.1 and 3.2), 'early' exposure to 0.5% O_2 severely stunted DT branch formation and fusion such that adjacent metameres appear as unconnected lumenal fragments (Figure 3.1C). Structures that form after DT fusion, for example the lateral trunk (LT), were less severely affected. At an organismal level, 'early' hypoxia also resulted in complete lethality prior to hatching. In contrast to the stunting effect of 'early' hypoxia on tracheal growth, 'late' exposure to 0.5% O_2 induced a convoluted tube overgrowth phenotype throughout the tracheal system (Figure 3.1D) at high penetrance (Figure 3.1G

and Tables 3.1 and 3.2). A similar hypoxia-induced tube overgrowth phenotype has been reported previously (Arquier et al., 2006). The major primary and secondary branches of these embryos are highly convoluted and sinuous, and show visceral branch (VB) and dorsal branch (DB) duplications (Figure 3.1E,F). Unlike the 'early' 0.5% O_2 treatment, these 'late' embryos showed no significant reduction in organismal viability. Interestingly, when these experiments were repeated under the weaker hypoxic condition of 1% O_2, the overall penetrance of tracheal phenotypes in 'early' embryos dropped considerably (from 97% [n=27] to 12% [n=42]; see Table 3.1) while the penetrance of tracheal overgrowth in 'late' embryos remained quite high (Figure 3.1G and Table 3.1). However, comparing DT length in 'late' embryos exposed to 1% or 0.5% O_2 (Figure 3.1H) reveals a progressive increase in tube length relative to normoxic controls (21 ± 1.1% longer in 1% O_2 [n=4] and 46 ± 3.1% longer in 0.5% O_2 [n=4]). Thus stronger hypoxic challenges produce a progressively stronger tracheal growth phenotype in the 'late' embryo. Overall, these patterns of tracheal sensitivity to 'early' and 'late' hypoxia suggest that hypoxic activation does not always lead to tracheal overgrowth, but can in fact also stunt tracheal branching during a specific window of 'early' embryonic development. However, the 'early' embryonic tracheal system is relatively resistant to these effects, while the 'late' embryonic tracheal system is sensitized to graded activation of the hypoxic response pathway.

To test whether *sima* is responsible for both 'early' and 'late' hypoxic tracheal phenotypes, embryos homozygous for the $sima^{07607}$ loss-of-function allele (Centanin et al., 2005) were exposed to the 'strong' 0.5% O_2 hypoxic

challenge at ‘early’ and ‘late’ time points. In both cases lack of wild type *sima* strongly suppressed the penetrance of the hypoxia-induced tracheal phenotypes (Figure 3.1G and Table 3.1), indicating that activation of the *sima* hypoxia response pathway in early stage embryos blocks tracheal cell migration and fusion, while in later stage embryos it promotes tracheal overgrowth and excess secondary branching.

Figure 3.1. Tracheal morphogenesis defects following exposure to hypoxia.

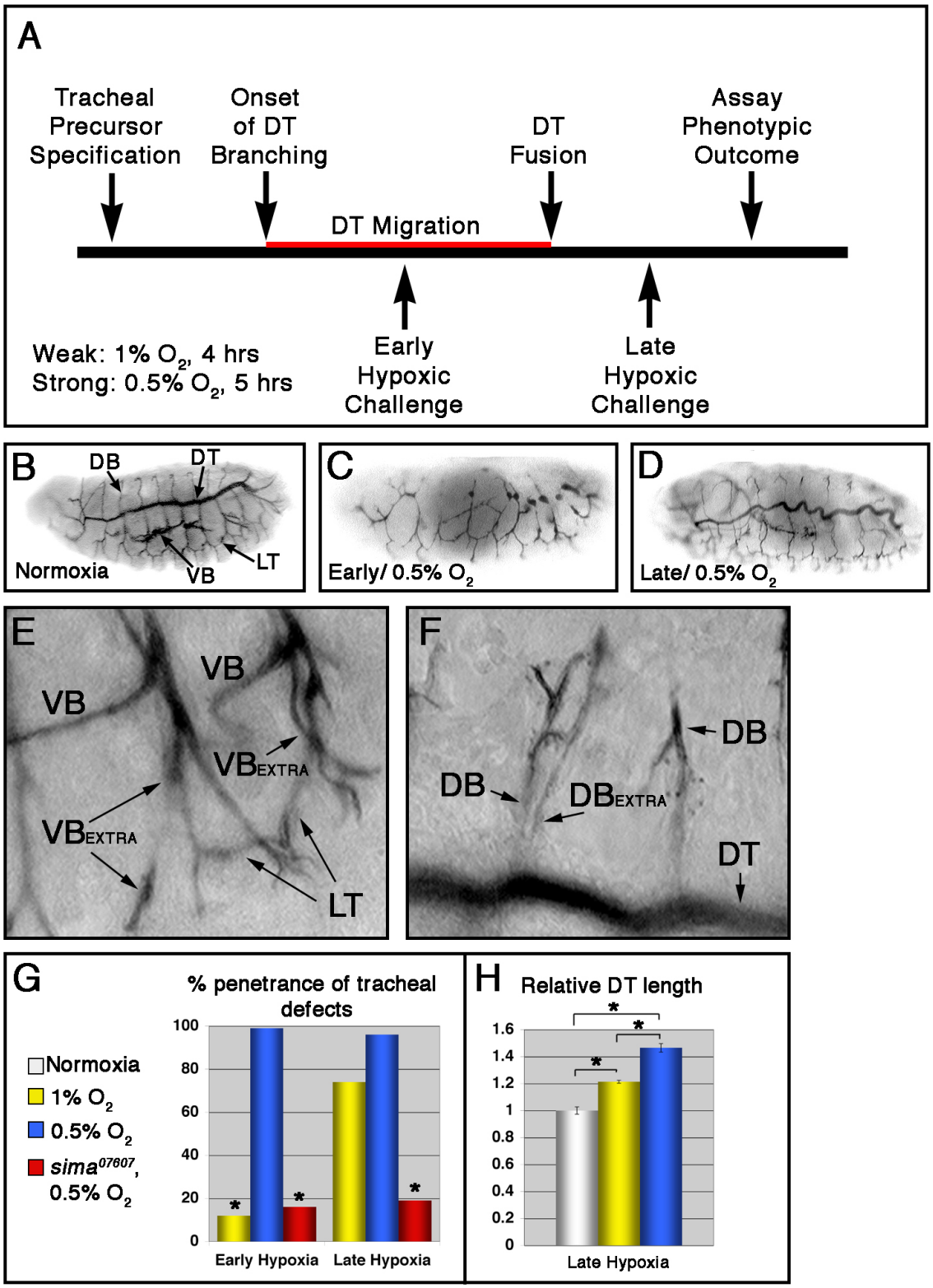

(A) Schematic representation of severity and timing of hypoxic challenges, relative to migration of dorsal trunk (DT) fusion cells (in red). (B-F) Lateral images of w^{1118} embryos stained with the tracheal lumen marker mAb2A12. Unless otherwise indicated, embryos are shown anterior left, and dorsal up. (B) Tracheal architecture of a normoxic embryo. The DT, dorsal branches (DBs), lateral trunk (LT) and visceral branches (VBs) are indicated. (C-F) Hypoxia treated embryos showing characteristic phenotypes following exposure to 0.5% O_2. (C) Early hypoxic exposure leads to defects in tracheal morphogenesis. (D) Sinuous overgrowth seen following late hypoxic exposure. (E,F) Late hypoxic exposure also causes duplications of the (E) VB and (F) DB within given segment. 'Extra' branches are indicated. (G) Quantification of penetrance of tracheal defects in the indicated hypoxic conditions and genotypes (* $p < 0.001$ relative to w^{1118} embryos in 0.5% O_2 [blue bars]). (H) Quantification of DT length in the indicated hypoxic conditions relative to normoxic control, showing a graded hypoxic response (* $p < 0.005$; error bars are ± standard error of the mean [SEM]).

Table 3.1. Hypoxia-induced embryonic tracheal phenotypes

Genotype	Total penetrance (%)	Migration defects (%)	n=
Normoxia			
WT	9	3	61
0.5% O_2			
WT, stage 11	99	86	45
sima^{07607}, stage 11	16*	8*	39
WT, stage 15	97	0	27
sima^{07607}, stage 15	19*	0	26
1% O_2			
WT, stage 11	12	5	42
ago^{3}*/+*, stage 11	41**	9	58
WT, stage 15	74	0	34
ago^{3}*/+*, stage 15	71	0	35

* $p < 0.01$ relative to *WT*: 0.5% O_2, ** $p < 0.01$ relative to *WT*: 1% O_2

Table 3.2. Tracheal RNAi phenotypes

Genotype	Total penetrance (%)	Migration defects (%)	n=
btl-Gal4:UAS-Adf1^{RNAi}	15	10	59
btl-Gal4:UAS-pigeon^{RNAi}	16	8	25
btl-Gal4:UAS-dVHL^{i4B2}	60*	16	32
btl-Gal4:UAS-dVHL^{i11A2}	50*	18	34
btl-Gal4:UAS-dVHL^{i34B3}	68*	32*	48
btl-Gal4:UAS-dVHL^{i4B6}	54*	33*	33
btl-Gal4:UAS-dVHL^{i31A2}	61*	38*	40
actin-Gal4:UAS-dVHL^{i34B3}	48*	24	29

* $p < 0.01$ relative to *btl-Gal4:UAS-Adf1^{i}*

3.C. *dVHL* is required to suppress the tracheal hypoxic response

By analogy to mammalian HIF-1α, dVHL-dependent degradation is predicted to be one of the major mechanisms that restricts *sima* activity in normoxia. Indeed analysis of *fga* mutants suggests that preventing dVHL from acting on Sima protein specifically within larval tracheal cells is a required element of the organismal response to hypoxia (Centanin et al., 2008). To explore its possible role in regulating the embryonic hypoxic response, *dVHL* expression was assayed during embryogenesis by reverse transcriptase-PCR (RT-PCR, Figure 3.2A). *dVHL* is expressed throughout embryonic development, beginning prior to the onset of tracheal development (stages 1-8, Figure 3.2A lane 1) and continuing throughout early (stages 9-11), mid (stages 12-14) and late (stages 15-17) tracheogenesis (Figure 3.2A lanes 2-4, respectively), with an apparent expression peak during mid tracheogenesis. This is consistent with a requirement to regulate *sima*, which is ubiquitously expressed during embryogenesis (Nambu et al., 1996).

However, testing the role of *dVHL* is complicated by the lack of available *dVHL* genomic alleles. Consequently we used a transgenic RNA interference (RNAi) approach to test the role of *dVHL* in tracheal morphogenesis. A *dVHL* RNAi transgene was constructed by inserting a DNA fragment corresponding to the single *dVHL* exon into the *pSymp* vector (Giordano et al., 2002). Flanking *UAS* sites allow for Gal4-driven production of a *dVHL* dsRNA that is processed by the Drosha/Dicer pathway into small interfering RNAs (Kim et al., 2006b). Multiple *UAS-dVHL*^{i} lines were generated and tested for knockdown efficiency by

Western blot of dVHL protein in animals expressing the ubiquitous 'driver' *actin-Gal4* (Figure 3.2B). A range of knockdown efficiencies was observed, ranging from strong (line *i31A2*) to mild reduction (lines *i11A2* and *i34B3*) of dVHL protein levels (Figure 3.2B).

To determine what role *dVHL* plays in embryonic tracheal development, *UAS-dVHL^{i}* transgenes were expressed in embryos using either the ubiquitous *actin-Gal4* driver or the tracheal cell-specific *btl-Gal4* driver (Shiga et al., 1996). Because each had a similar effect on tracheal patterning (Table 3.2), *btl-Gal4* was used for subsequent experiments. All *dVHL^{i}* lines had effects on tracheal development that were not observed in control embryos expressing RNAi against the neuronal genes *Adf1* or *pigeon* (Figure 3.2C and Table 3.2) or in embryos expressing *dVHL^{i}* in non-tracheal tissue with the *en-Gal4* driver. Expression of the strongest *dVHL^{i}* line, *i31A2*, produced migration defects in a significant percentage of embryos (Figure 3.2D) that resemble the effect of 'early' hypoxic challenge on DT migration, but are more severe in that they also include defective DB/VB migration and interruptions of the LT. Examination of a fusion cell marker (*esg-lacZ*) in this background reveals proper specification of fusion cells in segments with migration defects, suggesting that these defects are independent of fusion cell specification (Figure 3.2K-M). By contrast, expression of the more mild *dVHL^{i}* knock-down lines leads to an intermediate phenotype characterized by fewer migration and fusion defects per embryo, particularly in the DT and LT (Figure 3.2E), and sinuous overgrowth of the primary and secondary branches that resembles the 'late' response to hypoxia (Figure 3.2F).

dVHL knockdown also produces overgrown and intertwined secondary branches (Figure 3.2G,H) and secondary branch duplication (Figure 3.2J) similar to that observed in wild type embryos exposed to 'late' hypoxia (see Table 3.3 for a summary of embryonic phenotypes). In all combinations of *btl-Gal4* driver and *UAS-dVHL^{i}* transgene, a majority of animals develop through larval stages and die as pupae (see Section 3.D), indicating that persistent knockdown of *dVHL* in tracheal cells eventually leads to organismal death. This pupal lethality is specific to tracheal expression and is not seen in pupae expressing *dVHL^{i}* with the *en-Gal4* or *GMR-Gal4* drivers. During the 3rd instar, these larvae show increases in thick terminal branches (TTBs; Figure 3.3A,C) that can be phenocopied by exposing larvae to 1% O_2 (Figure 3.3B; TTBs quantified in Table 3.4 as in Centanin et al., 2008) They also show duplication of larval tertiary branches (see LG branches in Figure 3.3E), and failure of lateral trunk fusion associated with cells terminating in multiple, fine extensions (Figure 3.3F). *dVHL* is thus required within tracheal cells to pattern embryonic and larval tracheal development, and loss of the gene in these cells is sufficient to mimic the systemic effect of hypoxia on the embryonic and larval tracheal systems.

Figure 3.2. Tracheal specific knockdown of *dVHL* leads to defects in embryonic tracheal morphogenesis.

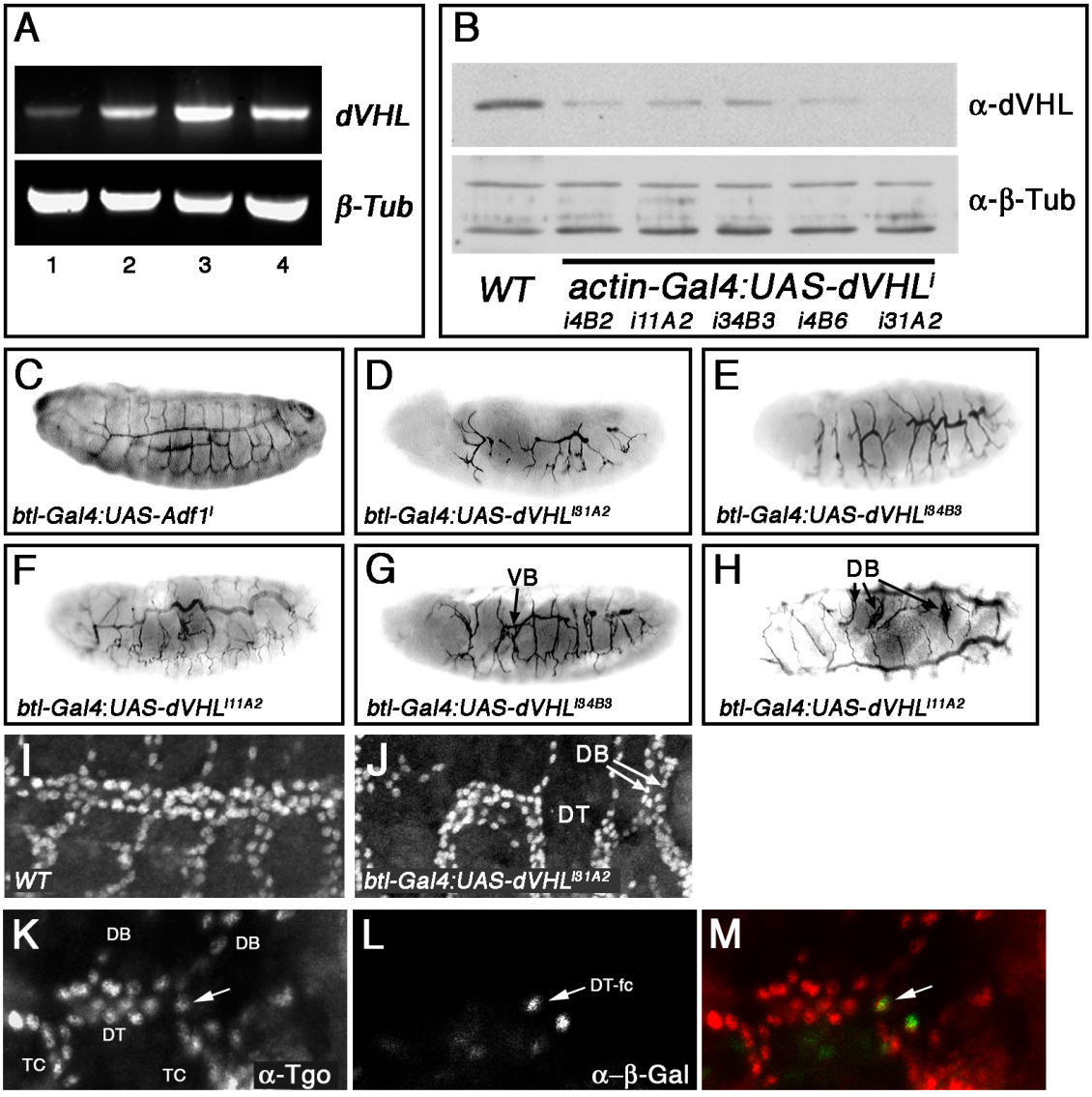

esg-lacZ; btl-Gal4:UAS-dVHL^{i31A2}

(A) RT-PCR analysis of *dVHL* (top) and *β-tubulin* (bottom) expression during embryonic stages 1-8 (lane 1), 9-11 (lane 2), 12-14 (lane 3) and 15-17 (lane 4). (B) Western blot analysis of dVHL (top panel) levels in whole embryo extracts from stage 13-16 control embryos (*WT*) and embryos expressing the indicated combination of *actin-Gal4* and *UAS-dVHL^{i}* lines. α-β-Tubulin is used a loading

control (bottom panel). (C-G) Lateral and (H) dorsal images of embryos stained with the tracheal lumen marker mAb2A12. (C) Normal tracheal architecture in a *btl-Gal4-UAS-Adf1* control RNAi embryo (D-F) Embryos of the indicated genotypes showing the range of tracheal defects seen following *btl-Gal4:UAS-dVHL^{i}* knockdown. (G,H) *btl-Gal4* driven *dVHL* knockdown also causes duplications of (G) VBs and (H) DBs as indicated. (I,J) Lateral images of (I) *w^{1118}* and (I) *btl-Gal4:UAS-dVHL^{i31A2}* embryos stained with α-Tgo to mark tracheal cells. (J) Magnified view of a *dVHL^{i}* embryonic trachea showing DT interruption, and missing (asterisk) or duplicated (arrows) DBs. (K-M) Lateral images of a stage 15 *esg-lacZ; btl-Gal4:UAS-dVHL^{i31A2}* embryo stained with (K) α-Tgo t mark tracheal cells and (L) α-β-Gal to mark *esg*-positive fusion cells. Tracheal branches and DT fusion cell are labeled. An *esg*-positive fusion cell from a misrouted secondary branch is also visible.

Figure 3.3. Tracheal cell specific *dVHL* knockdown causes defects in terminal cell branching and larval tracheal morphology.

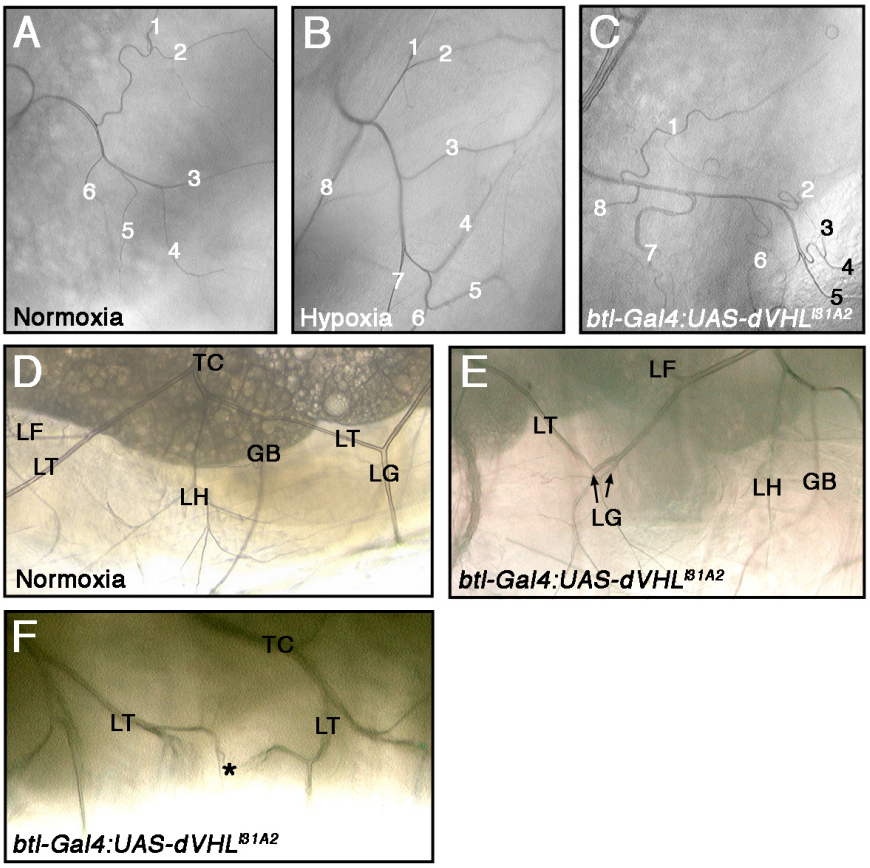

(A-C) Bright-field dorsal images of third instar larvae showing ramified branches of a dorsal branch terminal cell from tracheal segment 3 (Tr3). Thick terminal branch (TTB) number is increased by (B) exposure to 1% O_2 or (C) *btl-Gal4* driven expression of *UAS-dVHL^{i31A2}*. (D-F) Lateral images of third instar larvae. (D) Image of a single segment from a normoxic larva. The ganglionic branch (GB), transverse connective (TC), lateral trunk (LT), and LT terminal cells LF, LG and LH are indicated. *btl-Gal4:UAS-dVHL^{i31A2}* expression leads to duplications of lateral trunk terminal cells. (E) Two LG branches are indicated. (F) *btl-Gal4* driven

dVHL^{i31A2} knockdown also causes defects in migration/fusion of secondary branches. The LT branches from adjacent placodes should fuse at the point indicated by the asterisk, but instead fail to fuse leading to the ramification of multiple fine tracheal branches.

Table 3.3. Breakdown of embryonic phenotypes

Genotype	Migration defects	Tracheal convolutions	Duplicated / missing	n=
w^{1118}	3%	7%	0%	61
w^{1118}: Early, 0.5% O_2	86%	13%	0%	45
w^{1118}: Late, 0.5% O_2	0%	71%	26%	27
btl-Gal4:UAS-Adf1^{RNAi}	10%	5%	0%	59
btl-Gal4:UAS-pigeon^{RNAi}	8%	8%	0%	25
btl-Gal4:UAS-dVHL^{i4B2}	16%	44%	31%	32
btl-Gal4:UAS-dVHL^{i11A2}	18%	33%	ns	34
btl-Gal4:UAS-dVHL^{i34B3}	32%	33%	15%	48
btl-Gal4:UAS-dVHL^{i4B6}	33%	21%	ns	33
btl-Gal4:UAS-dVHL^{i31A2}	38%	23%	ns	40

ns: not scored

Table 3.4. Larval TTB phenotypes

Genotype	# of TTBs (per Tr3 DB)	n=
w^{1118}:normoxia	5.1	21
w^{1118}:hypoxia	7.4*	22
btl-Gal4/+	5.3	23
btl-Gal4:UAS-dVHL^{i31A2}	7.4**	24
btl-Gal4:btl^{EY01638}	7.2**	24
btl-Gal4:UAS-agoΔF	5.5	16
btl-Gal4:UAS-dVHL^{i31A2}*,UAS-agoΔF*	6.9**	22

* $p < 0.01$ relative to *w*^{1118}:normoxia, **$p < 0.01$ relative to *btl-Gal4/+*

3.D. *dVHL* genetically antagonizes *sima* in the embryonic trachea

Stronger *dVHL* knock-down correlates with more disruptive effects on primary and secondary branch migration and fusion in a manner similar to 'early' hypoxia, while less efficient knockdown produces a higher penetrance of tracheal overgrowth and excess branching in a manner similar to 'late' hypoxia. Given the graded tracheal phenotypes produced by 0.5% and 1% O_2 exposure, this range of $dVHL^i$ phenotypes seems very likely to reflect variable efficiency of dVHL knockdown. These data thus suggest that chronic activation of *sima* in the embryonic tracheal placodes impairs subsequent tracheal migration and fusion events, while more mild activation of *sima* leads to excess tracheal cell branching and growth later in embryonic development. Analysis of tracheal architecture in *btl-Gal4,UAS-sima* embryos confirms that overexpression of exogenous *sima* is sufficient block placode branching and migration in the embryo (Figure 3.4). To test whether endogenous *sima* is in fact required to promote both types of $dVHL^i$ tracheal phenotypes, the *btl-Gal4* driver was used to drive the $dVHL^i$ lines in the tracheal systems of $sima^{07607}/+$ or $sima^{07607}/sima^{07607}$ embryos (Figure 3.5), which can survive up to and through the pupal phase (Centanin et al., 2005) and our observations). Initial analysis was performed on multiple $dVHL^i$ lines, all of which gave a similar result (Figure 3.5A). As expected based on the evolutionarily conserved relationship between VHL and HIF-1α, removing one copy of *sima* significantly reduced the penetrance of $dVHL^{i34B3}$ tracheal phenotypes, from 68% (n=48) to 24% (n=53; Figure 3.5A and Table 3.5). Moreover, removing the remaining wild type copy of *sima* further suppressed the

frequency of *dVHL*^{i34B3} tracheal phenotypes to background levels equivalent to that seen in control *btl-Gal4,UAS-Adf1*^{i} RNAi embryos, indicating that *sima* is absolutely required for *dVHL*^{i} tracheal phenotypes. Reducing *sima* gene dosage by half is also sufficient to completely suppress the pupal lethality of the *btl-Gal4,UAS-dVHL*^{i34B3} genotype back to adult viability (Figure 3.5B and Table 3.6). Heterozygosity for a genomic deletion removing the *sima* locus (*Df(3R)BSC502*) is also sufficient to suppress *dVHL*^{i34B3} pupal lethality (Figure 3.5B and Table 3.6) suggesting the ability of the *sima*^{07607} allele to suppress *dVHL*^{i} phenotypes is due to loss of *sima* rather than some cryptic mutation in the genetic background. These strong genetic interactions between *dVHL* and *sima* validate the specificity of the *UAS-dVHL*^{i} system as a technique to antagonize dVHL activity in vivo, and indicate that *sima* is a major effector of the morphological changes that occur in the embryonic tracheal system in response to either reduced oxygen availability or loss of *dVHL*.

Figure 3.4. Transgenic over-expression of *sima* in tracheal cells arrests tracheal development.

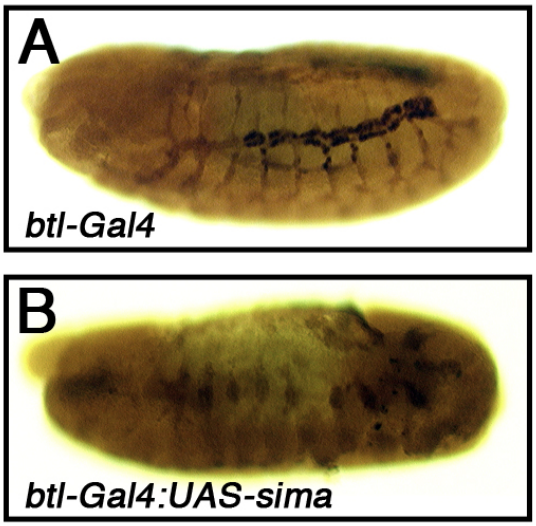

Lateral views of (A) *btl-Gal4* control and (B) *btl-Gal4:UAS-sima* embryos stained with α-Tgo to visualize tracheal cells.

Figure 3.5. *dVHL* knockdown phenotypes genetically require *sima*.

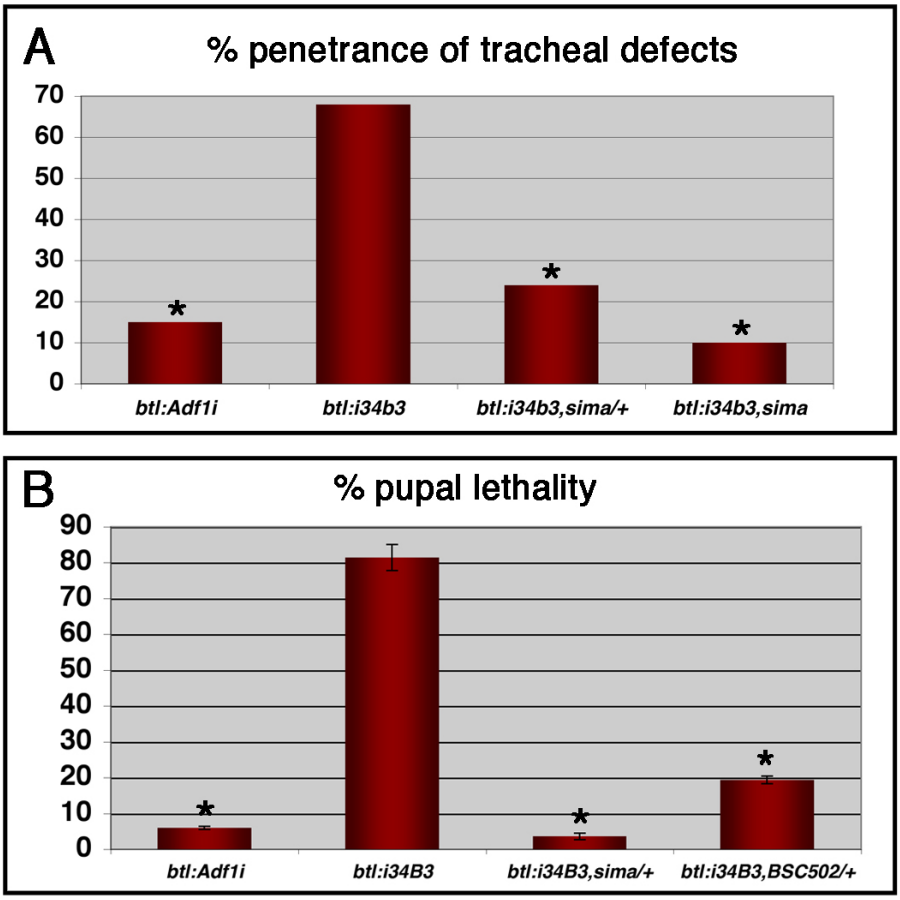

(A) Penetrance of tracheal defects in embryos with *btl-Gal4* driven expression of *UAS-Adf1^{i}* or the *UAS-dVHL^{i34B3}* transgene. *dVHL^{i}* phenotypes are suppressed by *sima* alleles in a dose-dependent manner (* $p < 0.001$ relative to *btl-Gal4:UAS-dVHL^{i34B3}*). (B) Frequency of pupal lethality in the indicated genotypes. *btl-Gal4:UAS-dVHL^{i34B3}* lethality is dominantly suppressed by *sima* or *Df(3R)BSC502* (* $p < 0.005$ relative to *btl-Gal4:UAS-dVHL^{i34B3}*; error bars are ± SEM).

Table 3.5. *dVHL* interacts genetically with *sima* and FGF pathway alleles

Genotype	Total penetrance (%)	n=
btl-Gal4:UAS-dVHL^{i34B3}	68	48
btl-Gal4:UAS-dVHL^{i34B3},sima^{07607}/+	24*	53
btl-Gal4:UAS-dVHL^{i34B3},sima^{07607}	10*	59
btl-Gal4:UAS-dVHL^{i34B3},trh^{10512}/+	54	52
btl-Gal4:UAS-dVHL^{i34B3},btl^{dev1}/+	26*	54
btl-Gal4:UAS-dVHL^{i34B3},bnl^{P1}/+	25*	55

* $p < 0.01$ relative to *btl-Gal4:UAS-dVHL^{i34B3}*

Table 3.6. Pupal lethality

Genotype	% lethality	n=
btl-Gal4:UAS-Adf1^{i}	6.0 ± 0.39	350
btl-Gal4:UAS-dVHL^{i31A2}	98.5 ± 1.12*	393
btl-Gal4:UAS-dVHL^{i34B3}	81.5 ± 3.62*	302
btl-Gal4:UAS-dVHL^{i34B3},sima^{07607}/+	3.6 ± 0.18**	278
btl-Gal4:UAS-dVHL^{i34B3},Df(3R)BSC502/+	19.4 ± 1.05**	193

* $p < 0.01$ relative to *btl-Gal4:UAS-Adf1^{i}*

** $p < 0.01$ relative to *btl-Gal4:UAS-dVHL^{i34B3}*

3.E. *dVHL* suppresses *btl* expression in the embryo

By analogy to the larval tracheal system in which *sima*-driven expression of the *btl* FGF receptor induces excess growth and branching of terminal cells (Centanin et al., 2008), we next sought to determine whether both aspects of *dVHL*^{i} embryonic tracheal phenotype – defective migration and sinuous overgrowth & branching – were also dependent on Btl/FGF signaling. Recessive lethal alleles of the *btl* receptor (*btl*^{dev1}, Kennison & Tamkun, 1988), the *bnl* ligand (*bnl*^{P1}, Sutherland et al., 1996), and the *trh* bHLH-PAS transcription factor responsible for induction of *btl* expression in the tracheal placode (*trh*^{10512}, Wilk et al., 1996), were placed in the background of *btl-Gal4,UAS-dVHL*^{i34B3}. Embryonic tracheal architecture was analyzed with the mAb2A12 antibody and the fraction of embryos showing either migration defects or excess growth/branching defects was calculated as a percentage of the total (Figure 3.6A and Table 3.5). Loss of one copy of either *btl* or *bnl* led to a significant reduction in the penetrance of *dVHL*^{i34B3} tracheal phenotypes from 68% (n=48) to 26% (n=54) and 25% (n=55) respectively, comparable to heterozygosity for the *sima*^{07607} allele. Tracheal phenotypes that result from reduced *dVHL* activity thus display equal sensitivity to reductions in Btl signal strength or to reduced activity of the *btl* transcriptional activator Sima. This sensitivity might reflect a role for *dVHL* as an antagonist of a pathway that operates in parallel to Btl or a role for dVHL as a direct antagonist of Btl (Hsu et al., 2006), although *dVHL* inactivation had little effect on the levels or trafficking of a Btl:GFP fusion protein (Figure 3.7). Precedent with the larval function of the HPH *fga* suggests that *dVHL* may act through Sima to control *btl*

transcription in the embryo more directly (Centanin et al., 2008). Consistent with this hypothesis, expression of a wild type *btl* transgene specifically in tracheal cells produces tracheal overgrowth (Figure 3.6B), DT breaks, and excess larval TTBs (Table 3.4) that resemble *dVHL*^{i} tracheal-specific knockdown phenotypes. A constitutively active *btl* allele (*btl*$^{\wedge}$) has previously been shown to block early migration events in the embryonic tracheal system and also lead to secondary branch duplication (Lee et al., 1996a). Moreover, expression of either of two downstream effectors of Btl – *Ras85D* (Lee et al., 1996b) or the *pnt* transcription factor (Klaes et al., 1994) – disrupts tracheal branching in the embryo (Figure 3.6C,D), consistent with the role of *pnt* in repressing fusion cell specification (Samakovlis et al., 1996a). To test whether *dVHL* restricts *btl* transcription in vivo, we first made use of the prior observation that ubiquitous overexpression of *sima* in the embryo is sufficient to induce specific groups of non-tracheal cells to form ectopic *btl*-positive placodes (Centanin et al., 2008). *sima* can induce two ectopic placodes (tp-1 and tp0) anterior to the first tracheal placode (tp1), and occasionally a third (tp11) distal to the last placode (tp10). These cryptic placodes also appear in response to *trh* (Wilk et al., 1996) and appear to be primed to adopt a tracheal fate by spatially restricted signals like *vvl* (Boube et al., 2000; Zelzer & Shilo, 2000) that sensitize the *btl* promoter to other *trans*-activators. Significantly, ubiquitous knockdown of *dVHL* leads to the appearance of an ectopic *btl*-positive placode at the tp0 position (Figure 3.6F,G). At lower frequency *btl*-expressing cells also appear at the tp-1 and tp11 positions as well (Figure 3.8). Loss of *dVHL* is thus capable of mimicking the effect of *trh* or *sima*

overexpression on patterns of *btl* transcription. There is no change in levels or localization of Trh in this genetic background (Figure 3.6P), again supporting the notion that expression of *dVHL^{i}* leads specifically to *sima*-mediated phenotypes. To test whether reduced dVHL activity also results in higher levels of *btl* transcription in differentiated tracheal cells, *UAS-dVHL^{i}/+* and *UAS-dVHL^{i}/ btl-Gal4,UAS-GFP* embryos at either stage 11 (pre-migratory) or stage 15 (post-migratory) were hybridized with a *btl* RNA probe and developed using a tyramide-amplification protocol (Merabet et al., 2005). Samples from each stage were processed together and genotyped afterward by *GFP* expression. At stage 11, levels of *btl* transcript are elevated in tracheal placodes expressing the *dVHL^{i}* knockdown transgene compared to control embryos (Figure 3.6I vs. 3.6M). Similarly stage 15 embryos carrying the *dVHL^{i}* knockdown transgene show increased levels of *btl* transcript in cells of the DT, the DBs, and the transverse connectives (Figure 3.6K vs. 3.6O). *dVHL* thus restricts *btl* transcription in tracheal cells at multiple stages of embryonic development. In view of the genetic requirement for *btl* in *dVHL^{i}* tracheal phenotypes, these data indicate that Sima-driven elevation in *btl* expression and activity is a major cause of both the ‘early’ and ‘late’ tracheal responses to hypoxia.

Figure 3.6. *dVHL^{i}* expression leads to ectopic *btl* transcription.

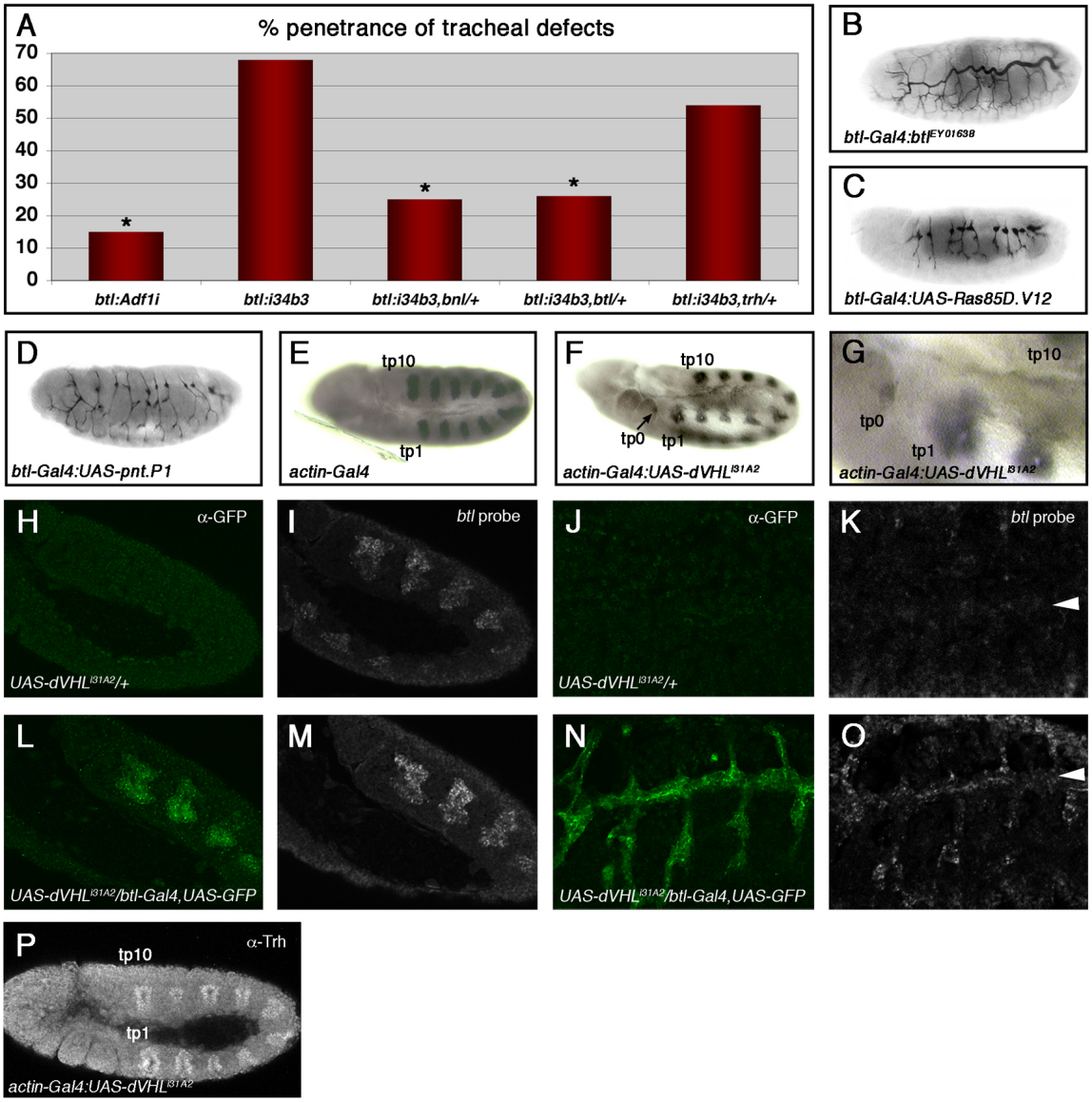

(A) Penetrance of tracheal defects in embryos with *btl-Gal4* driven expression of *UAS-Adf1^{i}* control RNAi or the *UAS-dVHL^{i34B3}* transgene in tracheal cells. *btl-Gal4:UAS-dVHL^{i34B3}* phenotypes are dominantly suppressed by alleles of the FGF pathway components *btl* or *bnl*, but not by alleles of the transcription factor *trh* (* $p < 0.001$ relative to *btl-Gal4:UAS-dVHL^{i34B3}*). (B-D) Lateral images of embryos stained with the tracheal lumen marker mAb2A12. *btl-Gal4:UAS-*

dVHL^{i34B3} phenotypes are phenocopied by *btl-Gal4* driven over-expression of (B) *btl*, or FGF downstream pathway components (C) *Ras85D.V12* (a constitutively active form of *Ras85D*), or (D) the MAPK transcriptional effector *pnt.P1*. (E-G) Lateral images of embryos hybridized with a *btl* anti-sense probe. (E) Control *actin-Gal4* embryos display the normal complement of ten *btl* positive tracheal placodes (tp1 through tp10). (F,G) *actin-Gal4* driven expression of *dVHL*^{i31A2} causes ectopic transcription of *btl* in cryptic tracheal placodes (indicated as tp0). Control *UAS-dVHL*^{i31A2} stage 11 (H,I) and stage 15 (J,K) embryos hybridized with a *btl* anti-sense probe and stained with α-GFP. *btl* is expressed in all cells of stage 11 tracheal placodes, but only in migrating tracheal cells of stage 15 embryos. *UAS-dVHL*^{i31A2}*/btl-Gal4,UAS-GFP* stage 11 (L,M) and stage 15 (N,O) embryos hybridized with a *btl* anti-sense probe and stained with α-GFP, showing elevated *btl* expression. Embryos were genotyped by expression of GFP. Arrowhead indicates DT. (P) Stage 11 *actin-Gal4:UAS-dVHL*^{i31A2} embryo stained with α-Trh. Trh staining shows the wild type pattern of ten Trh positive tracheal placodes (tp1 through tp10).

Figure 3.7. Expression of *dVHL^{i}* does not alter trafficking of Btl.

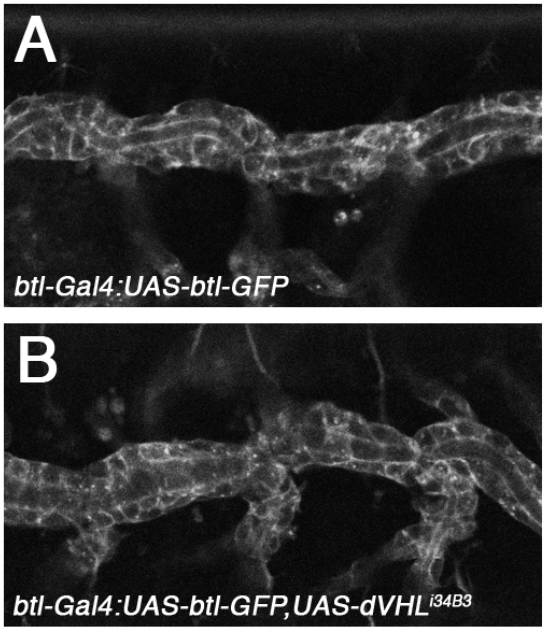

(A) *btl-Gal4* control and (B) *UAS-dVHL^{i34B3}* knockdown embryos expressing a Btl-GFP fusion protein (Dammai et al. 2003) show very similar Btl levels and localization.

Figure 3.8. Appearance of cryptic *btl* positive tracheal placodes in *dVHL* knockdown embryos.

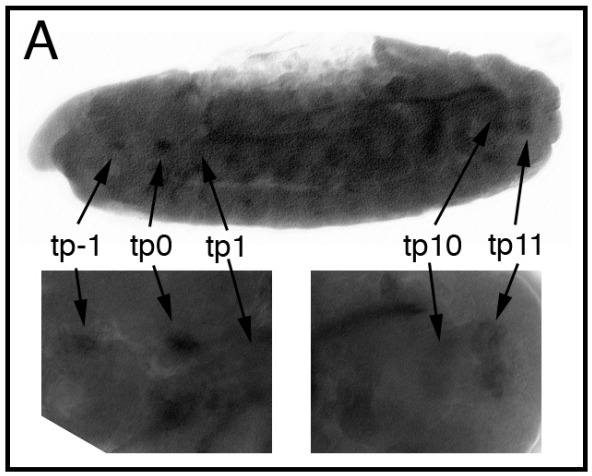

(A) Lateral view of an *actin-Gal4:UAS-dVHL*^{i31A2} embryo hybridized with a *btl* anti-sense probe. Three cryptic *btl* positive tracheal placodes are indicated (tp-1, tp0, tp11).

3.F. *dVHL* and *ago* synergize to control embryonic tracheogenesis

The *sima* and *trh* transcription factors are each capable of interacting with the *btl* promoter to induce *btl* expression in cultured cells (Centanin et al., 2008; Ohshiro & Saigo, 1997). Previous work has shown that *trh* alleles dominantly suppress tracheal migration defects resulting from ectopic expression of *btl* in DT fusion cells lacking the *archipelago* (*ago*) gene, which encodes an F-box protein that binds Trh and recruits it into a SCF ubiquitin ligase complex for polyubiquitination and proteasome-dependent degradation. Thus the observation that *dVHL*^{i} tracheal phenotypes require *sima* but are only minimally sensitive to *trh* gene dosage (Figure 3.6A and Table 3.5), along with the finding that Trh expression is not altered by loss of *dVHL* (Figure 3.6P), suggests that the *ago* and *dVHL* ubiquitin ligases restrict *btl* expression by genetically distinct pathways. To test if *dVHL* and *ago* alleles might then collaborate to deregulate *btl*-dependent branching and migration events, the frequency of the two types of *dVHL*^{i} embryonic tracheal phenotypes – stunted migration or ectopic branching and sinuous overgrowth – were examined in a background heterozygous for the *ago*^{3} strong loss-of-function allele (Moberg et al., 2001). Two 'weaker' *dVHL* lines (*i11A2* and *i4B2*) that gave a higher frequency of sinuous overgrowth and a somewhat lower frequency of migration defects were used for this analysis. In both cases, addition of the *ago* allele shifts the most frequent tracheal phenotype from sinuous overgrowth to stunted branch migration (Figure 3.9A,B) and increases the overall fraction of embryos with migration defects to 70-75% (Figure 3.9C and Table 3.7). Moreover, embryos *trans*-heterozygous for the *ago*^{3}

allele and a genomic deficiency that removes the *dVHL* locus (*Exel6060/+;ago^{3}/+*) show an elevated frequency of tracheal fusion and migration defects compared to either lesion alone (Figure 3.9D,E). The *dVHL* deficiency also dominantly enhances the number of DT breaks per affected *ago^{1}/ago^{3}* embryo from 1.2 ± 0.09 (n=39) to 2.5 ± 0.19 (n=41; $p<1\times10^{-6}$; Figure 3.9F,G). Thus, *dVHL* and *ago* act synergistically to control migration and fusion events in the developing tracheal system. Interestingly, examination of L3 larvae that co-express *dVHL^{i31A2}* and a dominant-negative form of *ago* (*UAS-ago*Δ*F*) in tracheal cells shows no enhancement of TTB branching beyond that observed with *dVHL* knockdown alone (Table 3.4). The synergy between *ago* and *dVHL* may thus be specific to the early embryonic tracheal system. To test whether the functional interaction between *dVHL* and *ago* is indeed specific to a particular developmental phase, the 'weak' dose of 1% O_2 was used as a switch to activate the *dVHL/sima* transcriptional program at 'early' or 'late' embryonic time points (according to the scheme depicted in Figure 3.1) in either wild type (*+/+*) embryos or *ago^{3}/+* embryos. Tracheal architecture was then analyzed with mAb2A12. As described above (Figure 3.1G), 'early' exposure to 1% O_2 produces tracheal phenotypes at only low penetrance (12%). Significantly, reducing the dose of *ago* leads to a more than 3-fold increase in the penetrance of tracheal phenotypes in response to this 1% O_2 treatment (Figure 3.9H and Table 3.1). This includes an approximate doubling of migration defects (from 5% to 9% of embryos), appearance of duplicated secondary branches (from 0% to 5% of embryos), and an increase in sinuous overgrowth (from 2% to 34% of embryos). Notably, this

enhancement is specific to the 'early' time point: exposure to 1% O_2 at the 'late' embryonic time point produced the same penetrance of tracheal phenotypes in *ago^3/+* and control *+/+* embryos (Figure 3.9H and Table 3.1). Moreover, *ago* heterozygosity did not affect the extent of DT growth induced in response to 'late' 1% O_2 (21 ± 3.1% longer in +/+ [n=4], [see yellow bar in Figure 3.1H]; 20 ± 2.6% longer in *ago^3/+* [n=4]), demonstrating that a phenotype that is a dose-sensitive readout of pathway activity is also unaffected by lowered *ago* activity. Reducing *ago* activity thus specifically sensitizes the 'early' embryonic tracheal system to architectural changes in response to mild hypoxia. As *ago* restricts *btl* transcription in the developing embryonic tracheal system, this stage-specific synergy between *ago* and hypoxia appears to define a window of development during which activation of the *dVHL/sima* pathway induces a program of gene expression that conflicts with normal *btl/bnl* migration cues. Removing a copy of *ago* is predicted to enhance this conflict by elevating Trh activity and *btl* transcription.

Figure 3.9. *ago* interacts with *dVHL* in tracheal morphogenesis.

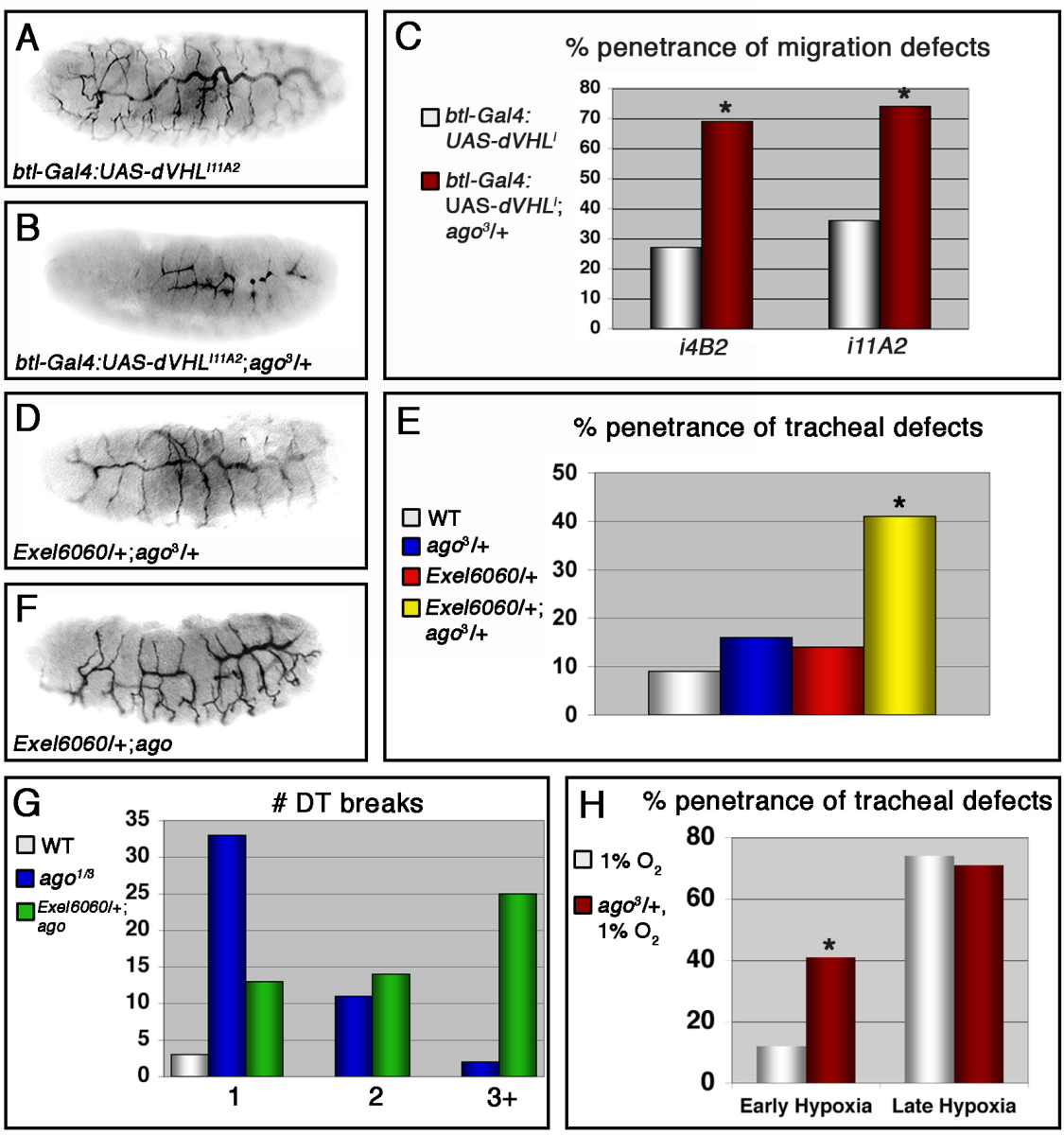

(A-D) Lateral views of embryos stained with the lumenal marker mAb2A12. The *btl-Gal4:UAS-dVHL^{i11A2}* phenotype (A) is enhanced by reducing the genetic dosage of *ago* (B). (C) Enhancement of the penetrance of migration defects in *btl-Gal4:UAS-dVHL^{i}* embryos by the *ago^{3}* allele (* $p < 0.05$ compared to *btl-Gal4:UAS-dVHL^{i}* alone). (D-G) Alleles of *ago* also interact with a deletion

(*Exel6060*) uncovering the *dVHL* locus. (D) Lateral view of an *Exel6060/+;ago^{3}/+* embryo stained with mAb2A12 displaying defects in tracheal morphogenesis. (E) Quantification of the *trans*-heterozygous interaction between *ago* and *Exel6060* in tracheal formation (* $p < 0.001$ compared to *wt*). (F) Lateral view of an *Exel6060/+;ago$^{1/3}$* embryo stained with mAb2A12. (G) Frequency of embryos with 1, 2, or 3+ DT breaks shows enhancement of the *ago$^{1/3}$* tracheal phenotype by *Exel6060*. (H) Penetrance of all classes of tracheal defects (breaks, overgrowth, missing or duplicated branches) in *w^{1118}* and *ago^{3}/+* embryos following exposure to 1% O_2. (* $p < 0.005$ relative to *w^{1118}*).

Table 3.7. Genetic interactions between *dVHL* and *ago*

Genotype	Penetrance (%)	Migration defects (%)	n=
btl-Gal4:UAS-dVHL^{i4B2}	60	16	32
btl-Gal4:UAS-dVHL^{i4B2},ago^{3}/+	59	41*	51
btl-Gal4:UAS-dVHL^{i11A2}	50	18	34
btl-Gal4:UAS-dVHL^{i11A2},ago^{3}/+	53	39*	48

* $p < 0.01$ relative to *btl-Gal4:UAS-dVHL^{i}*

3.G. Discussion of results

Hypoxia-induced remodeling of tracheal terminal cells represents the response of a developed larval tracheal system to reduced levels of oxygen in the environment. By contrast, the response of the developing embryonic tracheal system to systemic hypoxia has not been as well characterized. In light of the observation that embryonic tracheal cells display hypoxia-induced activation of a Sima-reporter (Lavista-Llanos et al., 2002) and that *sima* promotes *btl* expression in larval tracheal cells (Centanin et al., 2008), embryonic exposure to hypoxia may thus produce a situation in which hardwired *btl/bnl* patterning signals in the embryo come into conflict with the type of *sima/btl*-driven plasticity of tracheal cell branching seen in the larva. Here we examine the effect of hypoxia on embryonic tracheal branching and migration. We find that hypoxia has dramatic effects on the patterns of morphogenesis of the primary and secondary tracheal branches. Surprisingly, varying the timing and severity of hypoxic challenge is able to shift the outcome from severely stunted tracheal branching to excess branch number and enhanced branch growth. Genetic and molecular data indicate that both classes of phenotypes, stunting and overgrowth, involve regulation of *sima* activity and *btl* transcription by *dVHL*, and that the effects of hypoxia on tracheal development can be mimicked in normoxia by tracheal specific knockdown of *dVHL*. This observation confirms a central role for *dVHL* in restricting the hypoxic response in vivo, and identifies a role for *dVHL* as a required inhibitor of *sima* and *btl* during normal tracheogenesis.

Since Trh and Sima/HIF-1α share a consensus DNA binding site (Crews & Fan, 1999; Gorr et al., 2004; Jiang & Crews, 2007), it is likely that the tracheal phenotypes elicited by hypoxia or *dVHL* knockdown are largely the result of excess 'Trh-like' transcriptional activity in tracheal cells (Figure 3.10). This conclusion is supported by the phenotypic similarity between hypoxia/*dVHL* knockdown and *trh* overexpression, by the modest ability of *trh* alleles to suppress $dVHL^{i}$ phenotypes and by the previously demonstrated overlap of transcriptional activity between Trh and human HIF-1α (Zelzer et al., 1997). This excess activity occurs independently of a change in Trh expression and appears to be mediated specifically by *sima*.

Our analysis suggests that there are two distinct developmental 'windows' of embryogenesis during which hypoxia has opposite effects on tracheal branching. The first corresponds to a period immediately before and during primary branch migration that is relatively insensitive to hypoxia. Embryos in this stage show a minimal response to 1% O_2, but show a nearly complete arrest of migration in 0.5% O_2. Interestingly, a prior study found that similarly staged embryos (stage 11) respond to complete anoxia by prolonged developmental arrest, from which they can emerge and resume normal development (Wingrove & O'Farrell, 1999). These somewhat paradoxical results – that acute hypoxia is more detrimental to development than chronic anoxia – might be explained by the observation that chronic exposure to low oxygen induces Sima activity throughout the embryo while acute exposure activates Sima only in tracheal cells (Lavista-Llanos et al., 2002). The former scenario may result in coordinated

developmental and metabolic arrest throughout the organism, while in the latter scenario developmental patterns of gene expression in non-tracheal cells may proceed such that tracheal cells emerging from an 'early' hypoxic response find an embryonic environment in which developmentally hard-wired migratory signals emanating from non-tracheal cells have ceased.

The second type of tracheal response occurs during a later 'window' of embryogenesis after *btl/bnl*-driven primary and secondary branch migration and fusion are largely complete. It involves sinuous overgrowth of the primary and secondary branches (this study and Arquier et al., 2006), and duplication of secondary branches. As in the 'early' response, 'late' hypoxic phenotypes are controlled by the *dVHL/sima* pathway, yet unlike the 'early' response, these phenotypes occur at high penetrance even at 1% O_2. Thus the 'late' embryonic tracheal system is relatively sensitized to hypoxia and responds with increased branching in a manner similar to larval terminal cells. Indeed, much as larval branching increases with decreasing oxygen levels (Jarecki et al., 1999), we observe that dorsal trunk growth in the late embryo is graded to the degree of hypoxia. The mechanism underlying the differential sensitivity of the 'early' and 'late' tracheal system may be quite complex. However, we find that tracheogenesis can be sensitized to hypoxia by reducing activity of *ago*, a ubiquitin ligase component that restricts *btl* transcription in tracheal cells via its role in degrading the Trh transcription factor. Increasing transcriptional input on the *btl* promoter thus appears to sensitize 'early' tracheal cells to hypoxia. As Sima also controls *btl* transcription, one explanation of the difference in sensitivity

between different embryonic stages may thus lie in differences in the activation state of the *btl* promoter (Figure 3.10).

An organism can have its hypoxic response triggered in two ways, either by systemic exposure of the whole organism to a reduced oxygen environment or by localized hypoxia produced by increased oxygen consumption in metabolically active tissues. Data from this study and others (Centanin et al., 2008; Jarecki et al., 1999) suggests there may be distinctions between these two triggers. Exposing larvae or embryos to a systemic pulse of hypoxia results in a '*btl*-centric' response specifically in tracheal cells. Outside of an 'early' vulnerable period which corresponds to embryonic branch migration and fusion, elevated Btl activity in embryonic tracheal cells promotes branch duplications and overgrowth similar to that seen in larvae (Centanin et al., 2008). By contrast, tracheal growth induced by localized hypoxia in the larva has been suggested to involve a '*bnl*-centric' model in which the hypoxic tissue secretes Bnl and recruits new tracheal branching (Jarecki et al., 1999). Whether this type of mechanism operates in embryos, or whether embryos ever experience localized hypoxia in non-tracheal cells, has not been established.

Our data indicate that *dVHL* is a central player in the hypoxic response pathway in embryonic and larval tracheal cells. A prior study found that injection of *dVHL* dsRNA into syncytial embryos disrupted normal tracheogenesis (Adryan et al., 2000), but was technically limited in its ability to conduct a detailed analysis of *dVHL* function in development and homeostasis. We find that *dVHL* knockdown specifically in tracheal cells mimics the effect of systemic hypoxia on

embryonic tracheal architecture and larval terminal cell branching. *dVHL* knockdown thus phenocopies loss of the HPH gene *fga*, which normally functions to target Sima to the dVHL ubiquitin ligase in normoxia (Centanin et al., 2005). Moreover, all phenotypes that result from reduced *dVHL* expression can be rescued by reducing *sima* activity, suggesting that Sima is the major target of dVHL in the tracheal system. These data support a model in which *dVHL*, *fga*, and *sima* function as part of a conserved VHL/HPH/HIF-1α pathway to control tracheal morphogenesis in embryos and larvae. The *btl* receptor appears to be an important target of this pathway in embryonic (this study) and larval (Centanin et al., 2008) tracheal cells. Knockdown of *dVHL* elevates *btl* transcription in embryonic placodes and tracheal branches, and removal of a copy of the gene effectively suppresses *dVHL* tracheal phenotypes. Reciprocally, overexpression of wild type *btl* in embryonic tracheal cells can produce migration defects and sinuous overgrowth, while expression of a constitutively active *btl* chimera (*btl*$^{\wedge}$) also leads to primary branch stunting and duplication of secondary branches (Lee et al., 1996a). Interestingly, pupal lethality associated with tracheal-specific knockdown of *dVHL* is not sensitive to the dose of *btl*, but is dependent on *sima*. Thus the *dVHL/sima* pathway may have *btl* independent effects on tracheal cells in later stages of development.

In addition to *sima* and Btl/FGF pathway mutants, *dVHL* also shows very strong genetic interactions with alleles of the *ago* ubiquitin ligase subunit. The interactions are consistent with the ability of *ago* to modulate hypoxia sensitivity in the embryo, and suggest a speculative model in which each ligase acts

through its own target – Sima or Trh – to regulate *btl* transcription in tracheal cells. Given that the human orthologs of *dVHL* and *ago* are significant tumor suppressor genes, it is intriguing to consider whether their ability to co-regulate tubular morphogenesis in the *Drosophila* embryo is conserved in mammalian development and disease.

[2] Mortimer, N. T. and Moberg, K. H. (2009). Regulation of *Drosophila* embryonic tracheogenesis by *dVHL* and hypoxia**.** *Dev Biol,* in press.

Figure 3.10. Model for dVHL and Ago function in embryonic tracheal development.

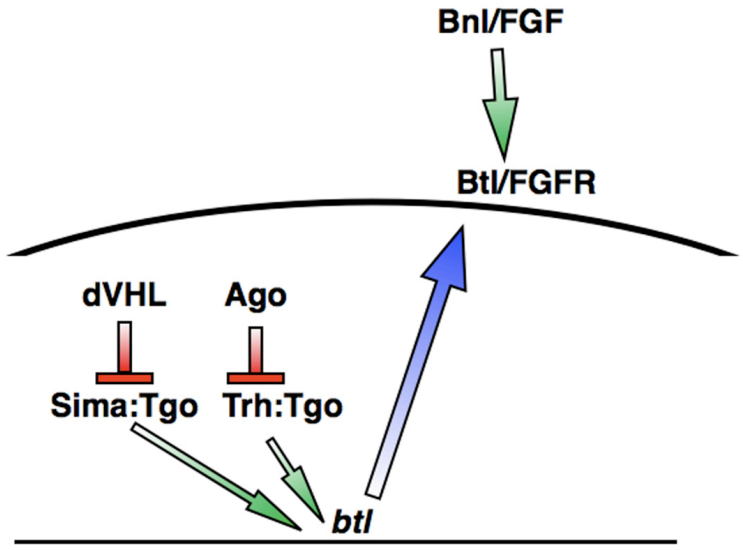

dVHL and Ago restrict *btl* transcription in embryonic tracheal cells. dVHL regulates levels of Sima, thus regulating the transcriptional activity of the Sima:Tgo heterodimer. Ago further acts to restrict Btl/FGF signaling via down-regulation of Trh, inhibiting Trh:Tgo-mediated transcription of *btl*.

Chapter Four: *ago* restricts activity of *Drosophila* HIF to regulate tracheal terminal branching and the *Drosophila* hypoxic response

4.A. Introduction

In order to function, metabolically active tissues require an adequate supply of oxygen; organismal viability is thus dependent on its sufficient delivery to internal tissues. Complex organisms have evolved branched oxygen-conducting networks to ensure that this oxygen demand is met. These organs arise through a process of tubular morphogenesis and are elaborated via multiple rounds of growth factor mediated cell growth and migration. Examples of such branched organs include the mammalian vasculature and the *Drosophila* tracheal system, and their morphogenesis is necessary for organismal development.

At the cellular level, oxygen is required both for the metabolic production of energy and as a necessary substrate for a variety of enzymatic functions (reviewed in Denko, 2008). Due to this requirement, metazoan cells are sensitive to decreases in oxygen availability. When faced with oxygen-poor, or hypoxic, conditions, a highly conserved pathway senses the decreased oxygen concentration and triggers a hypoxic response, resulting in both transient and long-term changes allowing cells to survive a period of decreased intracellular oxygen. The hypoxic response is characterized by a co-ordinate increase in oxygen-independent energy production and in the capacity of the oxygen-conducting organs (reviewed in Weidemann & Johnson, 2008).

Central to the hypoxic response is the activity of the hypoxia-inducible factor (HIF), a heterodimeric transcription factor required for cellular adaptation to hypoxic conditions (Semenza & Wang, 1992; Wang et al., 1995; Wang & Semenza, 1995). HIF is composed of an oxygen-regulated α subunit and a

constitutive β subunit; HIF activity is largely regulated at the level of HIF-1α stability (reviewed in Weidemann & Johnson, 2008). In normoxic conditions, HIF-1α is hydroxylated at conserved proline residues by the 2-oxoglutarate/ iron(II)-dependent prolyl-4-hydroxylase family member HIF prolyl hydroxylase (HPH, Bruick & McKnight, 2001; Epstein et al., 2001). Prolyl-hydroxylated HIF-1α is then recognized by the von Hippel Lindau (VHL) E3-ubiquitin ligase subunit, leading to its poly-ubiquitination and subsequent proteosome-dependent degradation (Cockman et al., 2000; Ivan et al., 2001; Jaakkola et al., 2001; Maxwell et al., 1999; Ohh et al., 2000). The enzymatic activity of HPH is dependent upon the availability of oxygen (Bruick & McKnight, 2001; Epstein et al., 2001). The HPH/VHL pathway can therefore function as a sensor of cellular oxygen levels, allowing HIF-1α stabilization only in hypoxic conditions and preventing HIF activity in normoxic cells (reviewed in Kaelin & Ratcliffe, 2008).

This hypoxic response pathway is conserved in *Drosophila* (reviewed in Gorr et al., 2006; Romero et al., 2007), where the *Drosophila* HIF (dHIF) α and β subunits are encoded by *similar* (*sima*, Bacon et al., 1998; Nambu et al., 1996) and *tango* (*tgo*, Ma & Haddad, 1999; Ohshiro & Saigo, 1997; Sonnenfeld et al., 1997), respectively. Activity of the HPH/VHL HIF-1α regulatory pathway has also been demonstrated in *Drosophila* (Arquier et al., 2006; Bruick & McKnight, 2001; Centanin et al., 2008; Centanin et al., 2005; Lavista-Llanos et al., 2002); the stability of Sima is dependent on the activity of the HPH homolog *fatiga* (*fga)*, and *dVHL*, the *Drosophila* VHL homolog. In hypoxic conditions, the dHIF complex translocates to the nucleus leading to expression of a conserved set of HIF target

genes (Liu et al., 2006) and physiological changes reminiscent of the mammalian hypoxic response including both increased oxygen-conducting capacity and altered metabolism (reviewed in Gorr et al., 2006; Hoogewijs et al., 2007). Unlike most vertebrates, *Drosophila* are able to survive extended periods of oxygen deprivation and are termed hypoxia tolerant. The *Drosophila* hypoxic response is characterized by metabolic changes (Zhou et al., 2008), reduced oxygen consumption (Krishnan et al., 1997; Ma et al., 1999), developmental arrest (Foe & Alberts, 1985; Wingrove & O'Farrell, 1999) and entry into a state of stupor (Csik, 1939; Krishnan et al., 1997). Recovery from this stupor is dependent upon genes necessary for survival in low-oxygen conditions (Haddad et al., 1997; Liu et al., 2006; Zhou et al., 2008).

The hypoxic response in *Drosophila* larvae also results in increased growth of the tracheal system, the oxygen-conducting organ of *Drosophila*. Elaboration of the tracheal system occurs during embryogenesis and is dependent on expression of the fibroblast growth factor (FGF) receptor homolog *breathless* (*btl*, Klambt et al., 1992) in tracheal cells and the FGF homolog *branchless* (*bnl*, Sutherland et al., 1996) in surrounding non-tracheal tissue. Bnl acts as an attractant for tracheal cells, and its dynamic expression allows the Btl/FGF pathway to drive tracheal cell migration in the establishment of the primary tracheal architecture during embryogenesis (Klambt et al., 1992; Sutherland et al., 1996).

During larval development, the Btl/FGF pathway is re-iteratively used to elaborate additional tracheal branches from this primary architecture in a

homeostatic process analogous to angiogenesis in the mammalian vasculature (Centanin et al., 2008; Jarecki et al., 1999). This larval homeostatic tracheogenesis is separable from embryonic developmental tracheal morphogenesis both temporally and in that it is sensitive to environmental and local oxygen concentration. *Drosophila* larvae raised in chronic hypoxia show an increase in branch number, whereas those raised in chronic hyperoxia have a greatly decreased extent of branch elaboration (Centanin et al., 2008; Jarecki et al., 1999). The hypoxic response leads to increased expression of *btl* in tracheal cells and *bnl* in oxygen-deficient tissues and thus increases activity of the Btl/ FGF pathway (Centanin et al., 2008; Jarecki et al., 1999), leading to increased tracheal branch growth. These hypoxia-induced branches form as cytoplasmic extensions of the tracheal terminal cells; a class of tracheal cells specified at the end of embryogenesis (Guillemin et al., 1996; Manning & Krasnow, 1993). These terminal branches serve as the site of gas exchange between the tracheal system and internal tissues (Lubarsky & Krasnow, 2003; Manning & Krasnow, 1993), and extend toward nearby Bnl expressing cells to conduct oxygen to the hypoxic tissue (Jarecki et al., 1999). When the oxygen demand is met, Bnl expression ceases, preventing excess tracheal growth. This oxygen responsiveness allows for growth of tracheal terminal branches specifically to localized areas of hypoxia to shape the mature tracheal architecture and to increase the oxygen-delivery capacity in hypoxic conditions.

Recent work in *Drosophila* has demonstrated the exquisite sensitivity of the hypoxic response. In adult *Drosophila*, differing transcriptional outputs are

observed depending upon the severity and length of the hypoxic treatment (Liu et al., 2006). This finding suggests that HIF activity is tightly regulated in order to trigger a hypoxic response that is appropriate to the environmental conditions. Regulation of HIF activity further plays an important role in development (reviewed in Covello & Simon, 2004; Gorr et al., 2006; Simon & Keith, 2008) and pathogenesis (reviewed in Semenza, 2000; Semenza, 2001; Semenza et al., 2000). Ectopic stability of HIF-α results in the development of a variety of pathologies including tumorigenesis, where HIF activity plays a major role in the metabolic switch to aerobic glycolysis characteristic of tumor cells and is linked to neoangiogenesis and increased tumor metastasis (reviewed in Rankin & Giaccia, 2008; Weidemann & Johnson, 2008; Zhou et al., 2006). Clearly the precise regulation of HIF activity plays a vital role in development, tumor suppression and in the response to changing environmental conditions.

Here we identify the *Drosophila* tumor suppressor homolog *archipelago* (*ago*) as a novel regulator of dHIF activity. *ago* encodes an F-box/WD-repeat domain containing protein which functions as the substrate specificity factor for an SCF type ubiquitin ligase (Koepp et al., 2001; Moberg et al., 2001; Strohmaier et al., 2001). *ago* was initially identified as a cell autonomous growth regulator in *Drosophila* and has been demonstrated to regulate levels of the proliferative proteins Cyclin E and dMyc (Moberg et al., 2001; Moberg et al., 2004); these functions are conserved in the mammalian *ago* homolog *Fbw7* (reviewed in Minella & Clurman, 2005; Tan et al., 2008; Welcker & Clurman, 2008). More recent work has begun to uncover non-proliferative roles for *ago*/*Fbw7* in

regulating growth factor signaling and metabolism which may be important for organismal development and tumor suppression (Olson et al., 2008; Sundqvist et al., 2005).

We find that loss of *ago* function leads to a post-transcriptional increase in dHIF activity in *Drosophila* larvae. This activity is reflected in a *sima*-dependent increase in tracheal terminal branching that is separable from the requirement for *ago* to restrict *btl* transcription in the post-mitotic morphogenesis of the embryonic tracheal system, and is due to increased *bnl* transcription in the larval body wall muscles. In this tissue, *ago* acts co-operatively with the established Fga/dVHL regulatory pathway to restrict tracheal terminal branching. We further demonstrate that loss of *ago* leads to an altered hypoxic response. Molecularly this phenotype is defined by differing levels of transcription of dHIF target genes both in normoxia and in varying degrees of hypoxia, where we find that loss of *ago* lessens the sensitivity of the hypoxic response. Finally this altered hypoxic response is reflected at the organismal level by differences in recovery from hypoxic stupor and in the ability to survive chronic oxygen deprivation. These findings define a role for *ago* in regulating dHIF activity and the *Drosophila* hypoxic response.

4.B. Loss of *ago* results in increased branching of tracheal terminal cells

We have found that null alleles of *ago* are embryonic lethal (Moberg et al., 2001). In order to investigate the post-embryonic roles of *ago* in non-proliferating tissues, we isolated a hypomorphic *ago* allele using transposase-mediated imprecise excision of a P-element transposon inserted 16 base pairs (bp) upstream of the *ago* genomic locus (*EP(3)1135*). The resulting $ago^{\Delta 3\text{-}7}$ allele is a 603 bp deletion removing the first exon of the *ago-RC* transcript (Figure 4.1). Alone or in combination with the null alleles ago^{1} and ago^{3} (Moberg et al., 2001), the $ago^{\Delta 3\text{-}7}$ deletion causes pupal lethality and larval tracheal phenotypes (Figure 4.2). The most prevalent phenotype is an increase in the number of cytoplasmic branches elaborated from multiple subtypes of terminal cells, including those found along the lateral trunk which serve to oxygenate the ventrolateral body wall muscles. This increase is reflected in an approximate doubling in the terminal branch number of lateral terminal cells (Figure 4.2E), including an increase in LH cell terminal branching, from 20.4 ± 0.64 branches (n=33) in control larvae to 39.5 ± 1.59 branches (n=34) in $ago^{\Delta 3\text{-}7/1}$ larvae ($p=2.6\text{x}10^{-16}$, Figure 4.2A,B,E), and LG cell terminal branching, from 19.6 ± 0.54 branches (n=33) in control larvae to 36.8 ± 1.94 branches (n=31) in $ago^{\Delta 3\text{-}7/1}$ larvae ($p=9.5\text{x}10^{-13}$, Figure 4.2C-E). This increase in terminal cell branch number is similar to that seen in larvae grown in hypoxic conditions (Centanin et al., 2008; Jarecki et al., 1999).

Loss of *ago* function also causes additional tracheal branch phenotypes. These phenotypes include the appearance of terminal branch tangles (Figure 4.2F) and the development of ringlet-shaped ganglionic branches (Figure

4.2G,H). These phenotypes are also seen in hypoxic larvae, or those in which the Fga/dVHL regulatory pathway is disrupted (Centanin et al., 2008). Additionally, we observe overlapping tracheal fields in *ago* mutant larvae (Figure 4.2D). This overlap is not seen in control larvae (Figure 4.2C and Romero et al., 2007) and is unexpected given the precise oxygen-driven mechanism of terminal branch development. Terminal branching is strictly regulated to meet the oxygen demand of larval tissues (Ghabrial et al., 2003), and the excess and overlapped branching seen in *ago* mutant larvae suggests that loss of *ago* uncouples terminal branch morphogenesis from oxygen demand.

Figure 4.1. The *ago*$^{\Delta 3\text{-}7}$ allele specifically deletes the *ago-RC* transcript and is enriched in body wall muscle cells.

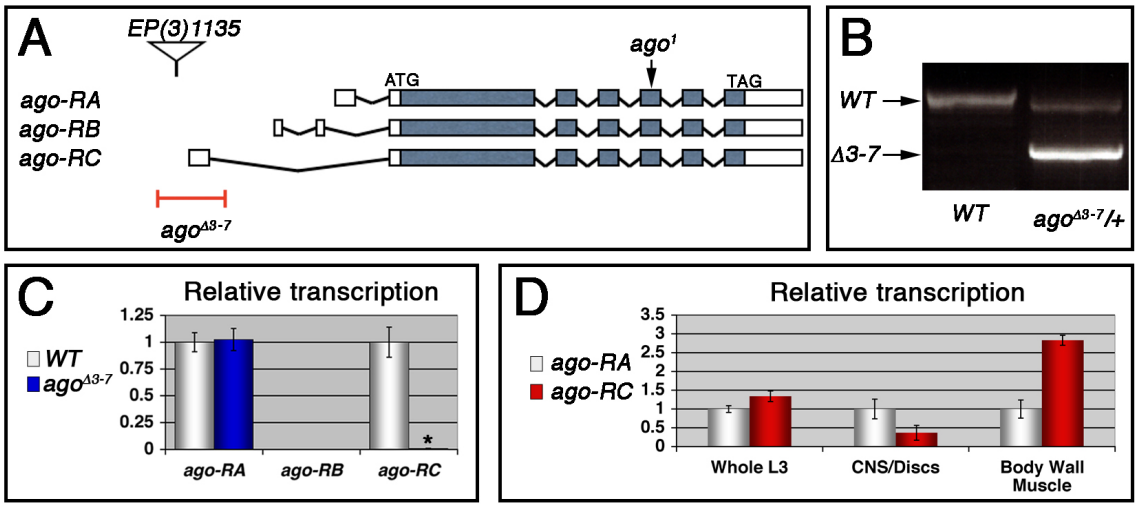

(A) Graphical representation of the *ago* genomic locus illustrating the three *ago* transcripts and alleles used in this study. (B) Genomic PCR to confirm the *ago*$^{\Delta 3\text{-}7}$ deletion. (C) Quantification of the relative transcription of the three *ago* transcripts in larvae in the indicated genotypes by quantitative real-time PCR (qRT-PCR). *p=2.7X10^{-5} relative to control. (D) Tissue specific qRT-PCR of the indicated *ago* transcripts to assay relative abundance in the indicated tissues.

Figure 4.2. *ago*$^{\Delta 3\text{-}7/1}$ larvae display a wide range of tracheal terminal branch phenotypes.

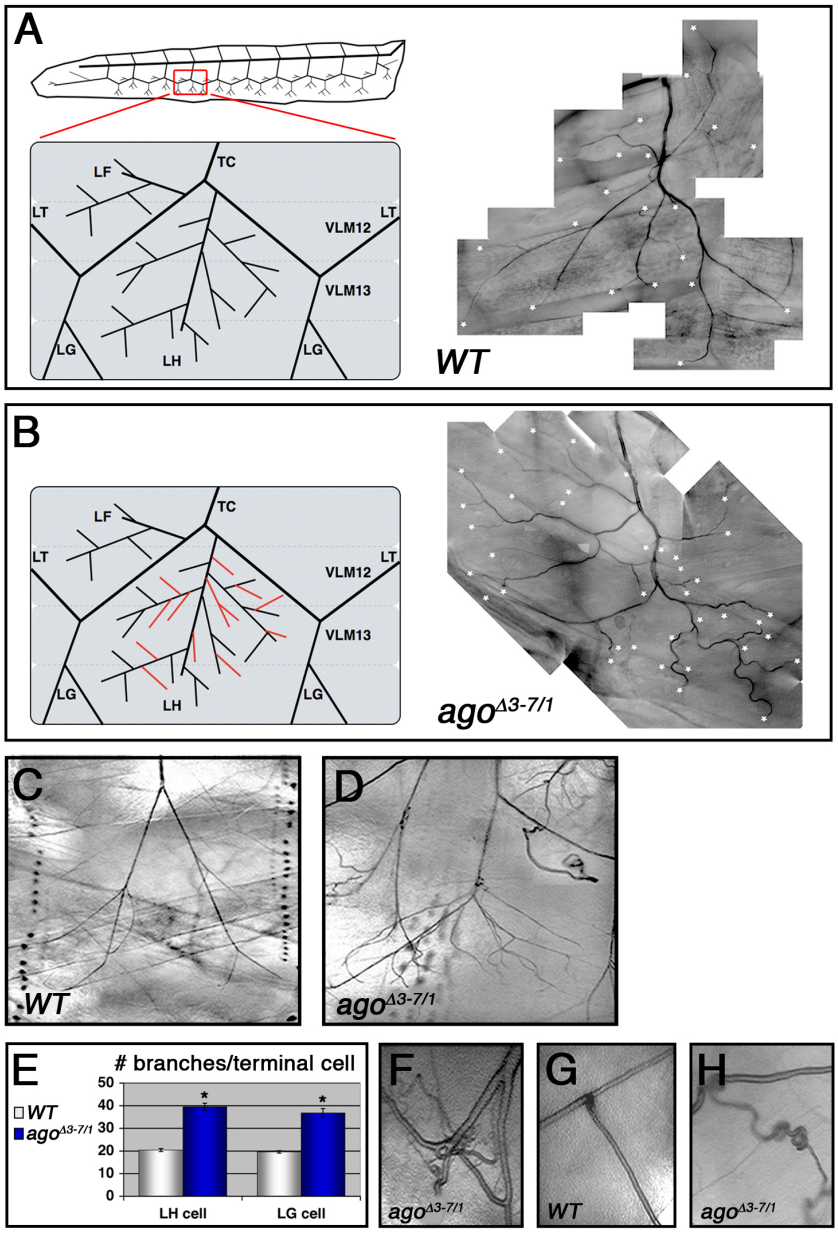

(A) Schematic representation (left) and photomicrograph showing branching of LH lateral terminal cells in control larvae. Branch termini are indicated with asterisks. (B) LH terminal cell branching is increased in *ago*$^{\Delta 3\text{-}7/1}$ larvae, indicated

schematically (red branches, left) and by increased number of branch termini (asterisks). (C,D) Representative images of LG lateral terminal cell branching in control larvae (C) and *ago*$^{\Delta 3\text{-}7/1}$ larvae (D). The *ago*$^{\Delta 3\text{-}7/1}$ mutant displays increased branching and overlapping tracheal fields. (E) Quantification of branch number per LH (left) and LG (right) terminal cell in the indicated genotypes. *$p<0.001$ relative to control (F) *ago*$^{\Delta 3\text{-}7/1}$ larva displaying terminal branch tangling. (G,H) Ganglionic branch development in control (G) and *ago*$^{\Delta 3\text{-}7/1}$ (H) larvae. Appearance of ringlet-shaped ganglionic branches is common in *ago*$^{\Delta 3\text{-}7/1}$ larvae.

4.C. *ago* acts non-autonomously to restrict post-embryonic tracheal branching

While the *ago* mutant terminal branch phenotypes are reminiscent of hypoxia-induced larval tracheal growth, this does not exclude an additional embryonic role for *ago* in regulating the growth of tracheal terminal cells. Post-embryonic induction of a dominant negative *ago* transgene (*UAS-agoΔF*) was used to determine the temporal requirement for *ago* in regulating tracheal terminal branching. Heat shock induction of *agoΔF* in larvae was sufficient to drive an increase in terminal branching (Figure 4.3A). Whereas there was no difference in LH cell branch number prior to transgene induction (22.2 ± 0.89 branches [n=27] vs 21.7 ± 0.69 branches [n=24]), excess LH cell branching was observed twenty-four hours post-induction with an increase in branch number from 22.6 ± 0.67 branches (n=24) in control larvae to 40.2 ± 1.48 branches (n=24) in *agoΔF* larvae ($p=3.0x10^{-14}$). This data demonstrates a role for *ago* in regulating post-embryonic homeostatically driven tracheal terminal branching.

Interestingly, *ago* function is not required in tracheal terminal cells. This suggests that unlike its role in developmental tracheogenesis, *ago* may act non-autonomously to control tracheal terminal branching. Tissue-specific quantitative real-time PCR (qRT-PCR) reveals that the *ago-rc* transcript is specifically enriched in the most highly tracheated tissues in the organism, the body wall muscle (Figure 4.1D) and the gut. That the specific loss of this transcript in the $ago^{\Delta 3-7}$ allele leads to excess terminal branching in these tissues supports this hypothesis.

To test the non-autonomy of the tracheal defects in *ago* mutant larvae, the *UAS-agoΔF* dominant negative transgene was expressed in the ventrolateral body wall muscle VLM12 using the *5053A-Gal4* driver. As indicated by the schematic in Figure 4.3C, *5053A-Gal4* drives expression specifically in VLM12 and excludes the surrounding body wall muscles and tracheal cells. VLM12 specific expression of *UAS-agoΔF* results in an increase in terminal branching relative to either the adjacent VLM13 or to VLM12 in control larvae (5.11 ± 0.16 branches [n=54] in control vs 9.54 ± 0.29 branches [n=50] in *agoΔF*, $p=4.67x10^{-24}$, Figure 4.3B). Expression of dominant negative *ago* does not change the pattern of terminal branching, VLM12 is still tracheated exclusively by the LF and LH terminal cells, but does change the extent of branching of these two terminal cell types, leading to an approximate doubling of both LF and LH branches terminating on VLM12 (Figure 4.3C,D). This data demonstrates that *ago* is required to restrict post-embryonic tracheal terminal branching in a non-autonomous manner.

Figure 4.3. Terminal branch phenotypes associated with post-embryonic and body wall muscle specific induction of *ago-ΔF*.

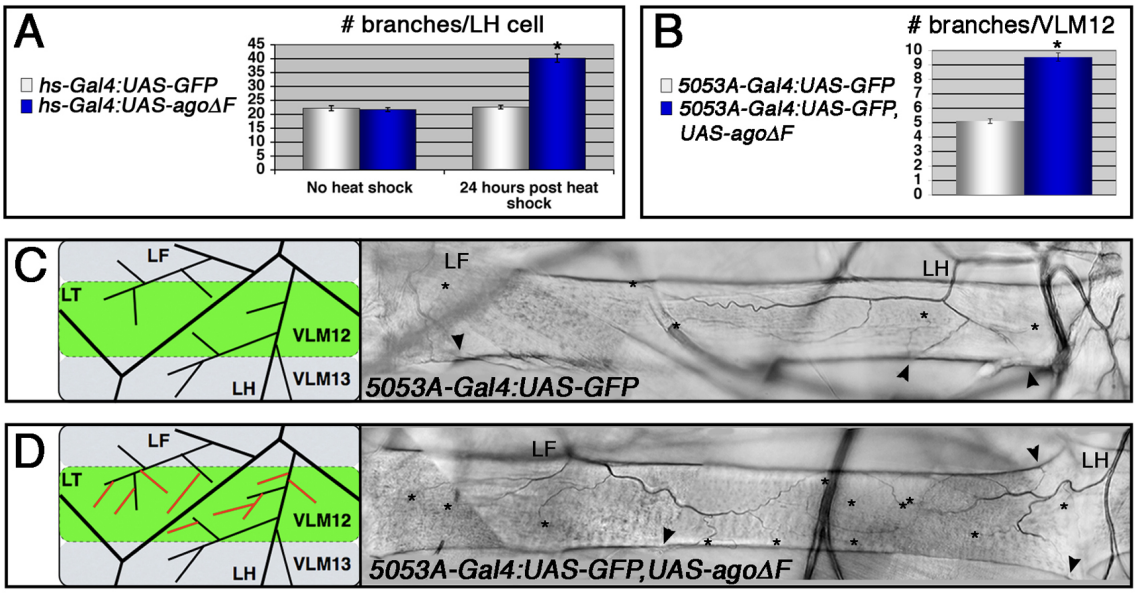

(A) Quantification of number of branches per LH terminal cell in the indicated genotypes before (left) and after (right) heat shock treatment. *$p=3.0x10^{-14}$ relative to heat shocked control. (B) Quantification of number of branches terminating on VLM12 in the indicated genotypes. *$p=4.67x10^{-24}$ relative to control. (C,D) Schematic (left) and photomicrograph depiction of LH and LF lateral terminal cell branch termini on VLM12 in *5053A-Gal4* control (C) and *5053A-Gal4:UAS-agoΔF* (D) larvae. Terminal branches terminating on VLM12 are indicated by asterisks. Arrowheads mark terminal branches with termini elsewhere.

4.D. The deregulation of tracheal terminal branching reveals a novel *ago* target

The *Drosophila ago* ubiquitin ligase subunit has multiple targets including the proliferative proteins CycE and dMyc (Moberg et al., 2001; Moberg et al., 2004), and the transcription factor Trachealess (Trh). Since the role of a ubiquitin ligase is to restrict levels of its target proteins, over-expression of these known *ago* targets, along with the putative target Notch, was assayed for the ability to phenocopy expression of *agoΔF* in VLM12. We find that muscle specific expression of Trh or Notch fails to stimulate excess terminal branch growth (Table 4.1), as does expression of dMyc, despite a 28.5% increase in VLM12 size (Tables 4.1 and 4.2). CycE expression does cause an increase in terminal branch number (Table 4.1), but as CycE protein levels are not affected by expression of *agoΔF* (Figure 4.4), deregulation of CycE is unlikely to account for the *ago* mutant phenotypes. Interestingly, *ago* does not appear to regulate the size (Table 4.2) or number of body wall muscles, suggesting that its role in regulating terminal branching is separable from any proliferative role. The failure of Trh overexpression to phenocopy loss of *ago* further suggests that these tracheal terminal phenotypes are separable from its developmental role and represent deregulation of a novel *ago* target.

Figure 4.4. Loss of *ago* does not deregulate Cyclin E levels in body wall muscle cells.

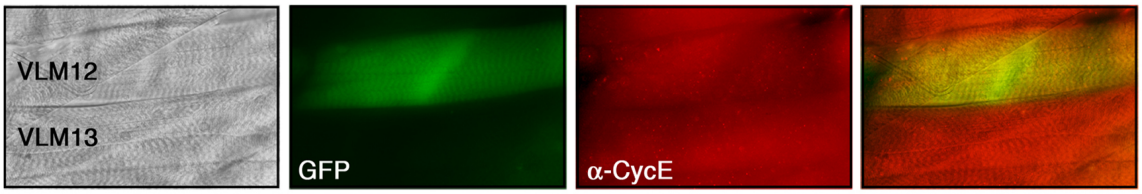

5053A-Gal4:UAS-GFP,UAS-agoΔF

Comparison of Cyclin E levels in VLM12 and VLM13 in *5053A-Gal4:UAS-GFP;UAS-agoΔF* larvae. Larvae were stained with α-Cyclin E antiserum (red). GFP marks VLM12 (green).

Table 4.1. Quantification of terminal tracheal branch phenotypes

Genotype	Branches/VLM12	n=
5053A-Gal4:UAS-GFP	5.11 ± 0.16	54
5053A-Gal4:UAS-GFP,UAS-trh	4.97 ± 0.25	31
5053A-Gal4:UAS-GFP,UAS-CycE	7.39 ± 0.49	18
5053A-Gal4:UAS-GFP,UAS-dMyc	4.86 ± 0.25	50
5053A-Gal4:UAS-GFP,UAS-N	4.27 ± 0.41	15
5053A-Gal4:UAS-GFP,UAS-sima	13.67 ± 0.61	48

Table 4.2. Size of VLM12

Genotype	VLM12 size (sq. μ)	n=
5053A-Gal4:UAS-GFP	16143 ± 520	22
5053A-Gal4:UAS-GFP,UAS-agoΔF	15515 ± 372	25
5053A-Gal4:UAS-GFP,UAS-dMyc	20740 ± 732[a]	22

[a]$p<0.001$ relative to *5053A-Gal4:UAS-GFP*

4.E. Loss of *ago* leads to deregulated dHIF activity

Based on the similarity of the increased *ago* mutant terminal branching with the tracheal growth seen in response to hypoxia, we hypothesized that the uncoupling of terminal branch growth from oxygen availability seen in *ago* mutants was due to deregulation of the hypoxic response. In support of this idea, we find that an allele of *sima* dominantly suppresses the *agoΔF* VLM12 phenotype, decreasing terminal branch number from 9.54 ± 0.29 (n=50) to 6.34 ± 0.27 branches (n=53, $p=4.36x10^{-12}$, Figure 4.5A). *sima* heterozygosity further suppresses the excess terminal branching seen in $ago^{\Delta 3-7/1}$ larvae from 39.5 ± 1.59 (n=34) to 29.0 ± 1.48 branches per LH cell (n=34, $p=7.45x10^{-6}$). We further find that unlike ectodermal cells (Centanin et al., 2008), ectopic expression of *sima* in muscle cells leads to an increase in terminal branching (Table 4.1).

This genetic dependence on *sima* suggests that dHIF transcriptional activity may be increased in *ago* mutant tissues. To test this idea, we assayed the transcription of *Drosophila lactate dehydrogenase* (*dLDH*), a known dHIF target (Bruick & McKnight, 2001), in the body wall muscle of $ago^{\Delta 3-7}$ and control larvae, and found a 27.3-fold increase in *dLDH* transcription in *ago* mutants (Figure 4.5B). Interestingly, this increase is not due to elevated *sima* transcription (Figure 4.5B), suggesting a post-transcriptional increase in dHIF activity.

Figure 4.5. *ago* terminal branch phenotypes are dependent on *sima* and *bnl*.

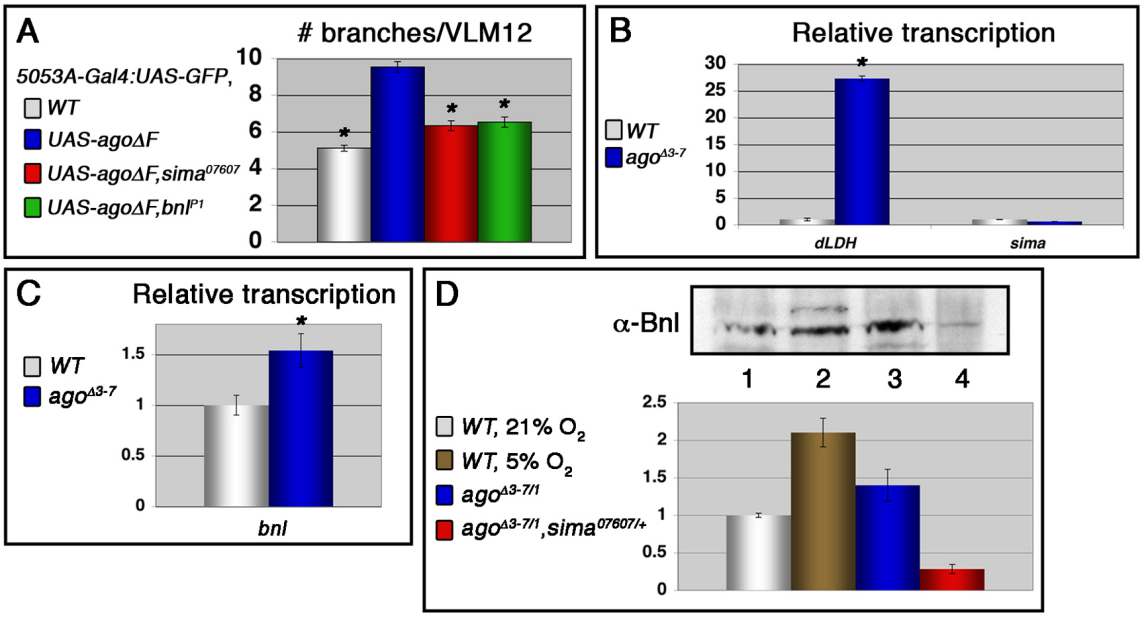

(A) Quantification of terminal branching on VLM12 in the indicated genotypes. *p<0.001 relative to *5053A-Gal4:UAS-GFP;UAS-agoΔF*. (B) Quantification of *dLDH* (left) and *sima* (right) transcription in the body wall muscles of larvae of the indicated genotypes by qRT-PCR. *p<0.001 relative to control. (C) Quantification of *bnl* transcription in the body wall muscles of larvae of the indicated genotypes by qRT-PCR. *p=3.2x10^{-2} relative to control. (D) Expression of Bnl. (Top) Representative Bnl immunoblot in normoxic (lane 1), hypoxic (lane 2), *ago*$^{\Delta 3\text{-}7/1}$ (lane 3) and *ago*$^{\Delta 3\text{-}7/1}$, *sima/+* (lane 4) larvae. (Bottom) Quantification of Bnl protein levels in the indicated genotypes normalized by larval equivalents.

4.F. Loss of *ago* induces terminal branching a via *sima* dependent increase in *bnl* expression

The *Drosophila* hypoxic response leads to a demonstrated increase in *bnl* expression (Figure 4.5D and Centanin et al., 2008; Ghabrial et al., 2003; Jarecki et al., 1999). Recent work has shown that this increase is, at least in part, due to a *sima* dependent increase in *bnl* transcription (Centanin et al., 2008). We therefore assayed the ability of the bnl^{P1} allele to suppress the *ago* mutant phenotype and found a dominant suppression of both the *agoΔF* VLM12 phenotype, from 9.54 ± 0.29 (n=50) to 6.54 ± 0.28 branches (n=54, $p=5.99x10^{-11}$, Figure 4.5A) and of the $ago^{\Delta 3-7/1}$ excess branching, from 39.5 ± 1.59 (n=34) to 28.4 ± 1.80 branches per LH cell (n=29, $p=1.75x10^{-5}$).

These findings suggest that *bnl* expression may be upregulated in *ago* mutant larvae. Accordingly we find a 53.9% upregulation of *bnl* transcription in body wall muscle of $ago^{\Delta 3-7}$ larvae relative to control (Figure 4.5C). Previous studies using a genomic duplication of the *bnl* locus have demonstrated that this 50% increase is sufficient to drive significant terminal branch growth (Jarecki et al., 1999). This transcriptional increase is reflected in an increase of Bnl protein levels in $ago^{\Delta 3-7/1}$ larvae (Figure 4.5D). This increased expression of Bnl in *ago* mutant larvae is dominantly suppressed by an allele of *sima* (Figure 4.5D). Heterozygosity for *sima* further leads to a significant decrease in Bnl levels relative to control larvae, suggesting that both endogenous expression of Bnl and the ectopic expression seen in *ago* mutant larvae are largely dependent on *sima*. Thus it appears that the excess tracheal branching observed in body wall

muscles lacking *ago* function is due to ectopic activation of dHIF resulting in increased Bnl expression (Figure 4.6).

Figure 4.6. Excess terminal branching in *ago* mutants to due deregulated Bnl signaling.

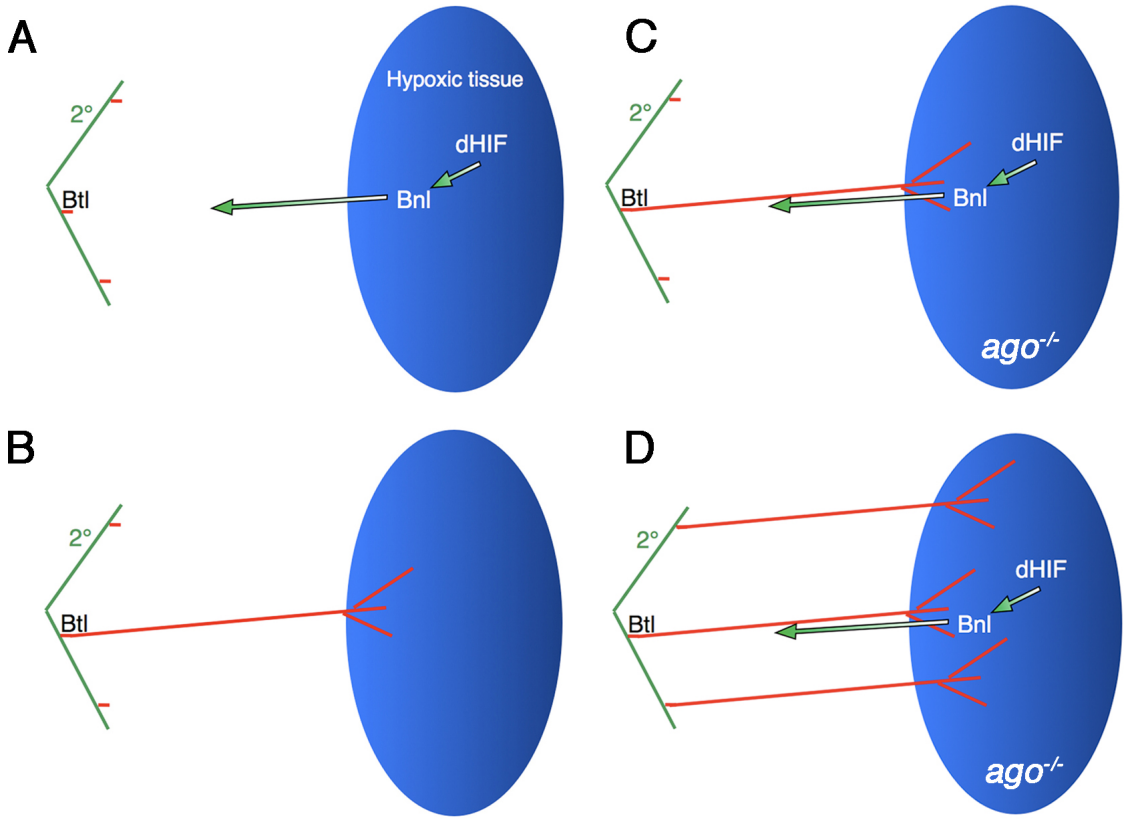

Shown schematically, (A) dHIF is stabilized in hypoxic tissue, driving expression of Bnl. In wild type larvae (B), the Bnl signal is recieved by the tracheal terminal cell causing it to elaborate a series of branches toward the hypoxic tissue. This oxygenation then turns off the hypoxic response. In *ago* mutants (C), Bnl expression persists in the oxygenated tissue, leading to excess terminal branch elaboration (D).

4.G. *ago* acts co-operatively with *dVHL* to regulate tracheal terminal branching

These data suggest that *ago* functions as a second dHIF regulatory mechanism, along with the Fga/dVHL pathway. This could reflect a tissue specificity for the roles of *ago* and *dVHL*, or may suggest that they act in parallel to provide increased regulation of dHIF activity. To address the tissue-specificity hypothesis, we first used reverse transcriptase-PCR (RT-PCR) to assay the presence of *dVHL* mRNA in the body wall muscles and found that this tissue does express *dVHL* (Figure 4.7). A highly efficient *dVHL* RNAi knock-down transgene (*dVHL^{i}*) was then expressed using the *5053A-Gal4* driver to determine the role of *dVHL* in regulating tracheal branching in this tissue. We find that expression of *dVHL^{i}* in VLM12 leads to an increase in terminal branching relative to a non-specific RNAi control (5.28 ± 0.20 branches [n=40] in *Adf1^{i}* control vs 7.48 ± 0.21 branches [n=89] in *dVHL^{i}*, $p=1.27x10^{-9}$, Figure 4.8A), suggesting that *dVHL* is required to regulate Sima stability in larval body wall muscle cells.

We further find that co-expression of *dVHL^{i}* with *agoΔF* has an additive effect on terminal branching (Figure 4.8A). The combined knock-down of *dVHL* and *ago* leads to the appearance of a phenotype not seen in either alone. Whereas expression of *agoΔF* or *dVHL^{i}* alone increases terminal branch number due to excess branching of the terminal cells that normally tracheate VLM12, the LF and LH lateral terminal cells, co-expression in VLM12 leads to both increased LF and LH branching along with the recruitment of ectopic branches from the LG lateral terminal cell (Figure 4.8B,C). This ectopic recruitment phenotype is also

seen when *sima* (data not shown) or *bnl* (Jarecki et al., 1999) are transgenically overexpressed in VLM12, suggesting that the combined knock-down of *ago* and *dVHL* leads to an increased tracheogenic signal strength.

To further understand the relationship between the roles of *ago* and *dVHL* in regulating terminal branching, we used transgenic overexpression and knock-down constructs for epistatic analysis. If *ago* and *dVHL* act in a linear pathway, these 'add-back' experiments should reveal an epistatic relationship with the prediction that over-expression of the 'down-stream' member should rescue loss of the 'up-stream' member, but that the reverse should not be true. However if they act in parallel on the same target, *ago* and *dVHL* should be able to 'replace' each other. We found that over-expression of wildtype *dVHL* showed a 66.4% suppression of the *agoΔF* branching phenotype ($p=6.55x10^{-12}$, Figure 4.8A and Table 4.3), and conversely that over-expression of wildtype *ago* showed a 54.1% suppression of the $dVHL^{i}$ branching phenotype ($p=2.73x10^{-4}$, Figure 4.8A and Table 4.3). This data supports the second hypothesis and suggests that the *ago* and *dVHL* ubiquitin ligases work in parallel on a common target to regulate dHIF activity.

Figure 4.7. *dVHL* is expressed in larval body wall muscles.

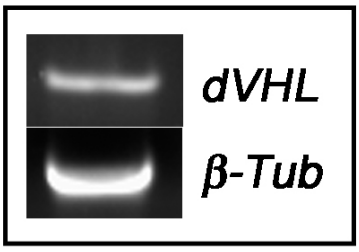

Reverse transcriptase PCR (RT-PCR) analysis of *dVHL* and *β-Tub* mRNA levels in larval body wall muscles.

Figure 4.8. *ago* and *dVHL* regulate terminal branching.

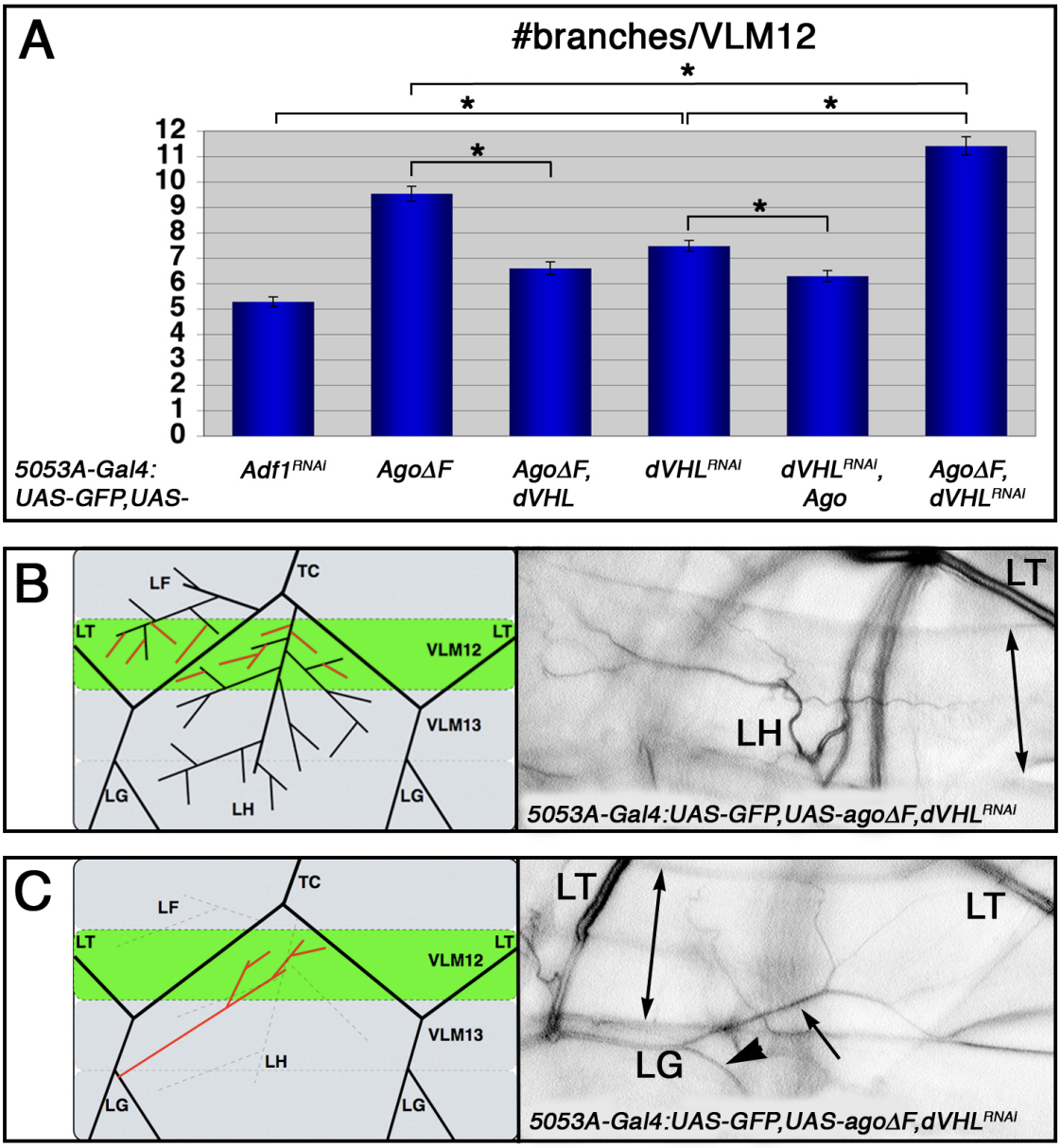

(A) Quantification of VLM12 terminal branching in larvae of the indicated genotypes. *p<0.001. (B,C) Terminal branch phenotypes of *ago* and *dVHL* double-knockdown larvae. (B) Schematic (left) and photomicrograph showing increased LF and LH cell terminal branching on VLM12. Double-headed arrow indicates VLM12. (C) Schematic (left) and photomicrograph showing ectopic

recruitment of LG cell terminal branches to VLM12. Arrow, LG branch recruited to VLM12; arrowhead, LG branch following its typical course; double-headed arrow indicates VLM12.

Table 4.3. Quantification of terminal tracheal branch phenotypes

Genotype	Branches/VLM12	n=
5053A-Gal4:UAS-GFP,UAS-Adf1^{RNAI}	5.28 ± 0.20	40
5053A-Gal4:UAS-GFP,UAS-agoΔF	9.54 ± 0.29[a]	50
5053A-Gal4:UAS-GFP,UAS-dVHL^{RNAi}	7.48 ± 0.21[a]	89
5053A-Gal4:UAS-GFP,UAS-agoΔF,UAS-dVHL^{RNAi}	11.42 ± 0.36[b.c]	52
5053A-Gal4:UAS-GFP,UAS-agoΔF,UAS-dVHL	6.60 ± 0.25[b]	55
5053A-Gal4:UAS-GFP,UAS-ago,UAS-dVHL^{RNAi}	6.29 ± 0.22[c]	52

$p<0.001$ relative to [a]*5053A-Gal4:UAS-GFP,UAS-Adf1^{RNAI}*; [b]*5053A-Gal4:UAS-GFP,UAS-agoΔF*; [c]*5053A-Gal4:UAS-GFP,UAS-dVHL^{RNAi}*

4.H. Loss of *ago* alters the sensitivity of the transcriptional response to hypoxia

The *Drosophila* hypoxic response is sensitive to the severity of hypoxia, driving transcription of distinct sets of target genes at differing oxygen concentrations (Liu et al., 2006), including genes predicted to be involved in tracheogenesis, metabolic adaptation and survival in low oxygen. Based on the novel role for *ago* in regulating dHIF activity, we would predict that loss of *ago* should change the sensitivity of this response. To assay the role of *ago* in global hypoxia-mediated transcription, expression of a subset of hypoxia-inducible target genes was measured by qRT-PCR in normoxic and hypoxic larvae. These target genes were chosen based on their differential transcription in hypoxic adult *Drosophila* (Liu et al., 2006) and predicted links to known mechanisms of the hypoxic response. Selected target genes include *dLDH* which is predicted to play a role in the metabolic switch to high flux glycolysis (Semenza, 2007), *lysyl oxidase* (*lox*), a gene induced by HIF in hypoxic mammalian cells leading to changes in cell adhesion (Erler et al., 2006) and predicted to play a role in vascular (and possibly tracheal) remodeling (Rodriguez et al., 2008), and *CG11825*/*dHIG1*, the *Drosophila* homolog of Hypoxia induced gene 1 (HIG1), the expression of which is associated with hypoxic survival in pancreatic cells (Wang et al., 2006). qRT-PCR analysis reveals that these targets are differentially induced in hypoxia in a manner consistent with findings in adult *Drosophila* (Liu et al., 2006), and are sensitive to loss of *ago* function.

The metabolic gene *dLDH* is minimally transcribed in normoxic control larvae, and with progressively higher transcription as the oxygen level falls (1.6 and 2.7-fold increases in 5% and 0.5% O_2 respectively, Figure 4.9A), suggesting that *dLDH* transcription is proportional to dHIF activity. In *ago* mutants it is ectopically transcribed in normoxic body wall muscles (Figure 4.5B) and whole larvae (8.1-fold induction, Figure 4.9B, top panel). Additionally, the hypoxic induction of *dLDH* is approximately 14-fold higher in $ago^{\Delta 3\text{-}7/1}$ larvae than control larvae at both 5% and 0.5% O_2 (Figure 4.9B, top panel). These findings indicate that unlike the Fga/dVHL mechanism, *ago* regulates dHIF activity with equal efficiency throughout the range of oxygen concentrations.

Analysis of *lox* transcription reveals that in control larvae this gene is not transcriptionally induced in the mild 5% O_2 hypoxic condition, but is upregulated in more severe conditions, with a 4.4-fold induction at 0.5% O_2 (Figure 4.9A). Loss of *ago* leads to a 2.2-fold increase in *lox* transcription in normoxia (Figure 4.9B, middle panel), and in 5% O_2 *lox* transcription reaches near maximal levels; the 3.4-fold induction seen in *ago* mutants in 5% O_2 is not significantly different from that seen in control larvae at 0.5% O_2 (Figure 4.9B, middle panel). The pattern of *lox* induction suggests that the promoter is sensitive only to the levels of dHIF activity normally achieved in severe hypoxic conditions, but that this threshold is more easily reached in *ago* mutants where dHIF activity is already deregulated.

The putative hypoxia survival gene *dHIG1* displays a similar pattern of hypoxic induction. Whereas *dHIG1* mRNA levels are only mildly (2-fold) elevated

in 5% O_2, transcription is strongly (19.9-fold) upregulated in 0.5% O_2 (Figure 4.9A), suggesting that like *lox*, *dHIG1* transcription is only activated by the level of dHIF activity specific to severe hypoxia. In contrast to the normoxic induction of *dLDH* and *lox*, loss of *ago* is not sufficient to drive ectopic *dHIG1* transcription in normoxic conditions (Figure 4.9B, bottom panel). However the promoter is strongly sensitized to hypoxia-induced transcription in $ago^{\Delta 3\text{-}7/1}$ larvae. *dHIG1* induction reaches maximal levels at 5% O_2, with no significant increase at 0.5% O_2 (Figure 4.9B, bottom panel), again suggesting that loss of *ago* alters the threshold of hypoxia required for maximal dHIF activation. The altered transcription of hypoxia induced genes in *ago* mutant larvae is consistent with a model in which *ago* acts to regulate dHIF activity across oxygen concentrations to provide increased specificity to the hypoxic response.

Figure 4.9. Altered transcriptional response to hypoxia in *ago* mutant larvae.

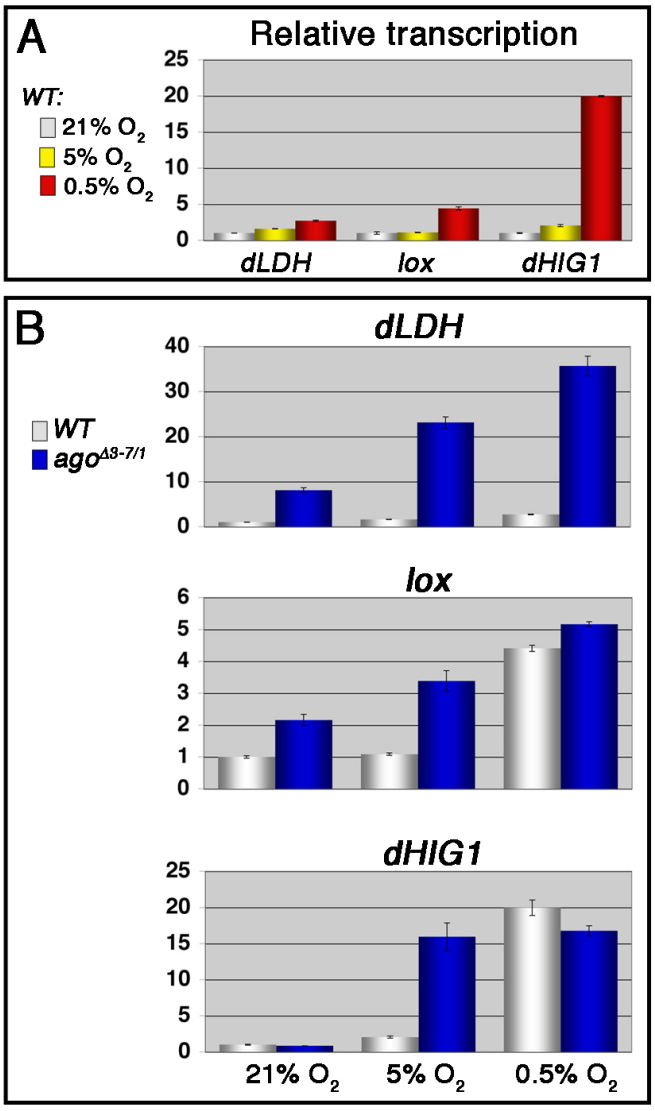

(A) Quantification of *dLDH* (left), *lox* (center) and *dHIG1* (right) transcription in control larvae in the indicated conditions by qRT-PCR. (B) Quantification of *dLDH* (top), *lox* (middle) and *dHIG1* (bottom) transcription in the indicated genotypes by qRT-PCR in 21% (left), 5% (center) and 0.5% (right) oxygen.

4.I. Hypoxia tolerance of adult *Drosophila* is regulated by *ago*

Drosophila respond to prolonged periods of oxygen deprivation by entering into a state of hypoxic stupor characterized by inactivity and reduced oxygen consumption (Krishnan et al., 1997). Adult flies enter stupor after approximately fifteen to twenty minutes in a 0.5% O_2 environment and remain unconscious until re-oxygenation. Based on the altered transcriptional response to hypoxia in *ago* mutant larvae, we hypothesized that decreased *ago* expression in adult flies would lead to an altered organismal response to hypoxia.

We assayed control and $ago^{\Delta 3\text{-}7/EP(3)1135}$ adult flies for two aspects of hypoxia tolerance: recovery time following acute (1 hour) hypoxia and survivability in chronic (16 hour) hypoxia. We find that $ago^{\Delta 3\text{-}7/EP(3)1135}$ flies display no obvious developmental phenotypes and enter into hypoxic stupor at the same rate as control flies. After one hour at 0.5% O_2 average recovery time was measured. Recovery from hypoxia was defined as the time required for a fly to resume walking following re-oxygenation. Shown in Figure 4.10A are average recovery times of five to seven day old control and *ago* mutant flies from seven independent experiments (*WT* n=90 flies, *ago* n=88 flies). While flies of both genotypes began to recover within the first minute of re-oxygenation, we find that the *ago* mutant flies recover significantly faster than controls (Figure 4.10A). Using linear regression analysis we estimate that the time for 50% recovery is reduced from 4.5 ± 0.75 minutes in control flies to 1.4 ± 0.16 minutes in $ago^{\Delta 3\text{-}7/EP(3)1135}$ flies (p=0.0015). We further find that 100% of *ago* mutant flies have resumed walking after ten minutes of recovery time, whereas the control flies

were not completely recovered at the end of the fifteen minute measurement period.

As a second measure of hypoxia tolerance, we assayed the survivability of five to seven day old control and *ago*$^{\Delta 3\text{-}7/EP(3)1135}$ adult flies after sixteen hours in 0.5% O_2. Survival rates were measured following a twenty-four hour recovery period (Figure 4.10B), and the data presented represents the average of six independent experiments (*WT* n=89 flies, *ago* n=84 flies). *ago* mutants show decreased survivability following exposure to chronic hypoxia; control flies had an 88.7 ± 6.1% survival rate compared to a 66.2 ± 3.7% survival rate in *ago*$^{\Delta 3\text{-}7/EP(3)1135}$ flies (p=0.011). This suggests that the ability to regulate dHIF is essential, even during prolonged periods of oxygen deprivation. These findings demonstrate a clear role for *ago* in the response to hypoxia at the organismal level.

Figure 4.10. Altered hypoxic response in *ago* mutant adult flies.

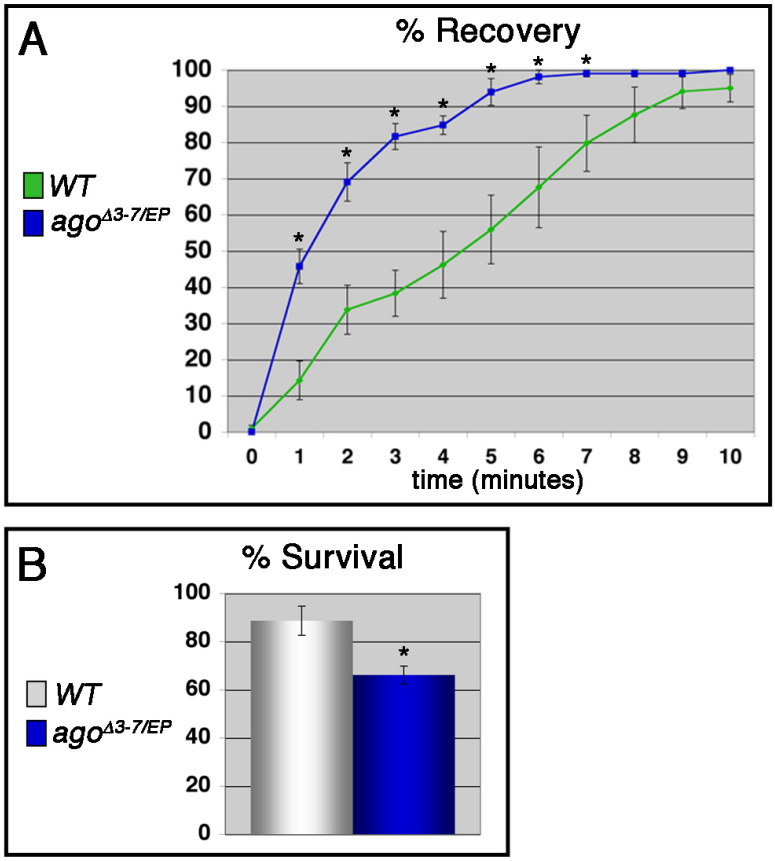

(A) Quantification of post-hypoxic recovery time in adult *Drosophila* of the indicated genotypes following acute hypoxia. *p<0.05 relative to control. (B) Survival of adult *Drosophila* following chronic hypoxia of the indicated genotypes. *p=0.011 relative to control.

4.J. Discussion of results

The *ago* ubiquitin ligase plays an important role in restricting Btl/FGF signaling during two distinct phases to regulate tracheogenesis. In the first phase *ago* acts to restrict *btl* transcription in tracheal cells by regulating levels of the transcription factor Trh during embryogenesis. Here we have described a novel second phase in which *ago* is required to restrict growth of tracheal terminal branches. Terminal branch growth is driven by the homeostatically-regulated induction of *bnl* via an oxygen/dHIF dependent mechanism. *ago* mutant larvae display a *sima* and *bnl* dependent increase in tracheal terminal branching in normoxic conditions, suggesting that loss of *ago* uncouples tracheogenesis from oxygen demand. This excess tracheogenesis is due to an upregulation of *bnl* mRNA and protein levels in *ago* mutant larval body wall muscles in a *sima* dependent manner, suggesting that *ago* acts to restrict *bnl* at the transcriptional level. Furthermore we find that while a genomic duplication of the *bnl* locus is sufficient to drive excess tracheal growth (Jarecki et al., 1999), the *ago* mutant phenotype is more severe, despite a similar increase in *bnl* levels. This suggests that other dHIF target genes may also play a role in this process.

In normoxic conditions, *ago* mutant larvae display evidence of an ectopic hypoxic response. Along with the excess recruitment of oxygen-conducting organs due to altered growth factor signaling, a subset of hypoxia inducible genes are ectopically transcribed in *ago* larvae. Transcription of the hypoxic response genes *dLDH*, *lox*, *hairy*, *amy-p* and *thor* is induced by hypoxia in *Drosophila* (Liu et al., 2006) and these targets are significantly upregulated in

normoxic *ago* larvae (Figure 4.9B and Table 4.4). These findings suggest that along with increased tracheogenesis, *ago* mutant larvae also likely display the switch to high-flux glycolysis and other hypoxia-induced changes characteristic of hypoxic cells. Furthermore, loss of *ago* leads to changes in the transcriptional response to hypoxia. In wild type larvae and adult flies this transcriptional response is strictly regulated such that different target genes are induced at 5% and 0.5% environmental O_2 (Figure 4.9A and Liu et al., 2006). In *ago* mutants this differential target gene induction is largely abolished; the induction of targets such as *lox* and *dHIG1* is virtually indistinguishable at 5% and 0.5% O_2.

Our findings demonstrate that *ago* regulates dHIF both in normoxic and hypoxic conditions. It further suggests that the role of *ago* is to limit overall levels of dHIF to allow for response sensitivity. We hypothesize that the hypoxic sensitivity is a product of the interaction between the Ago and Fga/dVHL HIF regulatory mechanisms. The HPH/VHL pathway has been demonstrated to act in graded manner, such that it effectively degrades HIF-1α at normoxia and then works with decreasing efficiency as the oxygen concentration drops (Jiang et al., 1996b). This leads to a gradient of HIF activity which is presumably required for the differential induction of target genes. Additionally, since *ago* regulates dHIF activity throughout all oxygen concentrations, we hypothesize that in its absence dHIF activity quickly accumulates and the amount of activity in 5% O_2 is no longer distinguishable from 0.5% O_2 leading to the altered response in *ago* mutant larvae. The data presented here provide further support for the hypothesis that *ago* acts in the regulation of oxygen homeostasis in *Drosophila*.

Table 4.4. Transcription of hypoxia inducible genes in normoxic *ago* larvae

Target gene	Relative Transcription[a]	p=[b]
dLDH	27.3 ± 0.47[c]	6.06×10^{-5}
dLDH	8.11 ± 0.52[d]	4.97×10^{-4}
lox	2.16 ± 0.17[d]	6.38×10^{-3}
hairy	1.19 ± 0.02[d]	1.11×10^{-3}
amy-p	2.03 ± 0.07[d]	9.87×10^{-5}
thor	1.18 ± 0.05[c]	2.99×10^{-2}

[a] transcription normalized to *WT* control larvae, [b] p value relative to control (Student's t-test), [c] body wall muscle, [d] whole larvae

Chapter Five: Discussion of findings and concluding remarks

5.A. *archipelago* plays a conserved role in tubular morphogenesis

Consistent with the vascular defects observed in the *archipelago* (*ago*)*/Fbw7* knock-out mouse model (Tetzlaff et al., 2004; Tsunematsu et al., 2004), our work has uncovered a role for *ago* in the development of the tracheal network in *Drosophila*. The elaboration of such branched oxygen-conducting networks plays an essential role in organismal development and oxygen homeostasis. The mechanisms driving the morphogenesis of these networks are conserved across species, and the F-box protein *ago* clearly plays a role in this process.

In *Drosophila, ago* regulates levels of the Trachealess (Trh) transcription factor in developing tracheal cells. Loss of function mutations in *ago* lead to an accumulation of Trh in tracheal cells and a subsequent increase in transcription of the FGF receptor homolog *breathless* (*btl*). This ectopic Btl/FGF signaling is sufficient to produce the tracheal morphogenetic defects seen in *ago* mutant embryos.

The model of *ago* function in regulating tubular morphogenesis in the *Drosophila* tracheal system differs from that proposed for *Fbw7* function in the mouse. The vascular defects in *Fbw7* mouse knock-out models have been attributed to deregulation of Notch levels in the developing vasculature (Tetzlaff et al., 2004; Tsunematsu et al., 2004). *Notch* plays similar roles in the development of both the *Drosophila* trachea and mammalian vascular system. In both cases, *Notch* is required for specification of the lead branch cell; known as the fusion cell in the *Drosophila* trachea or as the tip cell in mammalian angiogenesis (Hellstrom et al., 2007; Ikeya & Hayashi, 1999; Llimargas, 1999;

Steneberg et al., 1999; Suchting et al., 2007). However, all available evidence suggests that a putative role for *ago* in the regulation of Notch levels in *Drosophila* is separate from the mechanism by which *ago* regulates tracheal morphogenesis. *Notch* overexpression in tracheal cells leads to a failure to specify fusion cells and branch migration/fusion defects (Ikeya & Hayashi, 1999) but not the other defects seen in *ago* mutant embryos. Additionally, fusion cell specification is not affected in *ago* mutant embryos (see Figure 2.3), further discounting a role for deregulation of Notch in the *ago* tracheal phenotypes.

Based on the high degree of conservation between tubular morphogenetic processes in *Drosophila* and mammals, I would predict that the role of *ago* in restricting Btl/FGF signaling via regulation of Trh levels may also be conserved. Mammalian *trh* homologs include the *npas1* and *npas3* transcription factors. These genes were initially characterized by their neuronal expression (Brunskill et al., 1999; Zhou et al., 1997), but have more recently been shown to play roles in mediating FGF signaling via transcription of the FGF receptor (FGFR, Pieper et al., 2005) and tubular morphogenesis in the developing lung (Levesque et al., 2007). The potentially conserved roles of these Trh homologs may suggest a model in which *ago/Fbw7* regulates mammalian vascular formation by regulation of both Notch and FGF signaling and that the defects in the *Fbw7* knock-out mice may be due to a combined deregulation of these pathways.

If this model was confirmed, it may help to further understand the role of *ago*/*Fbw7* as a tumor suppressor. Ectopic FGF signaling is implicated in the progression of many forms of cancer. In a mouse model, inducible expression of

FGFR isoforms leads to tumorigenesis in both mammary and prostate tissue (Freeman et al., 2003; Welm et al., 2002). This ectopic FGF signaling has been shown to contribute to tumorigenesis by promoting both increased angiogenesis (Winter et al., 2007), and an epithelial-to-mesenchymal transition resulting in increased metastasis (Acevedo et al., 2007). Not surprisingly, over-expression of FGFR isoforms plays an important role in initiation of human cancers, including both oral and prostate cancer (Giri et al., 1999; Vairaktaris et al., 2006). Additionally, hyper-activating mutations in these genes also lead to formation of endometrial and bladder tumors (Pollock et al., 2007; Tomlinson et al., 2007). Interestingly, there are a subset of bladder tumors in which FGFR is over-expressed, leading to hyper-activated FGF signaling, in the absence of mutations in the *FGFR* genes (Tomlinson et al., 2007). This data implies that negative regulators of FGFR, potentially including *ago*/*Fbw7*, can play an important role in suppressing *FGFR*-mediated tumorigenesis.

5.B. Mechanisms of *ago*-mediated Trh regulation

There are two distinct mechanisms underlying the ability of *ago* to regulate Trh levels. Firstly, a tracheal-wide mechanism in which Ago physically interacts with Trh in both WD repeat-dependent and independent manners leading to a modest reduction in Trh levels in cultured S2 cells (see Figure 2.9). The *in vivo* role of this mechanism is to maintain levels of Trh within a developmentally defined limit. Accordingly, loss of *ago* leads to a slight overall increase in Trh levels in all tracheal cells (see Figure 2.6). Secondly, *ago* participates in the *dysfusion* (*dys*)-stimulated elimination of Trh in tracheal fusion cells. As previously shown, the fusion cell specific expression of *dys* leads to rapid elimination of Trh protein (see Figure 2.6; Jiang & Crews, 2003; Jiang & Crews, 2006), and expression of *dys* in cultured S2 cells also stimulates the complete elimination of Trh (see Figure 2.9). In this mechanism, the Ago:Trh interaction is entirely WD repeat-dependent, and *ago* is required for the *dys*-mediated elimination of Trh both *in vitro* and *in vivo* (see Figures 2.6, 2.9).

Analysis of *dys* loss of function mutations implies that both of these mechanisms are required for *ago* function in tracheal morphogenesis. *dys* mutant embryos are incapable of fusion cell specific elimination of Trh. However, this is not sufficient to cause dorsal trunk (DT) migration/fusion defects (although *dys* mutants show migration defects in other tracheal branches, see Jiang & Crews, 2003; Jiang & Crews, 2006). The high penetrance of DT migration/fusion defects in *ago* mutant embryos suggests that the regulation of baseline Trh levels, along

with *dys*-stimulated elimination of Trh in fusion cells, are both required to prevent ectopic *btl* transcription and Btl/FGF signaling in DT fusion cells.

Drosophila tracheal and S2 cells thus provide a good system in which to study this novel aspect of *ago* functional regulation. The switch between the low-level and rapid degradative mechanisms may reflect either a higher affinity of Ago for its substrate or a greater ubiquitination efficiency. The ability of Dys to flip this mechanistic switch is dependent on its ability to drive transcription of an unknown target in tracheal fusion cells (Jiang & Crews, 2006) and determining the identity of this unknown factor may serve to distinguish between these two possible explanations.

In a preliminary attempt to identify the unknown Dys-dependent target, several candidate genes were identified and assayed for their ability to produce *ago* or *dys*-like mutant phenotypes. These candidate genes encode the *Drosophila* homologs of proteins demonstrated to regulate the ability of Fbw7 to bind and polyubiquitinate its targets in human cell culture models. These candidates include GSK-3β, a kinase required to phosphorylate Fbw7 targets prior to binding (Wei et al., 2005; Welcker et al., 2004b; Welcker et al., 2003), the prolyl cis/trans isomerase Pin1 which isomerases a proline-proline bond in the Ago/Fbw7 phosphodegron (Drogen et al., 2006), and the protein phosphatase PP2A which has been shown to act in concert with Pin1 to regulate stability of Fbw7 targets (Yeh et al., 2004). *UAS-RNAi* lines specific to *shaggy* (*sgg*, the GSK-3β homolog, Siegfried et al., 1992; Siegfried et al., 1990), *dodo* (the Pin1 homolog, Maleszka et al., 1996), and multiple regulatory subunits of the PP2A

protein phosphatase complex (*tws*, *wdb*, *PR72* and *PP2A-B'*, Berry & Gehring, 2000; Mayer-Jaekel et al., 1993; Silverstein et al., 2002), were expressed in tracheal cells and assayed for phenotypic outcomes.

Tracheal cell specific knock-down of *sgg* phenocopies loss of *ago* (Figure 5.1). Levels of Trh are elevated in all tracheal cells (Figure 5.1A vs B) leading to defects in tracheal migration (Figure 5.1C) and lumenal convolutions (Figure 5.1D). These results suggest that *sgg* is required for both modes of Ago-mediated Trh down-regulation. Preliminary data also suggests that Pin1 and PP2A activities are required for tracheal morphogenesis (Figure 5.2 and data not shown). A closer examination of Trh levels in these genetic backgrounds is necessary to determine the nature of this requirement. These preliminary studies provide support for the hypothesis that the Dys-dependent factor acts to increase the affinity of Ago for its substrate, in this case Trh. Additional studies are required to gain further insight into this interesting aspect of *ago* function.

Figure 5.1. *sgg* is required for regulation of Trh levels in tracheal cells.

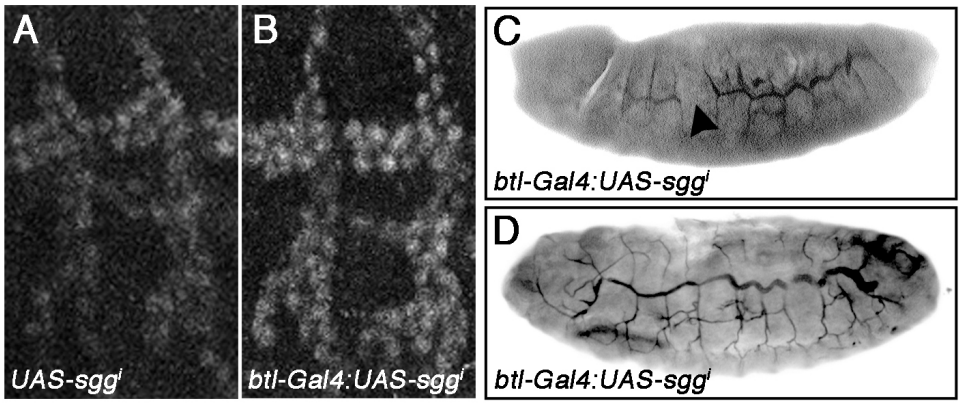

Embryos stained with α-Trh (A,B). Tracheal specific knockdown of *sgg* (B) leads to a general increase in Trh levels relative to control embryos (A). mAb2A12 staining of *sgg* knock-down embryos (C,D) shows migration/fusion defects (arrowhead in C) and lumenal convolutions (D, Erin Keebaugh and NTM).

Figure 5.2. Pin1 and PP2A are required for tracheal morphogenesis.

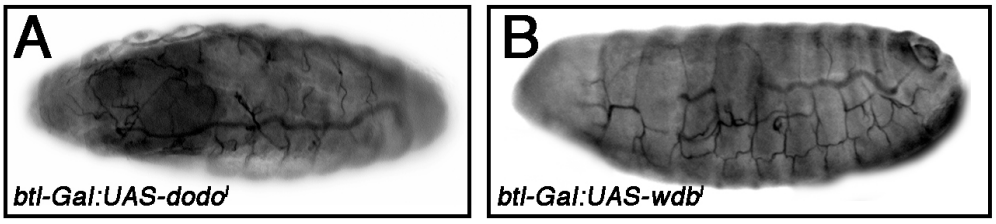

mAb2A12 staining of *dodo* and *wdb* knock-down embryos (A,B, Erin Keebaugh and NTM). (A) *dodo* knock-down leads to defects in branch migration. Similar defects are seen in embryos expressing dsRNA directed against *wdb* (B) and other PP2A subunits (data not shown).

5.C. Co-activation of developmental and homeostatic signaling leads to defects in tracheal morphogenesis

The Btl/FGF signaling pathway is reiteratively used to drive each stage of tracheogenesis during the embryonic and larval stages of *Drosophila* development. During embryogenesis, Btl/FGF signaling is induced by the developmentally regulated expression of *btl* in tracheal cells and *bnl* in surrounding non-tracheal tissue. Larval tracheogenesis is homeostatically regulated, such that transcription of *btl* and *bnl* is induced in regions of localized hypoxia or when the organism is deprived of oxygen as part of the larval hypoxic response. We found that the embryonic hypoxic response also leads to the tracheal cell-autonomous upregulation of *btl* transcription, allowing for an investigation of the consequence of simultaneous activation of developmental and homeostatic inputs into the Btl/FGF pathway.

Activation of the hypoxic response, either through exposure to hypoxia or knockdown of *dVHL*, leads to a range of tracheal phenotypes. These phenotypes are phenocopied by ectopic *btl* expression and are sensitive to dosage of Btl/FGF signaling pathway genes along with the transcriptional activators *trh* and *sima*. These findings indicate that the tracheal phenotypes due to induction of the hypoxic response are caused by excess Btl/FGF signaling and that the pathway is deregulated at the level of *btl* transcription (see Figure 3.10).

Interestingly, mutations in genes known to negatively regulate *btl* cause tracheal defects similar to those seen in hypoxic embryos. This includes mutations in the endocytic regulator *awd*, the transcriptional repressor *sal* and

ago, which restricts *btl* transcription. I have further found that hypoxia mediated tracheal defects are sensitive to *ago* dosage. Alleles of *ago* dominantly enhance *dVHL*^{i} phenotypes and show trans-heterozygous interactions with a deletion uncovering the *dVHL* genomic locus. Furthermore, heterozygosity for *ago* sensitizes embryos to hypoxia; whereas early exposure to a 1% O_2 environment is not sufficient to cause tracheal defects in control embryos, tracheogenesis is significantly perturbed in *ago/+* embryos (see Figure 3.9).

This suggests that, when simultaneously activated, the developmental and homeostatic mechanisms of *btl* regulation interact to shape the tracheal system. If so then the activity of the endogenous *btl* regulatory network (Boube et al., 2000; Kuhnlein & Schuh, 1996; Llimargas & Casanova, 1999; Ohshiro et al., 2002; Ohshiro & Saigo, 1997) may be an important determinant of the threshold of hypoxia required to elicit changes in tracheal architecture.

5.D. The role of *ago* in regulation of dHIF activity

We have demonstrated a novel role for *ago* in the regulation of dHIF activity, however the mechanism for this activity has not been determined. Based on the function of *ago* as a ubiquitin ligase subunit I would predict that it acts to regulate the stability of either the dHIF α or β subunit. This prediction is supported by the data already presented: *ago* appears to act post-transcriptionally, the *ago* phenotype is phenocopied by overexpression of the putative target *sima* and finally the ability of *agoΔF* (a form of *ago* which binds substrates but cannot interact with the ubiquitination machinery) to elicit phenotypes indicates that the role of *ago* is dependent on its ability to direct ubiquitination of a target protein.

All available evidence suggests that HIF stability is determined by the stability of the α subunit (reviewed in Kaelin & Ratcliffe, 2008; Weidemann & Johnson, 2008). However it is possible that a novel regulatory mechanism may act to regulate HIF-β stability. As a preliminary test of this hypothesis, we assayed the ability of Ago to co-immunoprecipitate with Tgo in cultured *Drosophila* cells. We found that unlike the known Tgo partner Trh (Figure 5.3, lane 1), neither wild type Ago nor AgoΔF were able to bind Tgo (Figure 5.3, lanes 2-3). This suggests that Ago may directly regulate Sima stability, and this hypothesis can be tested by assaying the ability of Ago to co-immunoprecipitate with Sima.

Initial evidence supports this hypothesis. The ability of *ago* and *dVHL* to functionally ‘replace’ each other (see Figure 4.7) suggests that they share a common target. Additional support for this idea comes from a novel form of

regulation of human HIF-1α stability. It has been demonstrated that GSK-3β phosphorylates HIF-1α, leading to its VHL independent, proteosomal dependent degradation (Flugel et al., 2007). GSK-3β phosphorylation has been shown to stimulate the ability of Ago/Fbw7 to bind its targets (Wei et al., 2005; Welcker et al., 2004b; Welcker et al., 2003). We find that expression of an RNAi knock-down construct directed against the *Drosophila* GSK-3β homolog *sgg* phenocopies the *ago* terminal branching phenotype (Figure 5.4). *sima* has a conserved putative GSK-3β phosphorylation site within a potential *ago*/*Fbw7* phosphodegron, providing further support for our hypothesis. Discovering the identity of the *ago* target in its regulation of dHIF activity may prove important in understanding its roles in development and tumor suppression.

Figure 5.3. Ago does not bind to Tgo.

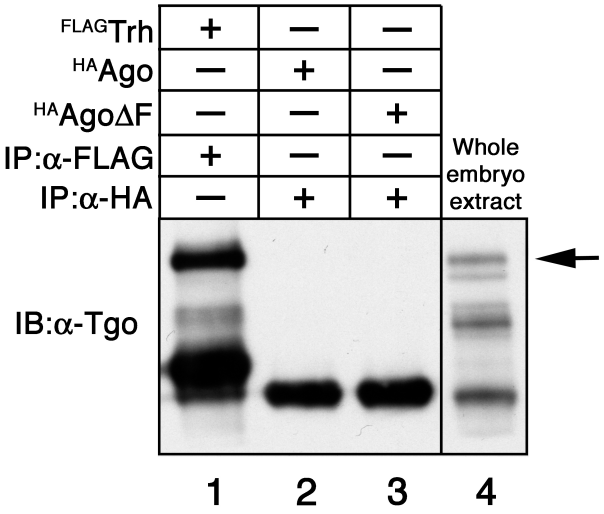

α-Tgo immunoblot of extracts from *Drosophila* S2 cells transfected with ^{FLAG}Trh and immunoprecipitated with α-FLAG (lane 1), transfected with ^{HA}Ago or ^{HA}AgoΔF and immunoprecipitated with α-HA (lanes 2 and 3, respectively) and whole embryo extract (lane 4) as a control for Tgo expression (arrow).

Figure 5.4. Expression of *sgg* RNAi causes excess terminal branching.

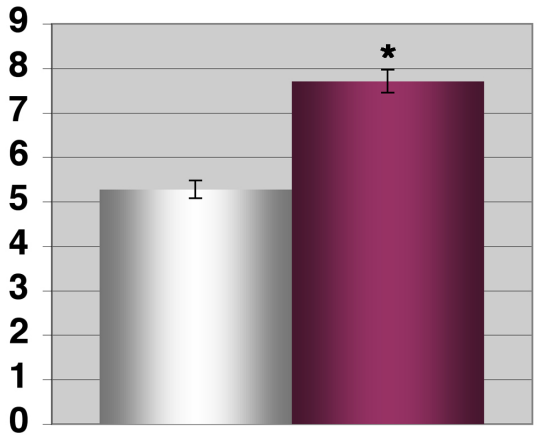

Quantification of VLM12 terminal branching in larvae of the indicated genotypes.

*$p=2.06x10^{-10}$ relative to control.

5.E. *ago* mutant larvae show characteristics of tumor cells

Features of the hypoxic response are also characteristic of tumor cells. Hypoxia-induced metabolic changes are characterized by an upregulation of glycolytic enzymes to compensate for the decreased function of other respiratory processes in low oxygen (reviewed in Hoogewijs et al., 2007; Webster, 2003). This switch to high-flux glycolysis is also a common property of tumor cells where it is known as aerobic glycolysis or the 'Warburg effect' (Denko, 2008; Warburg, 1956). *ago* mutant larvae display a transcriptional upregulation of *dLDH*, the human homolog of which is linked to aerobic glycolysis (Webster, 1987), suggesting that the metabolism of these larvae may be similar to that seen in tumor cells.

Another feature shared by hypoxic and tumor cells is the ability to affect an increase in the oxygen-conducting capacity of the vascular system. This is achieved via upregulation of the vascular endothelial growth factor (VEGF) and fibroblast growth factor (FGF) signaling pathways, resulting in angiogenesis, the elaboration of additional branches from the vasculature (Folkman & Klagsbrun, 1987; Kliche & Waltenberger, 2001; Presta et al., 2005). This aspect of the response is clearly mirrored in *ago* mutant larvae with the excess branching of tracheal terminal cells, in a tracheogenic process that is analogous to tumor angiogenesis.

A final characteristic of tumors linked to hypoxia and HIF activity is increased metastasis. The HIF-induced gene *lox* plays a role in vascular remodeling (Rodriguez et al., 2008) and has been found to be required for HIF-

induced metastasis, characteristic of many tumor types (Brahimi-Horn & Pouyssegur, 2006; Erler et al., 2006; Gort et al., 2008). Expression of *lox* alters cell adhesion properties to drive metastasis of tumor cells (Erler et al., 2006). Normoxic *ago* mutant larvae show elevated transcription of the *Drosophila lox* gene. Perhaps *lox* also plays a role in tracheogenesis and may suggest that *Drosophila* and vertebrate tumor cells lacking *ago* function have increased metastatic potential.

5.F. Loss of *ago* appears to shift the hypoxic 'threshold' required to trigger the hypoxic response

In adult *Drosophila*, more than sixty identified hypoxic response genes are induced by exposure to 0.5% O_2 conditions but not by the milder 5% O_2 treatment (Liu et al., 2006). I find that this pattern of transcriptional activation is also seen in the larval hypoxic response, where targets such as *lox* and *dHIG1* are normally strongly induced only in 0.5% O_2. *ago* mutants show a shift in *lox* and *dHIG1* transcription, such that these targets are now strongly induced in 5% O_2 and, in the case of *lox*, even upregulated in normoxia. This finding suggests that the hypoxic response threshold is shifted in *ago* mutants, such that 'mild' hypoxic responses are now triggered in normoxia, and 'severe' hypoxic responses are activated in more mild conditions (Figure 5.5).

This threshold shift seems to indicate that baseline levels of dHIF activity play a major role in determining the hypoxic threshold for triggering tracheogenic, metabolic and survival responses. If this aspect of the hypoxic response is conserved, it may provide an explanation for the appearance of aerobic glycolysis and angiogenic signaling in normoxic tumor cells. A shift in the hypoxic threshold may also explain why, relative to non-tumor tissue, hypoxic tumor cells have an increased ability to trigger a hypoxic survival response. This leads to increased survivability of tumor cells in conditions of oxygen deprivation. Based on our findings in *ago* mutants, this shift may be due to deregulation of baseline HIF levels in tumor cells, perhaps due to the loss of Fbw7 or GSK-3β.

Figure 5.5. Schematic representation of hypoxic threshold required to activate a range of hypoxic responses in control and *ago* mutant larvae.

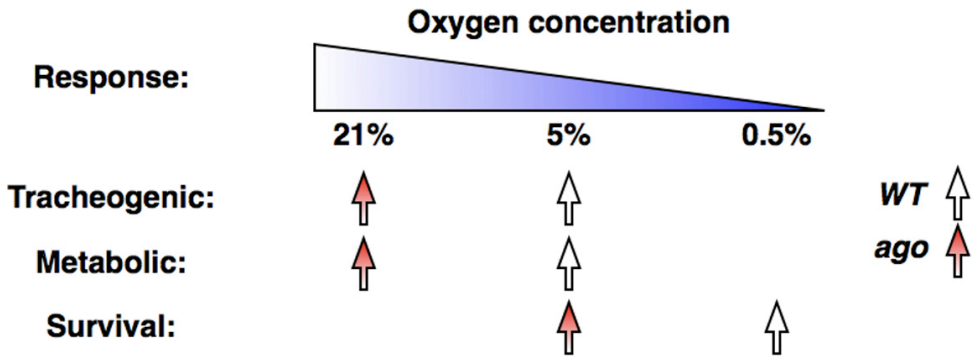

5.G. Concluding remarks

The data presented here provides interesting insights into the mechanisms regulating oxygen homeostasis in *Drosophila* and elucidates two novel roles of the *ago* tumor suppressor homolog. Tissue oxygenation is dependent on the development of an oxygen-conducting network and the ability of individual cells to respond to oxygen deprivation. We have found that *ago* acts to regulate both of these aspects of oxygen homeostasis.

During embryogenesis, *ago* limits levels of the Trh transcription factor in embryonic tracheal cells to restrict expression of the *btl* FGF receptor and subsequent FGF pathway activation. This function of *ago* is essential for the elaboration of the primary tracheal architecture. While it is not required in larval tracheal cells, *ago* does regulate larval tracheogenesis by restricting *bnl* expression in tracheal target tissues. The molecular requirement for *ago* in these tissues is in restricting the activity of dHIF. Loss of *ago* causes elevated dHIF activity leading to a shift in the hypoxic response such that mutant larvae activate transcription of tracheogenic and metabolic response genes in normoxia, and display a lowered threshold for transcription of other hypoxic response genes.

It remains to be determined whether these roles of *ago* are conserved in mammalian development. Early evidence suggests they may be; loss of *Fbw7* function impairs vascular development in mice (Tetzlaff et al., 2004; Tsunematsu et al., 2004) and *Fbw7* loss is associated with tumors displaying ectopically high levels of HIF activity, including glioblastoma and ovarian cancer (Gu et al., 2007; Hagedorn et al., 2007; Kwak et al., 2005; Moberg et al., 2001). Alterations in

growth factor signaling and metabolism are hallmarks of cancer (reviewed in Hanahan & Weinberg, 2000; Kroemer & Pouyssegur, 2008), suggesting that if conserved, these novel roles of *ago* may prove to have clinical relevance.

The main advance of this work is the identification of *ago* as a novel regulator of the hypoxic response. Oxygen homeostasis is dependent upon the tight regulation of the HIF-mediated transcriptional response to hypoxia; either insufficient or excess HIF activity can cause cell death and organismal lethality. Previous work has centered on the oxygen dependent HPH/VHL and FIH HIF regulatory pathways. However, the required degree of HIF regulation is not possible using just these oxygen sensing pathways; HIF must be regulated at oxygen concentrations below the threshold for activity of either HPH or FIH. This work is the first demonstration of a second protein degradative pathway which works in concert with HPH/VHL to control activity of HIF and identifies the F box protein *ago* as a key player in this second HIF regulatory pathway.

Appendix A. Materials and Methods

A.1. Stocks, genetics and statistics

The *ago* alleles ago^{1} and ago^{3} have been previously described (Moberg et al., 2001). Full-length *ago* and *agoΔF*, a version of *ago* lacking the core F-box domain (Moberg et al., 2004), were cloned as PCR products into the *EcoRI* site of the *pUAST* vector (Brand & Perrimon, 1993) and used to generate *UAS-ago* and *UAS-agoΔF* stocks. The *dVHL* open reading frame was cloned as a PCR product into the *Eco*RI site of the *pSymp* vector (Giordano et al., 2002) and used to generate $UAS\text{-}dVHL^{i}$ stocks (D. Rennie, Massachusetts General Hospital Transgenic *Drosophila* Core).

The *FRT80B* and w^{1118} strains were used as wild type controls. Other alleles used in this study were: btl^{dev1}, $btl^{EY01638}$, trh^{10512}, awd^{j2A4}, bnl^{P1}, $sima^{07607}$, $ago^{EP(3)1135}$, the genomic deletions *Df(3L)Exel9000* and *Df(2R)Exel6060* and *esg-lacZ* (all from the Bloomington *Drosophila* Stock Center) and *1-eve-1* (Perrimon et al., 1991). The following transgenes were also used: the *UAS* transgenes *UAS-CycE*, *UAS-dMyc*, *UAS-Ras85D.V12*, *UAS-pnt.P1*, *UAS-N* (all from the Bloomington *Drosophila* Stock Center), *UAS-trh* (Jin et al., 2001), *UAS-sima* (Lavista-Llanos et al., 2002), *UAS-btl-GFP* (Dammai et al., 2003) and *UAS-dVHL* (Arquier et al., 2006); the RNAi transgenes $UAS\text{-}Adf1^{RNAi}$, $UAS\text{-}wdb^{RNAi}$ (both from Vienna *Drosophila* RNAi Center), $UAS\text{-}pigeon^{RNAI}$ and $UAS\text{-}sgg^{RNAi}$ (both from NIG-Fly, National Institute of Genetics, Japan); and the *Gal-4* drivers *actin-Gal4*, *hs-Gal4*, *5053A-Gal4* (all from the Bloomington Drosophila Stock Center) and *btl-Gal4* (Shiga et al., 1996). Crosses involving the temperature-sensitive

UAS-Pros26^{1} and *UAS-Prosβ2*^{1} transgenes (Belote & Fortier, 2002) were performed at 21ºC.

Embryos were genotyped using the *TM6B, P{iab-2(1.7)lacZ}6B, Tb*^{1}, *TM6B,P{w*$^{+mC}$*=35UZ}DB1,Tb*^{1}, *SM6b,P{eve-lacZ8.0}SB1*, *CyO,P{ry*$^{+t7.2}$*=lArB}A208.1M2* and *CyO, P{elav-lacZ.H}YH2* 'blue' balancers, and the *TM3, P{Gal4-twi.G}2.3, P{UAS-2xEGFP}AH2.3, Sb*^{1}*Ser*^{1} and *CyO,P{ActGFP}JMR1* GFP balancers (all from the Bloomington *Drosophila* Stock Center).

Statistical comparisons were made using Student's t-Test (Microsoft Excel) with the indicated significance levels.

A.2. Immunohistochemistry and antibodies

Embryos were staged and fixed in 37% formaldehyde-saturated heptane, devitellinized in methanol and stored in ethanol at 4°C. These samples were rehydrated & washed in PBS with .05% Triton-X 100 (PBSTx), blocked in 5% milk powder/5% NGS in PBSTx, and incubated with the following primary antibodies: mouse anti-Tango (1:2, Developmental Studies Hybridoma Bank; DSHB), rat anti-Trh (1:200, Henderson et al., 1999), mouse mAb2A12 (1:5, DSHB), rabbit anti-β-Gal (1:250, Cappel), guinea pig anti-full length Ago (1:2500, Pocono Rabbit Farm & Laboratory), rat anti-Dys (1:200) and rabbit anti-Dys (1:800, Jiang & Crews, 2003) and rabbit anti-GFP (1:400, Molecular Probes). Third instar larvae were dissected in cold PBS, fixed in 4% paraformaldehyde and incubated with guinea pig anti-CycE (1:500). Secondary antibodies

conjugated to HRP, AP, Cy3 and Cy5 were used as recommended (Jackson ImmunoResearch).

A.3. Imaging of third instar larval trachea

To image the larval tracheal system, third instar larvae were dissected in cold PBS and fixed in 4% paraformaldehyde. The air-filled tracheal branches were then imaged using bright-field microscopy. High-magnification images were stitched together using Photomerge (Adobe Photoshop CS).

A.4. Western blot analysis

To analysis Trh levels, embryos from *w*^{1118} and *ago*^{1}*/ TM3, P{Gal4-twi.G}2.3, P{UAS-2xEGFP}AH2.3, Sb*^{1}*Ser*^{1} strains were collected at stages 13/14 and sorted by absence of GFP fluorescence. Extracts were prepared in sample buffer containing DTT and resolved on 7.5% SDS-PAGE prior to Western blotting with rat anti-Trh (1:2000), or anti-β-tubulin (1:2000, Santa Cruz Biotechnology).

To assay dVHL knock-down, embryos from *w*^{1118} and *UAS-dVHL*^{i} strains crossed to *actin-Gal4/CyO,P{ActGFP}JMR1* were collected at stages 13-16 and sorted by absence of GFP. Whole embryo extracts were prepared in sample buffer and resolved on 12% SDS-PAGE prior to Western blotting with rabbit anti-dVHL (1:1000, Arquier et al., 2006) and anti-β-tubulin.

Bnl protein levels were assayed in third instar larvae. Whole larval extracts were prepared in sample buffer and resolved on 7.5% SDS-PAGE prior to Western blotting with rabbit anti-Bnl (1:1000, Jarecki et al., 1999).

A.5. RNA in situ hybridization

Color RNA in situ hybridization was performed as described (Tautz, 2000). Briefly, embryos were fixed in 1.5% formaldehyde (in 0.1 M HEPES, pH 6.9, 2 mM $MgSO_4$, 1 mM EGTA)-saturated heptane, devitellinized and stored in methanol at -20°C. Embryos were washed in PBS with 0.1% Tween 20, treated with 15µg/ml Proteinase K for 2 minutes and post-fixed with 4% paraformaldehyde. Riboprobe hybridization and subsequent immunohistochemistry were performed as described (Tautz, 2000). Sense and anti-sense digoxigenin (DIG)-labeled riboprobes were synthesized from PCR fragments amplified from *btl* and *bnl* cDNAs and visualized by the anti-DIG-AP antibody (1:2000, Roche).

Fluorescent RNA in situ hybridization was performed as described (Merabet et al., 2005). DIG labeled riboprobes were synthesized from PCR fragments of *btl* or *bnl* cDNA and visualized with anti-DIG-Biotin (1:500, Sigma) followed by TSA-Biotin amplification (PerkinElmer) and incubation with SA-FITC.

A.6. Reverse transcription and quantitative real-time PCR (qRT-PCR)

For *dVHL* expression analysis, total RNA was isolated from staged whole embryos, and dissected third instar larval body wall muscles. cDNA was reverse-transcribed using random hexamer primers (Invitrogen) with Superscript II Reverse Transcriptase (Invitrogen). *dVHL* and *β-tubulin* transcripts were then amplified with gene-specific primers.

For quantification of mRNA levels, total RNA was isolated from whole third instar larvae or dissected larval tissues and reverse transcribed as described above. Levels of *Arp87c*, *ago-RA*,*RB* and *RC*, *dLDH*, *sima*, *bnl*, *lox*, *hairy*, *dHIG1*, *thor* and *amy-p* were then assayed with gene-specific primers using the SYBR green method of quantitative real-time PCR. Abundance of transcripts was then normalized to levels of *Arp87c*.

A.7. Plasmids and molecular biology

pMT-HA-ago expression plasmids have been described previously (Moberg et al., 2004). *pMT-Flag-trh* was generated by cloning the full-length *trh* ORF (Open Biosystems) into the *pMT* vector as an N-terminally Flag-tagged PCR product. The *pACT-HA-dys* plasmid (S. Crews) contains an N-terminally tagged version of the *dys* ORF under the control of a constitutively active fragment of the *actin* promoter. Transfected S2 cells were induced by the addition of 0.5mM $CuSO_4$ for 6 hours prior to lysis in buffer containing 0.5M KCl, 0.1% NP-40, 35% glycerol, 10mM HEPES pH 7.0, 5mM $MgCl_2$, 0.5mM EDTA pH 8.0, 25mM NaF, 1mM Na_2VO_4, 1mM DTT supplemented with protease inhibitors (Complete™ Protease Inhibitor Cocktail; Roche). Where indicated, 50uM MG132 (Calbiochem) was added 6 hrs prior to harvesting cells. Lysates were analyzed directly by immunoblot (IB), or diluted in immunoprecipitation (IP) buffer and subject to IP/IB analysis as described previously (Moberg et al., 2004). Anti-HA and anti-Flag antibodies (Sigma) were used according to manufacturer's instructions.

A.8. Hypoxia treatments

Hypoxia treatments were performed in a sealed Modular incubator chamber (Billups-Rothenberg Inc., Del Mar, CA) with separate gas intake and exhaust openings. To create hypoxic conditions the chamber was flooded with gas from a tank containing 0.5% O_2: 99.5% N_2. The rate of gas flow into the chamber was regulated by a flow meter and set to 15 L/min. The chamber was flooded with gas for a length of time appropriate to create the desired internal O_2 concentration which was measured with an electronic O_2 sensor (OX-01, RKI Instruments, Inc., Union City, CA), at which time the intake and exhaust openings were sealed. That the chamber maintained a constant environment was again monitored by the O_2 sensor.

To assay recovery from hypoxia, 5-7 day old adult flies were put into plain glass tubes in groups of 9-15. The flies were then placed into the hypoxia chamber at 0.5% O_2 for one hour and then removed to normoxia. Following hypoxic treatment more than 99% of the flies had fallen into hypoxic stupor (178 of 179). Recovery time was defined as the time required for each individual fly to resume walking following reoxygenation.

Hypoxia survival rates were assayed in 5-7 day old flies in groups of 8-16 following sixteen hours in 0.5% O_2. After being returned to normoxia, flies were given 24 hours to recover before the number of surviving flies was determined.

Appendix B. References

Acevedo, V. D., Gangula, R. D., Freeman, K. W., Li, R., Zhang, Y., Wang, F., Ayala, G. E., Peterson, L. E., Ittmann, M., and Spencer, D. M. (2007). Inducible FGFR-1 activation leads to irreversible prostate adenocarcinoma and an epithelial-to-mesenchymal transition. *Cancer Cell, 12*(6), 559–571.

Adryan, B., Decker, H. J., Papas, T. S., and Hsu, T. (2000). Tracheal development and the von Hippel-Lindau tumor suppressor homolog in *Drosophila*. *Oncogene, 19*(24), 2803–2811.

Anderson, M. G., Certel, S. J., Certel, K., Lee, T., Montell, D. J., and Johnson, W. A. (1996). Function of the *Drosophila* POU domain transcription factor *drifter* as an upstream regulator of *breathless* receptor tyrosine kinase expression in developing trachea. *Development, 122*(12), 4169–4178.

Arquier, N., Vigne, P., Duplan, E., Hsu, T., Therond, P. P., Frelin, C., and D'Angelo, G. (2006). Analysis of the hypoxia-sensing pathway in *Drosophila* melanogaster. *Biochem J, 393*(Pt 2), 471–480.

Artavanis-Tsakonas, S., Matsuno, K., and Fortini, M. E. (1995). Notch signaling. *Science, 268*(5208), 225–232.

Aso, T., Yamazaki, K., Aigaki, T., and Kitajima, S. (2000). *Drosophila* von Hippel-Lindau tumor suppressor complex possesses E3 ubiquitin ligase activity. *Biochem Biophys Res Commun, 276*(1), 355–361.

Bacon, N. C., Wappner, P., O'Rourke, J. F., Bartlett, S. M., Shilo, B., Pugh, C. W., and Ratcliffe, P. J. (1998). Regulation of the *Drosophila* bHLH-PAS protein Sima by hypoxia: functional evidence for homology with mammalian HIF-1 alpha. *Biochem Biophys Res Commun, 249*(3), 811–816.

Balakrishnan, A., Bleeker, F. E., Lamba, S., Rodolfo, M., Daniotti, M., Scarpa, A., van Tilborg, A. A., Leenstra, S., Zanon, C., and Bardelli, A. (2007). Novel somatic and germline mutations in cancer candidate genes in glioblastoma, melanoma, and pancreatic carcinoma. *Cancer Res, 67*(8), 3545–3550.

Beiman, M., Shilo, B. Z., and Volk, T. (1996). Heartless, a *Drosophila* FGF receptor homolog, is essential for cell migration and establishment of several mesodermal lineages. *Genes Dev, 10*(23), 2993–3002.

Belote, J. M. and Fortier, E. (2002). Targeted expression of dominant negative proteasome mutants in *Drosophila* melanogaster. *Genesis, 34*(1-2), 80–82.

Berry, M. and Gehring, W. (2000). Phosphorylation status of the SCR homeodomain determines its functional activity: essential role for protein phosphatase 2A,B'. *EMBO J, 19*(12), 2946–2957.

Boube, M., Llimargas, M., and Casanova, J. (2000). Cross-regulatory interactions among tracheal genes support a co-operative model for the induction of tracheal fates in the *Drosophila* embryo. *Mech Dev, 91*(1-2), 271–278.

Bouck, N., Stellmach, V., and Hsu, S. C. (1996). How tumors become angiogenic. *Adv Cancer Res, 69*, 135–174.

Boutilier, R. G. (2001). Mechanisms of cell survival in hypoxia and hypothermia. *J Exp Biol, 204*(Pt 18), 3171–3181.

Bracken, C. P., Fedele, A. O., Linke, S., Balrak, W., Lisy, K., Whitelaw, M. L., and Peet, D. J. (2006). Cell-specific regulation of hypoxia-inducible factor (HIF)-1alpha and HIF-2alpha stabilization and transactivation in a graded oxygen environment. *J Biol Chem, 281*(32), 22575–22585.

Brahimi-Horn, C. and Pouyssegur, J. (2006). The role of the hypoxia-inducible factor in tumor metabolism growth and invasion. *Bull Cancer, 93*(8), E73–80.

Brand, A. H. and Perrimon, N. (1993). Targeted gene expression as a means of altering cell fates and generating dominant phenotypes. *Development, 118*(2), 401–415.

Bredel, M., Bredel, C., Juric, D., Harsh, G. R., Vogel, H., Recht, L. D., and Sikic, B. I. (2005). Functional network analysis reveals extended gliomagenesis pathway maps and three novel MYC-interacting genes in human gliomas. *Cancer Res, 65*(19), 8679–8689.

Brodu, V. and Casanova, J. (2006). The RhoGAP *crossveinless-c* links *trachealess* and EGFR signaling to cell shape remodeling in *Drosophila* tracheal invagination. *Genes Dev, 20*(13), 1817–1828.

Brown, S., Hu, N., and Hombria, J. C. (2001). Identification of the first invertebrate interleukin JAK/STAT receptor, the *Drosophila* gene *domeless*. *Curr Biol, 11*(21), 1700–1705.

Bruick, R. K. and McKnight, S. L. (2001). A conserved family of prolyl-4-hydroxylases that modify HIF. *Science, 294*(5545), 1337–1340.

Brunskill, E. W., Witte, D. P., Shreiner, A. B., and Potter, S. S. (1999). Characterization of *npas3*, a novel basic helix-loop-helix PAS gene expressed in the developing mouse nervous system. *Mech Dev, 88*(2), 237–241.

Cabernard, C. and Affolter, M. (2005). Distinct roles for two receptor tyrosine kinases in epithelial branching morphogenesis in *Drosophila*. *Dev Cell, 9*(6), 831–842.

Calhoun, E. S., Jones, J. B., Ashfaq, R., Adsay, V., Baker, S. J., Valentine, V., Hempen, P. M., Hilgers, W., Yeo, C. J., Hruban, R. H., and Kern, S. E. (2003). BRAF and FBXW7 (CDC4, FBW7, AGO, SEL10) mutations in distinct subsets of pancreatic cancer: potential therapeutic targets. *Am J Pathol, 163*(4), 1255–1260.

Carmeliet, P. and Jain, R. K. (2000). Angiogenesis in cancer and other diseases. *Nature, 407*(6801), 249–257.

Cassia, R., Moreno-Bueno, G., Rodriguez-Perales, S., Hardisson, D., Cigudosa, J. C., and Palacios, J. (2003). Cyclin E gene (CCNE) amplification and hCDC4 mutations in endometrial carcinoma. *J Pathol, 201*(4), 589–595.

Centanin, L., Dekanty, A., Romero, N., Irisarri, M., Gorr, T. A., and Wappner, P. (2008). Cell autonomy of HIF effects in *Drosophila*: tracheal cells sense hypoxia and induce terminal branch sprouting. *Dev Cell, 14*(4), 547–558.

Centanin, L., Ratcliffe, P. J., and Wappner, P. (2005). Reversion of lethality and growth defects in Fatiga oxygen-sensor mutant flies by loss of hypoxia-inducible factor-alpha/Sima. *EMBO Rep, 6*(11), 1070–1075.

Chaudary, N. and Hill, R. P. (2007). Hypoxia and metastasis. *Clin Cancer Res, 13*(7), 1947–1949.

Cobb, M. H., Hepler, J. E., Cheng, M., and Robbins, D. (1994). The mitogen-activated protein kinases, ERK1 and ERK2. *Semin Cancer Biol, 5*(4), 261–268.

Cockman, M. E., Masson, N., Mole, D. R., Jaakkola, P., Chang, G. W., Clifford, S. C., Maher, E. R., Pugh, C. W., Ratcliffe, P. J., and Maxwell, P. H. (2000). Hypoxia inducible factor-alpha binding and ubiquitylation by the von Hippel-Lindau tumor suppressor protein. *J Biol Chem, 275*(33), 25733–25741.

Covello, K. L. and Simon, M. C. (2004). HIFs, hypoxia, and vascular development. *Curr Top Dev Biol, 62*, 37–54.

Cramer, T., Yamanishi, Y., Clausen, B. E., Forster, I., Pawlinski, R., Mackman, N., Haase, V. H., Jaenisch, R., Corr, M., Nizet, V., Firestein, G. S., Gerber, H. P., Ferrara, N., and Johnson, R. S. (2003). HIF-1alpha is essential for myeloid cell-mediated inflammation. *Cell, 112*(5), 645–657.

Crews, S. T. and Fan, C. M. (1999). Remembrance of things PAS: regulation of development by bHLH-PAS proteins. *Curr Opin Genet Dev, 9*(5), 580–587.

Csik, L. (1939). The susceptibility to oxygen want of different *Drosophila* species. *Zeitschrift fur vergleichende Physiologie, 27*, 304–310.

Dammai, V., Adryan, B., Lavenburg, K. R., and Hsu, T. (2003). *Drosophila awd*, the homolog of human *nm23*, regulates FGF receptor levels and functions synergistically with *shi/dynamin* during tracheal development. *Genes Dev, 17*(22), 2812–2824.

Dayan, F., Roux, D., Brahimi-Horn, M. C., Pouyssegur, J., and Mazure, N. M. (2006). The oxygen sensor factor-inhibiting hypoxia-inducible factor-1 controls expression of distinct genes through the bifunctional transcriptional character of hypoxia-inducible factor-1alpha. *Cancer Res, 66*(7), 3688–3698.

Demidenko, Z. N., Rapisarda, A., Garayoa, M., Giannakakou, P., Melillo, G., and Blagosklonny, M. V. (2005). Accumulation of hypoxia-inducible factor-1alpha is limited by transcription-dependent depletion. *Oncogene, 24*(30), 4829–4838.

Denko, N. (2008). Hypoxia, HIF1 and glucose metabolism in the solid tumour. *Nat Rev Cancer,* .

DiGregorio, P. J., Ubersax, J. A., and O'Farrell, P. H. (2001). Hypoxia and nitric oxide induce a rapid, reversible cell cycle arrest of the *Drosophila* syncytial divisions. *J Biol Chem, 276*(3), 1930–1937.

Douglas, R. M., Xu, T., and Haddad, G. G. (2001). Cell cycle progression and cell division are sensitive to hypoxia in *Drosophila* melanogaster embryos. *Am J Physiol Regul Integr Comp Physiol, 280*(5), R1555-63.

Ebbesen, P., Eckardt, K., Ciampor, F., and Pettersen, E. O. (2004). Linking measured intercellular oxygen concentration to human cell functions. *Acta Oncol, 43*(6), 598–600.

Epstein, A. C., Gleadle, J. M., McNeill, L. A., Hewitson, K. S., O'Rourke, J., Mole, D. R., Mukherji, M., Metzen, E., Wilson, M. I., Dhanda, A., Tian, Y. M., Masson, N., Hamilton, D. L., Jaakkola, P., Barstead, R., Hodgkin, J., Maxwell, P. H., Pugh, C. W., Schofield, C. J., and Ratcliffe, P. J. (2001). *C. elegans* EGL-9 and mammalian homologs define a family of dioxygenases that regulate HIF by prolyl hydroxylation. *Cell, 107*(1), 43–54.

Erler, J. T., Bennewith, K. L., Nicolau, M., Dornhofer, N., Kong, C., Le, Q., Chi, J. A., Jeffrey, S. S., and Giaccia, A. J. (2006). Lysyl oxidase is essential for hypoxia-induced metastasis. *Nature, 440*(7088), 1222–1226.

Ferrara, N. and Davis-Smyth, T. (1997). The biology of vascular endothelial growth factor. *Endocr Rev, 18*(1), 4–25.

Flamme, I., Frolich, T., and Risau, W. (1997). Molecular mechanisms of vasculogenesis and embryonic angiogenesis. *J Cell Physiol, 173*(2), 206–210.

Flugel, D., Gorlach, A., Michiels, C., and Kietzmann, T. (2007). Glycogen synthase kinase 3 phosphorylates hypoxia-inducible factor 1alpha and mediates its destabilization in a VHL-independent manner. *Mol Cell Biol, 27*(9), 3253–3265.

Foe, V. E. and Alberts, B. M. (1985). Reversible chromosome condensation induced in *Drosophila* embryos by anoxia: visualization of interphase nuclear organization. *J Cell Biol, 100*(5), 1623–1636.

Folkman, J. (1971). Tumor angiogenesis: therapeutic implications. *N Engl J Med, 285*(21), 1182–1186.

Folkman, J. and Klagsbrun, M. (1987). Angiogenic factors. *Science, 235*(4787), 442–447.

Fong, G. and Takeda, K. (2008). Role and regulation of prolyl hydroxylase domain proteins. *Cell Death Differ, 15*(4), 635–641.

Forneris, F., Binda, C., Vanoni, M. A., Mattevi, A., and Battaglioli, E. (2005). Histone demethylation catalysed by LSD1 is a flavin-dependent oxidative process. *FEBS Lett, 579*(10), 2203–2207.

Forsythe, J. A., Jiang, B. H., Iyer, N. V., Agani, F., Leung, S. W., Koos, R. D., and Semenza, G. L. (1996). Activation of vascular endothelial growth factor gene transcription by hypoxia-inducible factor 1. *Mol Cell Biol, 16*(9), 4604–4613.

Freeman, K. W., Gangula, R. D., Welm, B. E., Ozen, M., Foster, B. A., Rosen, J. M., Ittmann, M., Greenberg, N. M., and Spencer, D. M. (2003). Conditional activation of fibroblast growth factor receptor (FGFR) 1, but not FGFR2, in prostate cancer cells leads to increased osteopontin induction, extracellular signal-regulated kinase activation, and in vivo proliferation. *Cancer Res, 63*(19), 6237–6243.

Friedkin, M. and Lehninger, A. L. (1949). Esterification of inorganic phosphate coupled to electron transport between dihydrodiphosphopyridine nucleotide and oxygen. *J Biol Chem, 178*(2), 611–623.

Fryer, C. J., White, J. B., and Jones, K. A. (2004). Mastermind recruits CycC:CDK8 to phosphorylate the Notch ICD and coordinate activation with turnover. *Mol Cell, 16*(4), 509–520.

Gabay, L., Seger, R., and Shilo, B. Z. (1997). MAP kinase in situ activation atlas during *Drosophila* embryogenesis. *Development, 124*(18), 3535–3541.

Gasparini, G., Longo, R., Toi, M., and Ferrara, N. (2005). Angiogenic inhibitors: a new therapeutic strategy in oncology. *Nat Clin Pract Oncol, 2*(11), 562–577.

Genbacev, O., Joslin, R., Damsky, C. H., Polliotti, B. M., and Fisher, S. J. (1996). Hypoxia alters early gestation human cytotrophoblast differentiation/invasion in vitro and models the placental defects that occur in preeclampsia. *J Clin Invest, 97*(2), 540–550.

Genbacev, O., Zhou, Y., Ludlow, J. W., and Fisher, S. J. (1997). Regulation of human placental development by oxygen tension. *Science, 277*(5332), 1669–1672.

Gerber, H. P., Condorelli, F., Park, J., and Ferrara, N. (1997). Differential transcriptional regulation of the two vascular endothelial growth factor receptor genes. Flt-1, but not Flk-1/KDR, is up-regulated by hypoxia. *J Biol Chem, 272*(38), 23659–23667.

Ghabrial, A. S. and Krasnow, M. A. (2006). Social interactions among epithelial cells during tracheal branching morphogenesis. *Nature, 441*(7094), 746–749.

Ghabrial, A., Luschnig, S., Metzstein, M. M., and Krasnow, M. A. (2003). Branching Morphogenesis of the *Drosophila* Tracheal System. *Annu Rev Cell Dev Biol, 19*, 623–47.

Giaccia, A. (1996). Hypoxic Stress Proteins: Survival of the Fittest. *Semin Radiat Oncol, 6*(1), 46–58.

Giordano, E., Rendina, R., Peluso, I., and Furia, M. (2002). RNAi triggered by symmetrically transcribed transgenes in *Drosophila* melanogaster. *Genetics, 160*(2), 637–648.

Giri, D., Ropiquet, F., and Ittmann, M. (1999). Alterations in expression of basic fibroblast growth factor (FGF) 2 and its receptor FGFR-1 in human prostate cancer. *Clin Cancer Res, 5*(5), 1063–1071.

Gisselbrecht, S., Skeath, J. B., Doe, C. Q., and Michelson, A. M. (1996). *heartless* encodes a fibroblast growth factor receptor (DFR1/DFGF-R2) involved in the directional migration of early mesodermal cells in the *Drosophila* embryo. *Genes Dev, 10*(23), 3003–3017.

Glazer, L. and Shilo, B. Z. (1991). The *Drosophila* FGF-R homolog is expressed in the embryonic tracheal system and appears to be required for directed tracheal cell extension. *Genes Dev, 5*(4), 697–705.

Gleadle, J. M. and Ratcliffe, P. J. (1997). Induction of hypoxia-inducible factor-1, erythropoietin, vascular endothelial growth factor, and glucose transporter-1 by hypoxia: evidence against a regulatory role for Src kinase. *Blood, 89*(2), 503–509.

Gnarra, J. R., Tory, K., Weng, Y., Schmidt, L., Wei, M. H., Li, H., Latif, F., Liu, S., Chen, F., and Duh, F. M. (1994). Mutations of the VHL tumour suppressor gene in renal carcinoma. *Nat Genet, 7*(1), 85–90.

Gnarra, J. R., Ward, J. M., Porter, F. D., Wagner, J. R., Devor, D. E., Grinberg, A., Emmert-Buck, M. R., Westphal, H., Klausner, R. D., and Linehan, W. M. (1997). Defective placental vasculogenesis causes embryonic lethality in VHL-deficient mice. *Proc Natl Acad Sci U S A, 94*(17), 9102–9107.

Gorr, T. A., Cahn, J. D., Yamagata, H., and Bunn, H. F. (2004). Hypoxia-induced synthesis of hemoglobin in the crustacean *Daphnia magna* is hypoxia-inducible factor-dependent. *J Biol Chem, 279*(34), 36038–36047.

Gorr, T. A., Gassmann, M., and Wappner, P. (2006). Sensing and responding to hypoxia via HIF in model invertebrates. *J Insect Physiol, 52*(4), 349–364.

Gort, E. H., Groot, A. J., van der Wall, E., van Diest, P. J., and Vooijs, M. A. (2008). Hypoxic regulation of metastasis via hypoxia-inducible factors. *Curr Mol Med, 8*(1), 60–67.

Grieshaber, M. K., Hardewig, I., Kreutzer, U., and Portner, H. O. (1994). Physiological and metabolic responses to hypoxia in invertebrates. *Rev Physiol Biochem Pharmacol, 125*, 43–147.

Gu, Y. Z., Moran, S. M., Hogenesch, J. B., Wartman, L., and Bradfield, C. A. (1998). Molecular characterization and chromosomal localization of a third alpha-class hypoxia inducible factor subunit, HIF3alpha. *Gene Expr, 7*(3), 205–213.

Gu, Z., Inomata, K., Ishizawa, K., and Horii, A. (2007). The FBXW7 beta-form is suppressed in human glioma cells. *Biochem Biophys Res Commun, 354*(4), 992–998.

Guillemin, K., Groppe, J., Ducker, K., Treisman, R., Hafen, E., Affolter, M., and Krasnow, M. A. (1996). The *pruned* gene encodes the *Drosophila* serum response factor and regulates cytoplasmic outgrowth during terminal branching of the tracheal system. *Development, 122*(5), 1353–1362.

Gupta-Rossi, N., Le Bail, O., Gonen, H., Brou, C., Logeat, F., Six, E., Ciechanover, A., and Israel, A. (2001). Functional interaction between SEL-10, an F-box protein, and the nuclear form of activated Notch1 receptor. *J Biol Chem, 276*(37), 34371–34378.

Haddad, G. G., Sun, Y. A., Wyman, R. J., and Xu, T. (1997). Genetic basis of tolerance to O_2 deprivation in *Drosophila* melanogaster. *Proc Natl Acad Sci U S A, 94*(20), 10809–10812.

Hagedorn, M., Delugin, M., Abraldes, I., Allain, N., Belaud-Rotureau, M., Turmo, M., Prigent, C., Loiseau, H., Bikfalvi, A., and Javerzat, S. (2007). FBXW7/ hCDC4 controls glioma cell proliferation in vitro and is a prognostic marker for survival in glioblastoma patients. *Cell Div, 2*, 9.

Hagen, T., Taylor, C. T., Lam, F., and Moncada, S. (2003). Redistribution of intracellular oxygen in hypoxia by nitric oxide: effect on HIF1alpha. *Science, 302*(5652), 1975–1978.

Hanahan, D. and Folkman, J. (1996). Patterns and emerging mechanisms of the angiogenic switch during tumorigenesis. *Cell, 86*(3), 353–364.

Hanahan, D. and Weinberg, R. A. (2000). The hallmarks of cancer. *Cell, 100*(1), 57–70.

Hellstrom, M., Phng, L., Hofmann, J. J., Wallgard, E., Coultas, L., Lindblom, P., Alva, J., Nilsson, A., Karlsson, L., Gaiano, N., Yoon, K., Rossant, J., Iruela-Arispe, M. L., Kalen, M., Gerhardt, H., and Betsholtz, C. (2007). Dll4 signalling through Notch1 regulates formation of tip cells during angiogenesis. *Nature, 445*(7129), 776–780.

Hemphala, J., Uv, A., Cantera, R., Bray, S., and Samakovlis, C. (2003). Grainy head controls apical membrane growth and tube elongation in response to Branchless/FGF signalling. *Development, 130*(2), 249–258.

Henderson, K. D., Isaac, D. D., and Andrew, D. J. (1999). Cell fate specification in the *Drosophila* salivary gland: the integration of homeotic gene function with the DPP signaling cascade. *Dev Biol, 205*(1), 10–21.

Henry, J. R. and Harrison, J. F. (2004). Plastic and evolved responses of larval tracheae and mass to varying atmospheric oxygen content in *Drosophila* melanogaster. *J Exp Biol, 207*(Pt 20), 3559–3567.

Herst, P. M. and Berridge, M. V. (2007). Cell surface oxygen consumption: a major contributor to cellular oxygen consumption in glycolytic cancer cell lines. *Biochim Biophys Acta, 1767*(2), 170–177.

Hewitson, K. S., McNeill, L. A., Riordan, M. V., Tian, Y., Bullock, A. N., Welford, R. W., Elkins, J. M., Oldham, N. J., Bhattacharya, S., Gleadle, J. M., Ratcliffe, P. J., Pugh, C. W., and Schofield, C. J. (2002). Hypoxia-inducible factor (HIF) asparagine hydroxylase is identical to factor inhibiting HIF (FIH) and is related to the cupin structural family. *J Biol Chem, 277*(29), 26351–26355.

Hochachka, P. W., Buck, L. T., Doll, C. J., and Land, S. C. (1996). Unifying theory of hypoxia tolerance: molecular/metabolic defense and rescue mechanisms for surviving oxygen lack. *Proc Natl Acad Sci U S A, 93*(18), 9493–9498.

Hogan, B. L. (1999). Morphogenesis. *Cell, 96*(2), 225–233.

Hoogewijs, D., Terwilliger, N. B., Webster, K. A., Powell-Coffman, J. A., Tokishita, S., Yamagata, H., Hankeln, T., Burmester, T., Rytkonen, K. T., Nikinmaa, M., Abele, D., Heise, K., Lucassen, M., Fandrey, J., Maxwell, P. H., Pahlman, S., and Gorr, T. A. (2007). From critters to cancers: bridging comparative and clinical research on oxygen sensing, HIF signaling, and adaptations towards hypoxia. *Integrative and Comparative Biology, 47*(4), 552–577.

Hsu, T., Adereth, Y., Kose, N., and Dammai, V. (2006). Endocytic function of von Hippel-Lindau tumor suppressor protein regulates surface localization of fibroblast growth factor receptor 1 and cell motility. *J Biol Chem, 281*(17), 12069–12080.

Huang, Y., Hickey, R. P., Yeh, J. L., Liu, D., Dadak, A., Young, L. H., Johnson, R. S., and Giordano, F. J. (2004). Cardiac myocyte-specific HIF-1alpha deletion alters vascularization, energy availability, calcium flux, and contractility in the normoxic heart. *FASEB J, 18*(10), 1138–1140.

Ikeya, T. and Hayashi, S. (1999). Interplay of Notch and FGF signaling restricts cell fate and MAPK activation in the *Drosophila* trachea. *Development, 126*(20), 4455–4463.

Imai, T., Horiuchi, A., Wang, C., Oka, K., Ohira, S., Nikaido, T., and Konishi, I. (2003). Hypoxia attenuates the expression of E-cadherin via up-regulation of SNAIL in ovarian carcinoma cells. *Am J Pathol, 163*(4), 1437–1447.

Imam, F., Sutherland, D., Huang, W., and Krasnow, M. A. (1999). *stumps*, a *Drosophila* gene required for fibroblast growth factor (FGF)-directed migrations of tracheal and mesodermal cells. *Genetics, 152*(1), 307–318.

Isaac, D. D. and Andrew, D. J. (1996). Tubulogenesis in *Drosophila*: a requirement for the *trachealess* gene product. *Genes Dev, 10*(1), 103–117.

Ivan, M., Kondo, K., Yang, H., Kim, W., Valiando, J., Ohh, M., Salic, A., Asara, J. M., Lane, W. S., and Kaelin, W. G. J. (2001). HIFalpha targeted for VHL-mediated destruction by proline hydroxylation: implications for O_2 sensing. *Science, 292*(5516), 464–468.

Iwai, K., Yamanaka, K., Kamura, T., Minato, N., Conaway, R. C., Conaway, J. W., Klausner, R. D., and Pause, A. (1999). Identification of the von Hippel-lindau tumor-suppressor protein as part of an active E3 ubiquitin ligase complex. *Proc Natl Acad Sci U S A, 96*(22), 12436–12441.

Jaakkola, P., Mole, D. R., Tian, Y. M., Wilson, M. I., Gielbert, J., Gaskell, S. J., Hebestreit, H. F., Mukherji, M., Schofield, C. J., Maxwell, P. H., Pugh, C. W., and Ratcliffe, P. J. (2001). Targeting of HIF-alpha to the von Hippel-Lindau ubiquitylation complex by O_2-regulated prolyl hydroxylation. *Science, 292*(5516), 468–472.

Jarecki, J., Johnson, E., and Krasnow, M. A. (1999). Oxygen regulation of airway branching in *Drosophila* is mediated by *branchless* FGF. *Cell, 99*(2), 211–220.

Jiang, B. H., Rue, E., Wang, G. L., Roe, R., and Semenza, G. L. (1996a). Dimerization, DNA binding, and transactivation properties of hypoxia-inducible factor 1. *J Biol Chem, 271*(30), 17771–17778.

Jiang, B. H., Semenza, G. L., Bauer, C., and Marti, H. H. (1996b). Hypoxia-inducible factor 1 levels vary exponentially over a physiologically relevant range of O_2 tension. *Am J Physiol, 271*(4 Pt 1), C1172-80.

Jiang, B. and Liu, L. (2008a). PI3K/PTEN signaling in tumorigenesis and angiogenesis. *Biochim Biophys Acta, 1784*(1), 150–158.

Jiang, B. and Liu, L. (2008b). AKT signaling in regulating angiogenesis. *Curr Cancer Drug Targets, 8*(1), 19–26.

Jiang, L. and Crews, S. T. (2003). The *Drosophila dysfusion* basic helix-loop-helix (bHLH)-PAS gene controls tracheal fusion and levels of the *trachealess* bHLH-PAS protein. *Mol Cell Biol, 23*(16), 5625–5637.

Jiang, L. and Crews, S. T. (2006). Dysfusion transcriptional control of *Drosophila* tracheal migration, adhesion, and fusion. *Mol Cell Biol, 26*(17), 6547–6556.

Jiang, L. and Crews, S. T. (2007). Transcriptional specificity of *Drosophila* dysfusion and the control of tracheal fusion cell gene expression. *J Biol Chem, 282*(39), 28659–28668.

Jin, J., Anthopoulos, N., Wetsch, B., Binari, R. C., Isaac, D. D., Andrew, D. J., Woodgett, J. R., and Manoukian, A. S. (2001). Regulation of Drosophila tracheal system development by protein kinase B. *Dev Cell, 1*(6), 817–827.

Kaelin, W. G. J. (2005). The von Hippel-Lindau protein, HIF hydroxylation, and oxygen sensing. *Biochem Biophys Res Commun, 338*(1), 627–638.

Kaelin, W. G. J. and Ratcliffe, P. J. (2008). Oxygen sensing by metazoans: the central role of the HIF hydroxylase pathway. *Mol Cell, 30*(4), 393–402.

Kamura, T., Koepp, D. M., Conrad, M. N., Skowyra, D., Moreland, R. J., Iliopoulos, O., Lane, W. S., Kaelin, W. G. J., Elledge, S. J., Conaway, R. C., Harper, J. W., and Conaway, J. W. (1999). Rbx1, a component of the VHL

tumor suppressor complex and SCF ubiquitin ligase. *Science, 284*(5414), 657–661.

Kapitsinou, P. P. and Haase, V. H. (2008). The VHL tumor suppressor and HIF: insights from genetic studies in mice. *Cell Death Differ, 15*(4), 650–659.

Kennison, J. A. and Tamkun, J. W. (1988). Dosage-dependent modifiers of *polycomb* and *antennapedia* mutations in *Drosophila*. *Proc Natl Acad Sci U S A, 85*(21), 8136–8140.

Kibel, A., Iliopoulos, O., DeCaprio, J. A., and Kaelin, W. G. J. (1995). Binding of the von Hippel-Lindau tumor suppressor protein to Elongin B and C. *Science, 269*(5229), 1444–1446.

Kim, J., Tchernyshyov, I., Semenza, G. L., and Dang, C. V. (2006a). HIF-1-mediated expression of pyruvate dehydrogenase kinase: a metabolic switch required for cellular adaptation to hypoxia. *Cell Metab, 3*(3), 177–185.

Kim, K., Lee, Y. S., Harris, D., Nakahara, K., and Carthew, R. W. (2006b). The RNAi pathway initiated by Dicer-2 in *Drosophila*. *Cold Spring Harb Symp Quant Biol, 71*, 39–44.

Klaes, A., Menne, T., Stollewerk, A., Scholz, H., and Klambt, C. (1994). The Ets transcription factors encoded by the *Drosophila* gene *pointed* direct glial cell differentiation in the embryonic CNS. *Cell, 78*(1), 149–160.

Klambt, C. (1993). The *Drosophila* gene *pointed* encodes two ETS-like proteins which are involved in the development of the midline glial cells. *Development, 117*(1), 163–176.

Klambt, C., Glazer, L., and Shilo, B. Z. (1992). *breathless*, a *Drosophila* FGF receptor homolog, is essential for migration of tracheal and specific midline glial cells. *Genes Dev, 6*(9), 1668–1678.

Kliche, S. and Waltenberger, J. (2001). VEGF receptor signaling and endothelial function. *IUBMB Life, 52*(1-2), 61–66.

Klose, R. J., Kallin, E. M., and Zhang, Y. (2006). JmjC-domain-containing proteins and histone demethylation. *Nat Rev Genet, 7*(9), 715–727.

Koepp, D. M., Schaefer, L. K., Ye, X., Keyomarsi, K., Chu, C., Harper, J. W., and Elledge, S. J. (2001). Phosphorylation-dependent ubiquitination of cyclin E by the SCFFbw7 ubiquitin ligase. *Science, 294*(5540), 173–177.

Koh, M. S., Ittmann, M., Kadmon, D., Thompson, T. C., and Leach, F. S. (2006). CDC4 gene expression as potential biomarker for targeted therapy in prostate cancer. *Cancer Biol Ther, 5*(1), 78–83.

Koh, M. Y., Darnay, B. G., and Powis, G. (2008). Hypoxia-Associated Factor, a Novel E3-Ubiquitin Ligase, Binds and Ubiquitinates Hypoxia-Inducible Factor 1alpha, Leading to Its Oxygen-Independent Degradation. *Mol Cell Biol, 28*(23), 7081–7095.

Koivunen, P., Hirsila, M., Gunzler, V., Kivirikko, K. I., and Myllyharju, J. (2004). Catalytic properties of the asparaginyl hydroxylase (FIH) in the oxygen sensing pathway are distinct from those of its prolyl 4-hydroxylases. *J Biol Chem, 279*(11), 9899–9904.

Krebs, H. A. (1972). The Pasteur effect and the relations between respiration and fermentation. *Essays Biochem, 8*, 1–34.

Krebs, H. A. and Johnson, W. A. (1937). Metabolism of ketonic acids in animal tissues. *Biochem J, 31*(4), 645–650.

Krishnan, S., Sun, Y., Mohsenin, A., Wyman, R., and Haddad, G. (1997). Behavioral and Electrophysiologic Responses of *Drosophila melanogaster* to Prolonged Periods of Anoxia. *J Insect Physiol, 43*(3), 203–210.

Kroemer, G. and Pouyssegur, J. (2008). Tumor cell metabolism: cancer's Achilles' heel. *Cancer Cell, 13*(6), 472–482.

Kuhnlein, R. P. and Schuh, R. (1996). Dual function of the region-specific homeotic gene *spalt* during *Drosophila* tracheal system development. *Development, 122*(7), 2215–2223.

Kuo, Y. M., Jones, N., Zhou, B., Panzer, S., Larson, V., and Beckendorf, S. K. (1996). Salivary duct determination in *Drosophila*: roles of the EGF receptor signalling pathway and the transcription factors *fork head* and *trachealess*. *Development, 122*(6), 1909–1917.

Kwak, E. L., Moberg, K. H., Wahrer, D. C. R., Quinn, J. E., Gilmore, P. M., Graham, C. A., Hariharan, I. K., Harkin, D. P., Haber, D. A., and Bell, D. W. (2005). Infrequent mutations of Archipelago (hAGO, hCDC4, Fbw7) in primary ovarian cancer. *Gynecol Oncol, 98*(1), 124–128.

Lando, D., Peet, D. J., Gorman, J. J., Whelan, D. A., Whitelaw, M. L., and Bruick, R. K. (2002a). FIH-1 is an asparaginyl hydroxylase enzyme that regulates the transcriptional activity of hypoxia-inducible factor. *Genes Dev, 16*(12), 1466–1471.

Lando, D., Peet, D. J., Whelan, D. A., Gorman, J. J., and Whitelaw, M. L. (2002b). Asparagine hydroxylation of the HIF transactivation domain a hypoxic switch. *Science, 295*(5556), 858–861.

Lavista-Llanos, S., Centanin, L., Irisarri, M., Russo, D. M., Gleadle, J. M., Bocca, S. N., Muzzopappa, M., Ratcliffe, P. J., and Wappner, P. (2002). Control of the hypoxic response in *Drosophila melanogaster* by the basic helix-loop-helix PAS protein *similar*. *Mol Cell Biol, 22*(19), 6842–6853.

Lee, T., Feig, L., and Montell, D. J. (1996b). Two distinct roles for Ras in a developmentally regulated cell migration. *Development, 122*(2), 409–418.

Lee, T., Hacohen, N., Krasnow, M., and Montell, D. J. (1996a). Regulated Breathless receptor tyrosine kinase activity required to pattern cell migration and branching in the *Drosophila* tracheal system. *Genes Dev, 10*(22), 2912–2921.

Lee, Y. M., Jeong, C. H., Koo, S. Y., Son, M. J., Song, H. S., Bae, S. K., Raleigh, J. A., Chung, H. Y., Yoo, M. A., and Kim, K. W. (2001). Determination of hypoxic region by hypoxia marker in developing mouse embryos in vivo: a possible signal for vessel development. *Dev Dyn, 220*(2), 175–186.

Levesque, B. M., Zhou, S., Shan, L., Johnston, P., Kong, Y., Degan, S., and Sunday, M. E. (2007). NPAS1 regulates branching morphogenesis in embryonic lung. *Am J Respir Cell Mol Biol, 36*(4), 427–434.

Li, J., Pauley, A. M., Myers, R. L., Shuang, R., Brashler, J. R., Yan, R., Buhl, A. E., Ruble, C., and Gurney, M. E. (2002). SEL-10 interacts with presenilin 1, facilitates its ubiquitination, and alters A-beta peptide production. *J Neurochem, 82*(6), 1540–1548.

Li, Y., Gazdoiu, S., Pan, Z., and Fuchs, S. Y. (2004). Stability of homologue of Slimb F-box protein is regulated by availability of its substrate. *J Biol Chem, 279*(12), 11074–11080.

Lisy, K. and Peet, D. J. (2008). Turn me on: regulating HIF transcriptional activity. *Cell Death Differ, 15*(4), 642–649.

Lisztwan, J., Imbert, G., Wirbelauer, C., Gstaiger, M., and Krek, W. (1999). The von Hippel-Lindau tumor suppressor protein is a component of an E3 ubiquitin-protein ligase activity. *Genes Dev, 13*(14), 1822–1833.

Liu, G., Roy, J., and Johnson, E. A. (2006). Identification and function of hypoxia-response genes in *Drosophila* melanogaster. *Physiol Genomics, 25*(1), 134–141.

Llimargas, M. (1999). The Notch pathway helps to pattern the tips of the *Drosophila* tracheal branches by selecting cell fates. *Development, 126*(11), 2355–2364.

Llimargas, M. and Casanova, J. (1999). EGF signalling regulates cell invagination as well as cell migration during formation of tracheal system in *Drosophila*. *Dev Genes Evol, 209*(3), 174–179.

Locke, M. (1957). The Structure of Insect Tracheae. *Quarterly Journal of Microscopical Science, s3-98*, 487–492.

Locke, M. (1958). The Co-ordination of Growth in the Tracheal System of Insects. *Quarterly Journal of Microscopical Science, s3-99*, 373–391.

Lonser, R. R., Glenn, G. M., Walther, M., Chew, E. Y., Libutti, S. K., Linehan, W. M., and Oldfield, E. H. (2003). von Hippel-Lindau disease. *Lancet, 361*(9374), 2059–2067.

Lubarsky, B. and Krasnow, M. A. (2003). Tube morphogenesis: making and shaping biological tubes. *Cell, 112*(1), 19–28.

Ma, E. and Haddad, G. G. (1999). Isolation and characterization of the hypoxia-inducible factor 1beta in *Drosophila melanogaster*. *Brain Res Mol Brain Res, 73*(1-2), 11–16.

Ma, E., Xu, T., and Haddad, G. G. (1999). Gene regulation by O_2 deprivation: an anoxia-regulated novel gene in *Drosophila melanogaster*. *Brain Res Mol Brain Res, 63*(2), 217–224.

Mahon, P. C., Hirota, K., and Semenza, G. L. (2001). FIH-1: a novel protein that interacts with HIF-1alpha and VHL to mediate repression of HIF-1 transcriptional activity. *Genes Dev, 15*(20), 2675–2686.

Maleszka, R., Hanes, S. D., Hackett, R. L., de Couet, H. G., and Miklos, G. L. (1996). The *Drosophila melanogaster dodo* (*dod*) gene, conserved in humans, is functionally interchangeable with the ESS1 cell division gene of *Saccharomyces cerevisiae*. *Proc Natl Acad Sci U S A, 93*(1), 447–451.

Malyukova, A., Dohda, T., von der Lehr, N., Akhoondi, S., Corcoran, M., Heyman, M., Spruck, C., Grander, D., Lendahl, U., and Sangfelt, O. (2007). The tumor suppressor gene hCDC4 is frequently mutated in human T-cell acute lymphoblastic leukemia with functional consequences for Notch signaling. *Cancer Res, 67*(12), 5611–5616.

Manalo, D. J., Rowan, A., Lavoie, T., Natarajan, L., Kelly, B. D., Ye, S. Q., Garcia, J. G. N., and Semenza, G. L. (2005). Transcriptional regulation of vascular endothelial cell responses to hypoxia by HIF-1. *Blood, 105*(2), 659–669.

Manning, G. and Krasnow, M. A. (1993). Development of the *Drosophila* tracheal system. In The Development of *Drosophila melanogaster*. M. Bate and A. M. Arias (Eds.), (609–685). Cold Spring Harbor Press.

Mao, J., Perez-Losada, J., Wu, D., Delrosario, R., Tsunematsu, R., Nakayama, K. I., Brown, K., Bryson, S., and Balmain, A. (2004). Fbxw7/Cdc4 is a p53-dependent, haploinsufficient tumour suppressor gene. *Nature, 432*(7018), 775–779.

Maser, R. S., Choudhury, B., Campbell, P. J., Feng, B., Wong, K., Protopopov, A., O'Neil, J., Gutierrez, A., Ivanova, E., Perna, I., Lin, E., Mani, V., Jiang, S., McNamara, K., Zaghlul, S., Edkins, S., Stevens, C., Brennan, C., Martin, E. S., Wiedemeyer, R., Kabbarah, O., Nogueira, C., Histen, G., Aster, J., Mansour, M., Duke, V., Foroni, L., Fielding, A. K., Goldstone, A. H., Rowe, J. M., Wang, Y. A., Look, A. T., Stratton, M. R., Chin, L., Futreal, P. A., and DePinho, R. A. (2007). Chromosomally unstable mouse tumours have genomic alterations similar to diverse human cancers. *Nature, 447*(7147), 966–971.

Maxwell, P. H. (2005). The HIF pathway in cancer. *Semin Cell Dev Biol, 16*(4-5), 523–530.

Maxwell, P. H., Wiesener, M. S., Chang, G. W., Clifford, S. C., Vaux, E. C., Cockman, M. E., Wykoff, C. C., Pugh, C. W., Maher, E. R., and Ratcliffe, P. J. (1999). The tumour suppressor protein VHL targets hypoxia-inducible factors for oxygen-dependent proteolysis. *Nature, 399*(6733), 271–275.

Mayer-Jaekel, R. E., Ohkura, H., Gomes, R., Sunkel, C. E., Baumgartner, S., Hemmings, B. A., and Glover, D. M. (1993). The 55 kd regulatory subunit of

Drosophila protein phosphatase 2A is required for anaphase. *Cell, 72*(4), 621–633.

Merabet, S., Ebner, A., and Affolter, M. (2005). The *Drosophila* Extradenticle and Homothorax selector proteins control *branchless*/FGF expression in mesodermal bridge-cells. *EMBO Rep, 6*(8), 762–768.

Metzger, R. J. and Krasnow, M. A. (1999). Genetic control of branching morphogenesis. *Science, 284*(5420), 1635–1639.

Meyerhof, O. (1920a). Die energieumwandlungen im muskel. I. Uber die beziehungen der milchsaure zur warmebildung und arbeits- leistung des muskels in der anaerobiose. *Arch Ges Physiol, 182*, 232–283.

Meyerhof, O. (1920b). Uber die energieumwandlungen im muskel. II. Das Schicksal der milchsaure in der Erholungsperiode des muskels. *Arch Ges Physiol, 182*, 284–317.

Meyerhof, O. (1920c). Die energieumwandlungen im muskel. III. Kohlenhydrat- und milchsaureumsatz im froschmuskel. *Arch Ges Physiol, 185*, 11–32.

Michelson, A. M., Gisselbrecht, S., Buff, E., and Skeath, J. B. (1998 Nov). Heartbroken is a specific downstream mediator of FGF receptor signalling in *Drosophila*. *Development, 125*(22), 4379–4389.

Min, H., Danilenko, D. M., Scully, S. A., Bolon, B., Ring, B. D., Tarpley, J. E., DeRose, M., and Simonet, W. S. (1998). Fgf-10 is required for both limb and lung development and exhibits striking functional similarity to *Drosophila branchless*. *Genes Dev, 12*(20), 3156–3161.

Minella, A. C. and Clurman, B. E. (2005). Mechanisms of tumor suppression by the SCF(Fbw7). *Cell Cycle, 4*(10), 1356–1359.

Minella, A. C., Welcker, M., and Clurman, B. E. (2005). Ras activity regulates cyclin E degradation by the Fbw7 pathway. *Proc Natl Acad Sci U S A, 102*(27), 9649–9654.

Mitchell, P. D. (1961). Coupling of Phosphorylation to Electron and Hydrogen Transfer by a Chemi-Osmotic type of Mechanism. *Nature, 191*(4784), 144–148.

Moberg, K. H., Bell, D. W., Wahrer, D. C., Haber, D. A., and Hariharan, I. K. (2001). Archipelago regulates Cyclin E levels in *Drosophila* and is mutated in human cancer cell lines. *Nature, 413*(6853), 311–316.

Moberg, K. H., Mukherjee, A., Veraksa, A., Artavanis-Tsakonas, S., and Hariharan, I. K. (2004). The *Drosophila* F box protein *archipelago* regulates dMyc protein levels in vivo. *Curr Biol, 14*(11), 965–974.

Mohammadi, M., Olsen, S. K., and Ibrahimi, O. A. (2005). Structural basis for fibroblast growth factor receptor activation. *Cytokine Growth Factor Rev, 16*(2), 107–137.

Myat, M. M., Lightfoot, H., Wang, P., and Andrew, D. J. (2005). A molecular link between FGF and Dpp signaling in branch-specific migration of the *Drosophila* trachea. *Dev Biol, 281*(1), 38–52.

Nagao, M., Ebert, B. L., Ratcliffe, P. J., and Pugh, C. W. (1996). *Drosophila melanogaster* SL2 cells contain a hypoxically inducible DNA binding complex which recognises mammalian HIF-binding sites. *FEBS Lett, 387*(2-3), 161–166.

Nambu, J. R., Chen, W., Hu, S., and Crews, S. T. (1996). The *Drosophila melanogaster similar* bHLH-PAS gene encodes a protein related to human hypoxia-inducible factor 1 alpha and *Drosophila single-minded*. *Gene, 172*(2), 249–254.

Nateri, A. S., Riera-Sans, L., Da Costa, C., and Behrens, A. (2004). The ubiquitin ligase SCFFbw7 antagonizes apoptotic JNK signaling. *Science, 303*(5662), 1374–1378.

O'Neil, J., Grim, J., Strack, P., Rao, S., Tibbitts, D., Winter, C., Hardwick, J., Welcker, M., Meijerink, J. P., Pieters, R., Draetta, G., Sears, R., Clurman, B. E., and Look, A. T. (2007). FBW7 mutations in leukemic cells mediate NOTCH pathway activation and resistance to gamma-secretase inhibitors. *J Exp Med, 204*(8), 1813–1824.

Oberg, C., Li, J., Pauley, A., Wolf, E., Gurney, M., and Lendahl, U. (2001). The Notch intracellular domain is ubiquitinated and negatively regulated by the mammalian Sel-10 homolog. *J Biol Chem, 276*(38), 35847–35853.

Ohh, M., Park, C. W., Ivan, M., Hoffman, M. A., Kim, T. Y., Huang, L. E., Pavletich, N., Chau, V., and Kaelin, W. G. (2000). Ubiquitination of hypoxia-inducible factor requires direct binding to the beta-domain of the von Hippel-Lindau protein. *Nat Cell Biol, 2*(7), 423–427.

Ohshiro, T., Emori, Y., and Saigo, K. (2002). Ligand-dependent activation of *breathless* FGF receptor gene in *Drosophila* developing trachea. *Mech Dev, 114*(1-2), 3–11.

Ohshiro, T. and Saigo, K. (1997). Transcriptional regulation of *breathless* FGF receptor gene by binding of TRACHEALESS/dARNT heterodimers to three central midline elements in *Drosophila* developing trachea. *Development, 124*(20), 3975–3986.

Olson, B. L., Hock, M. B., Ekholm-Reed, S., Wohlschlegel, J. A., Dev, K. K., Kralli, A., and Reed, S. I. (2008). SCFCdc4 acts antagonistically to the PGC-1alpha transcriptional coactivator by targeting it for ubiquitin-mediated proteolysis. *Genes Dev, 22*(2), 252–264.

Onoyama, I., Tsunematsu, R., Matsumoto, A., Kimura, T., de Alboran, I. M., Nakayama, K., and Nakayama, K. I. (2007). Conditional inactivation of Fbxw7 impairs cell-cycle exit during T cell differentiation and results in lymphomatogenesis. *J Exp Med, 204*(12), 2875–2888.

Ouiddir, A., Planes, C., Fernandes, I., VanHesse, A., and Clerici, C. (1999). Hypoxia upregulates activity and expression of the glucose transporter GLUT1 in alveolar epithelial cells. *Am J Respir Cell Mol Biol, 21*(6), 710–718.

Paffett, M. L. and Walker, B. R. (2007). Vascular adaptations to hypoxia: molecular and cellular mechanisms regulating vascular tone. *Essays Biochem, 43*, 105–119.

Papandreou, I., Cairns, R. A., Fontana, L., Lim, A. L., and Denko, N. C. (2006). HIF-1 mediates adaptation to hypoxia by actively downregulating mitochondrial oxygen consumption. *Cell Metab, 3*(3), 187–197.

Patel, S. A. and Simon, M. C. (2008). Biology of hypoxia-inducible factor-2alpha in development and disease. *Cell Death Differ, 15*(4), 628–634.

Pause, A., Lee, S., Worrell, R. A., Chen, D. Y., Burgess, W. H., Linehan, W. M., and Klausner, R. D. (1997). The von Hippel-Lindau tumor-suppressor gene product forms a stable complex with human CUL-2, a member of the Cdc53 family of proteins. *Proc Natl Acad Sci U S A, 94*(6), 2156–2161.

Perrimon, N., Noll, E., McCall, K., and Brand, A. (1991). Generating lineage-specific markers to study *Drosophila* development. *Dev Genet, 12*(3), 238–252.

Peyssonnaux, C., Cejudo-Martin, P., Doedens, A., Zinkernagel, A. S., Johnson, R. S., and Nizet, V. (2007). Cutting edge: Essential role of hypoxia inducible factor-1alpha in development of lipopolysaccharide-induced sepsis. *J Immunol, 178*(12), 7516–7519.

Pfander, D., Swoboda, B., and Cramer, T. (2006). The role of HIF-1alpha in maintaining cartilage homeostasis and during the pathogenesis of osteoarthritis. *Arthritis Res Ther, 8*(1), 104.

Pieper, A. A., Wu, X., Han, T. W., Estill, S. J., Dang, Q., Wu, L. C., Reece-Fincanon, S., Dudley, C. A., Richardson, J. A., Brat, D. J., and McKnight, S. L. (2005). The neuronal PAS domain protein 3 transcription factor controls FGF-mediated adult hippocampal neurogenesis in mice. *Proc Natl Acad Sci U S A, 102*(39), 14052–14057.

Pollock, P. M., Gartside, M. G., Dejeza, L. C., Powell, M. A., Mallon, M. A., Davies, H., Mohammadi, M., Futreal, P. A., Stratton, M. R., Trent, J. M., and Goodfellow, P. J. (2007). Frequent activating FGFR2 mutations in endometrial carcinomas parallel germline mutations associated with craniosynostosis and skeletal dysplasia syndromes. *Oncogene, 26*(50), 7158–7162.

Poole, T. J., Finkelstein, E. B., and Cox, C. M. (2001). The role of FGF and VEGF in angioblast induction and migration during vascular development. *Dev Dyn, 220*(1), 1–17.

Presta, M., Dell'Era, P., Mitola, S., Moroni, E., Ronca, R., and Rusnati, M. (2005). Fibroblast growth factor/fibroblast growth factor receptor system in angiogenesis. *Cytokine Growth Factor Rev, 16*(2), 159–178.

Priestley, J. (1775). An Account of Further Discoveries in Air. *Philosophical Transactions, 65*, 384–394.

Provot, S., Zinyk, D., Gunes, Y., Kathri, R., Le, Q., Kronenberg, H. M., Johnson, R. S., Longaker, M. T., Giaccia, A. J., and Schipani, E. (2007). Hif-1alpha regulates differentiation of limb bud mesenchyme and joint development. *J Cell Biol, 177*(3), 451–464.

Punga, T., Bengoechea-Alonso, M. T., and Ericsson, J. (2006). Phosphorylation and ubiquitination of the transcription factor sterol regulatory element-binding protein-1 in response to DNA binding. *J Biol Chem, 281*(35), 25278–25286.

Rajagopalan, H., Jallepalli, P. V., Rago, C., Velculescu, V. E., Kinzler, K. W., Vogelstein, B., and Lengauer, C. (2004). Inactivation of hCDC4 can cause chromosomal instability. *Nature, 428*(6978), 77–81.

Rankin, E. B. and Giaccia, A. J. (2008). The role of hypoxia-inducible factors in tumorigenesis. *Cell Death Differ, 15*(4), 678–685.

Ratan, R. R., Siddiq, A., Smirnova, N., Karpisheva, K., Haskew-Layton, R., McConoughey, S., Langley, B., Estevez, A., Huerta, P. T., Volpe, B., Roy, S., Sen, C. K., Gazaryan, I., Cho, S., Fink, M., and LaManna, J. (2007). Harnessing hypoxic adaptation to prevent, treat, and repair stroke. *J Mol Med, 85*(12), 1331–1338.

Reichman-Fried, M., Dickson, B., Hafen, E., and Shilo, B. Z. (1994). Elucidation of the role of *breathless*, a *Drosophila* FGF receptor homolog, in tracheal cell migration. *Genes Dev, 8*(4), 428–439.

Reichman-Fried, M. and Shilo, B. Z. (1995). Breathless, a *Drosophila* FGF receptor homolog, is required for the onset of tracheal cell migration and tracheole formation. *Mech Dev, 52*(2-3), 265–273.

Richard, D. E., Berra, E., and Pouyssegur, J. (1999). Angiogenesis: how a tumor adapts to hypoxia. *Biochem Biophys Res Commun, 266*(3), 718–722.

Risau, W. and Flamme, I. (1995). Vasculogenesis. *Annu Rev Cell Dev Biol, 11*, 73–91.

Rodriguez, C., Martinez-Gonzalez, J., Raposo, B., Alcudia, J. F., Guadall, A., and Badimon, L. (2008). Regulation of lysyl oxidase in vascular cells: lysyl oxidase as a new player in cardiovascular diseases. *Cardiovasc Res, 79*(1), 7–13.

Romero, N. M., Dekanty, A., and Wappner, P. (2007). Cellular and developmental adaptations to hypoxia: a *Drosophila* perspective. *Methods Enzymol, 435*, 123–144.

Rosenfeld, E., Beauvoit, B., Rigoulet, M., and Salmon, J. (2002). Non-respiratory oxygen consumption pathways in anaerobically-grown *Saccharomyces cerevisiae*: evidence and partial characterization. *Yeast, 19*(15), 1299–1321.

Ryan, H. E., Lo, J., and Johnson, R. S. (1998). HIF-1 alpha is required for solid tumor formation and embryonic vascularization. *EMBO J, 17*(11), 3005–3015.

Samakovlis, C., Hacohen, N., Manning, G., Sutherland, D. C., Guillemin, K., and Krasnow, M. A. (1996a). Development of the *Drosophila* tracheal system occurs by a series of morphologically distinct but genetically coupled branching events. *Development, 122*(5), 1395–1407.

Samakovlis, C., Manning, G., Steneberg, P., Hacohen, N., Cantera, R., and Krasnow, M. A. (1996b). Genetic control of epithelial tube fusion during *Drosophila* tracheal development. *Development, 122*(11), 3531–3536.

Scheele, C. W. (1777). *Chemische Abhandlung von der Luft und dem Feuer.* M. Swederus.

Scholz, H., Schurek, H. J., Eckardt, K. U., and Bauer, C. (1990). Role of erythropoietin in adaptation to hypoxia. *Experientia, 46*(11-12), 1197–1201.

Scortegagna, M., Ding, K., Oktay, Y., Gaur, A., Thurmond, F., Yan, L., Marck, B. T., Matsumoto, A. M., Shelton, J. M., Richardson, J. A., Bennett, M. J., and Garcia, J. A. (2003). Multiple organ pathology, metabolic abnormalities and impaired homeostasis of reactive oxygen species in Epas1-/- mice. *Nat Genet, 35*(4), 331–340.

Seagroves, T. N., Ryan, H. E., Lu, H., Wouters, B. G., Knapp, M., Thibault, P., Laderoute, K., and Johnson, R. S. (2001). Transcription factor HIF-1 is a necessary mediator of the pasteur effect in mammalian cells. *Mol Cell Biol, 21*(10), 3436–3444.

Seger, R. and Krebs, E. G. (1995). The MAPK signaling cascade. *FASEB J, 9*(9), 726–735.

Semenza, G. L. (2000). HIF-1 and human disease: one highly involved factor. *Genes Dev, 14*(16), 1983–1991.

Semenza, G. L. (2001). Hypoxia-inducible factor 1: control of oxygen homeostasis in health and disease. *Pediatr Res, 49*(5), 614–617.

Semenza, G. L. (2003). Targeting HIF-1 for cancer therapy. *Nat Rev Cancer, 3*(10), 721–732.

Semenza, G. L. (2007). Oxygen-dependent regulation of mitochondrial respiration by hypoxia-inducible factor 1. *Biochem J, 405*(1), 1–9.

Semenza, G. L., Agani, F., Feldser, D., Iyer, N., Kotch, L., Laughner, E., and Yu, A. (2000). Hypoxia, HIF-1, and the pathophysiology of common human diseases. *Adv Exp Med Biol, 475*, 123–130.

Semenza, G. L. and Wang, G. L. (1992). A nuclear factor induced by hypoxia via de novo protein synthesis binds to the human erythropoietin gene enhancer at a site required for transcriptional activation. *Mol Cell Biol, 12*(12), 5447–5454.

Shen, J., Khan, N., Lewis, L. D., Armand, R., Grinberg, O., Demidenko, E., and Swartz, H. (2003). Oxygen consumption rates and oxygen concentration in

molt-4 cells and their mtDNA depleted (rho0) mutants. *Biophys J, 84*(2 Pt 1), 1291–1298.

Shiga, Y., Tanaka-Matakatsu, M., and Hayashi, S. (1996). A nuclear GFP/ beta-galactosidase fusion protein as a marker for morphogenesis in living *Drosophila*. *Dev Growth Diffn, 38*, 99–106.

Shishido, E., Higashijima, S., Emori, Y., and Saigo, K. (1993). Two FGF-receptor homologues of *Drosophila*: one is expressed in mesodermal primordium in early embryos. *Development, 117*(2), 751–761.

Shishido, E., Ono, N., Kojima, T., and Saigo, K. (1997). Requirements of DFR1/ Heartless, a mesoderm-specific *Drosophila* FGF-receptor, for the formation of heart, visceral and somatic muscles, and ensheathing of longitudinal axon tracts in CNS. *Development, 124*(11), 2119–2128.

Shohet, R. V. and Garcia, J. A. (2007). Keeping the engine primed: HIF factors as key regulators of cardiac metabolism and angiogenesis during ischemia. *J Mol Med, 85*(12), 1309–1315.

Shweiki, D., Itin, A., Soffer, D., and Keshet, E. (1992). Vascular endothelial growth factor induced by hypoxia may mediate hypoxia-initiated angiogenesis. *Nature, 359*(6398), 843–845.

Siegfried, E., Chou, T. B., and Perrimon, N. (1992). *wingless* signaling acts through *zeste-white 3*, the *Drosophila* homolog of glycogen synthase kinase-3, to regulate engrailed and establish cell fate. *Cell, 71*(7), 1167–1179.

Siegfried, E., Perkins, L. A., Capaci, T. M., and Perrimon, N. (1990). Putative protein kinase product of the *Drosophila* segment-polarity gene *zeste-white 3*. *Nature, 345*(6278), 825–829.

Silverstein, A. M., Barrow, C. A., Davis, A. J., and Mumby, M. C. (2002). Actions of PP2A on the MAP kinase pathway and apoptosis are mediated by distinct regulatory subunits. *Proc Natl Acad Sci U S A, 99*(7), 4221–4226.

Simon, M. C. and Keith, B. (2008). The role of oxygen availability in embryonic development and stem cell function. *Nat Rev Mol Cell Biol, 9*(4), 285–296.

Skowyra, D., Craig, K. L., Tyers, M., Elledge, S. J., and Harper, J. W. (1997). F-box proteins are receptors that recruit phosphorylated substrates to the SCF ubiquitin-ligase complex. *Cell, 91*(2), 209–219.

Skuli, N., Monferran, S., Delmas, C., Lajoie-Mazenc, I., Favre, G., Toulas, C., and Cohen-Jonathan-Moyal, E. (2006). Activation of RhoB by hypoxia controls hypoxia-inducible factor-1alpha stabilization through glycogen synthase kinase-3 in U87 glioblastoma cells. *Cancer Res, 66*(1), 482–489.

Smith, T. G., Robbins, P. A., and Ratcliffe, P. J. (2008). The human side of hypoxia-inducible factor. *Br J Haematol, 141*(3), 325–334.

Song, J. H., Schnittke, N., Zaat, A., Walsh, C. S., and Miller, C. W. (2008). FBXW7 mutation in adult T-cell and B-cell acute lymphocytic leukemias. *Leuk Res, 32*(11), 1751–1755.

Sonnenfeld, M., Ward, M., Nystrom, G., Mosher, J., Stahl, S., and Crews, S. (1997). The *Drosophila tango* gene encodes a bHLH-PAS protein that is orthologous to mammalian Arnt and controls CNS midline and tracheal development. *Development, 124*(22), 4571–4582.

Sporn, M. B. (1996). The war on cancer. *Lancet, 347*(9012), 1377–1381.

Spradling, A. C., Stern, D., Beaton, A., Rhem, E. J., Laverty, T., Mozden, N., Misra, S., and Rubin, G. M. (1999). The Berkeley *Drosophila* Genome Project gene disruption project: Single P-element insertions mutating 25% of vital *Drosophila* genes. *Genetics, 153*(1), 135–177.

Spruck, C. H., Strohmaier, H., Sangfelt, O., Muller, H. M., Hubalek, M., Muller-Holzner, E., Marth, C., Widschwendter, M., and Reed, S. I. (2002). hCDC4 gene mutations in endometrial cancer. *Cancer Res, 62*(16), 4535–4539.

Stathopoulos, A., Tam, B., Ronshaugen, M., Frasch, M., and Levine, M. (2004). *pyramus* and *thisbe*: FGF genes that pattern the mesoderm of *Drosophila* embryos. *Genes Dev, 18*(6), 687–699.

Stebbins, C. E., Kaelin, W. G. J., and Pavletich, N. P. (1999). Structure of the VHL-ElonginC-ElonginB complex: implications for VHL tumor suppressor function. *Science, 284*(5413), 455–461.

Steneberg, P., Hemphala, J., and Samakovlis, C. (1999). Dpp and Notch specify the fusion cell fate in the dorsal branches of the *Drosophila* trachea. *Mech Dev, 87*(1-2), 153–163.

Strohmaier, H., Spruck, C. H., Kaiser, P., Won, K. A., Sangfelt, O., and Reed, S. I. (2001). Human F-box protein hCdc4 targets cyclin E for proteolysis and is mutated in a breast cancer cell line. *Nature, 413*(6853), 316–322.

Suchting, S., Freitas, C., le Noble, F., Benedito, R., Breant, C., Duarte, A., and Eichmann, A. (2007). The Notch ligand Delta-like 4 negatively regulates endothelial tip cell formation and vessel branching. *Proc Natl Acad Sci U S A, 104*(9), 3225–3230.

Sundqvist, A., Bengoechea-Alonso, M. T., Ye, X., Lukiyanchuk, V., Jin, J., Harper, J. W., and Ericsson, J. (2005). Control of lipid metabolism by phosphorylation-dependent degradation of the SREBP family of transcription factors by SCF(Fbw7). *Cell Metab, 1*(6), 379–391.

Sutherland, D., Samakovlis, C., and Krasnow, M. A. (1996). *branchless* encodes a *Drosophila* FGF homolog that controls tracheal cell migration and the pattern of branching. *Cell, 87*(6), 1091–1101.

Tabbara, I. A. and Robinson, B. E. (1991). Hematopoietic growth factors. *Anticancer Res, 11*(1), 81–90.

Takeda, K., Ho, V. C., Takeda, H., Duan, L., Nagy, A., and Fong, G. (2006). Placental but not heart defects are associated with elevated hypoxia-inducible factor alpha levels in mice lacking prolyl hydroxylase domain protein 2. *Mol Cell Biol, 26*(22), 8336–8346.

Talks, K. L., Turley, H., Gatter, K. C., Maxwell, P. H., Pugh, C. W., Ratcliffe, P. J., and Harris, A. L. (2000). The expression and distribution of the hypoxia-inducible factors HIF-1alpha and HIF-2alpha in normal human tissues, cancers, and tumor-associated macrophages. *Am J Pathol, 157*(2), 411–421.

Tan, Y., Sangfelt, O., and Spruck, C. (2008). The Fbxw7/hCdc4 tumor suppressor in human cancer. *Cancer Lett,* .

Tanaka-Matakatsu, M., Uemura, T., Oda, H., Takeichi, M., and Hayashi, S. (1996). Cadherin-mediated cell adhesion and cell motility in *Drosophila* trachea regulated by the transcription factor Escargot. *Development, 122*(12), 3697–3705.

Tannock, I. F. (1968). The relation between cell proliferation and the vascular system in a transplanted mouse mammary tumour. *Br J Cancer, 22*(2), 258–273.

Tannock, I. F. (1972). Oxygen diffusion and the distribution of cellular radiosensitivity in tumours. *Br J Radiol, 45*(535), 515–524.

Tautz, D. (2000). Whole mount in situ hybridization for the detection of mRNA in *Drosophila* embryos. In Nonradioactive Analysis of Biomolecules. C. Kessler (Ed.), (573–580). Springer.

Tetzlaff, M. T., Yu, W., Li, M., Zhang, P., Finegold, M., Mahon, K., Harper, J. W., Schwartz, R. J., and Elledge, S. J. (2004). Defective cardiovascular development and elevated cyclin E and Notch proteins in mice lacking the Fbw7 F-box protein. *Proc Natl Acad Sci U S A, 101*(10), 3338–3345.

Thisse, B. and Thisse, C. (2005). Functions and regulations of fibroblast growth factor signaling during embryonic development. *Dev Biol, 287*(2), 390–402.

Thompson, B. J., Buonamici, S., Sulis, M. L., Palomero, T., Vilimas, T., Basso, G., Ferrando, A., and Aifantis, I. (2007). The SCFFBW7 ubiquitin ligase complex as a tumor suppressor in T cell leukemia. *J Exp Med, 204*(8), 1825–1835.

Tian, H., Hammer, R. E., Matsumoto, A. M., Russell, D. W., and McKnight, S. L. (1998). The hypoxia-responsive transcription factor EPAS1 is essential for catecholamine homeostasis and protection against heart failure during embryonic development. *Genes Dev, 12*(21), 3320–3324.

Tian, H., McKnight, S. L., and Russell, D. W. (1997). Endothelial PAS domain protein 1 (EPAS1), a transcription factor selectively expressed in endothelial cells. *Genes Dev, 11*(1), 72–82.

Tomlinson, D. C., Baldo, O., Harnden, P., and Knowles, M. A. (2007). FGFR3 protein expression and its relationship to mutation status and prognostic variables in bladder cancer. *J Pathol, 213*(1), 91–98.

Tsarouhas, V., Senti, K., Jayaram, S. A., Tiklova, K., Hemphala, J., Adler, J., and Samakovlis, C. (2007). Sequential pulses of apical epithelial secretion and endocytosis drive airway maturation in *Drosophila*. *Dev Cell, 13*(2), 214–225.

Tsunematsu, R., Nakayama, K., Oike, Y., Nishiyama, M., Ishida, N., Hatakeyama, S., Bessho, Y., Kageyama, R., Suda, T., and Nakayama, K. I. (2004). Mouse Fbw7/Sel-10/Cdc4 is required for notch degradation during vascular development. *J Biol Chem, 279*(10), 9417–9423.

Tu, B. P. and Weissman, J. S. (2002). The FAD- and O_2-dependent reaction cycle of Ero1-mediated oxidative protein folding in the endoplasmic reticulum. *Mol Cell, 10*(5), 983–994.

Vairaktaris, E., Ragos, V., Yapijakis, C., Derka, S., Vassiliou, S., Nkenke, E., Yannopoulos, A., Spyridonidou, S., Vylliotis, A., Papakosta, V., Loukeri, S., Lazaris, A., Tesseromatis, C., Tsigris, C., and Patsouris, E. (2006). FGFR-2 and -3 play an important role in initial stages of oral oncogenesis. *Anticancer Res, 26*(6B), 4217–4221.

van Drogen, F., Sangfelt, O., Malyukova, A., Matskova, L., Yeh, E., Means, A. R., and Reed, S. I. (2006). Ubiquitylation of cyclin E requires the sequential function of SCF complexes containing distinct hCdc4 isoforms. *Mol Cell, 23*(1), 37–48.

Van Vlierberghe, P., Homminga, I., Zuurbier, L., Gladdines-Buijs, J., van Wering, E. R., Horstmann, M., Beverloo, H. B., Pieters, R., and Meijerink, J. P. P. (2008). Cooperative genetic defects in TLX3 rearranged pediatric T-ALL. *Leukemia, 22*(4), 762–770.

Vaupel, P. and Mayer, A. (2007). Hypoxia in cancer: significance and impact on clinical outcome. *Cancer Metastasis Rev, 26*(2), 225–239.

Viault, F. (1890). Sur l'augmentation considérable du nombre des globules rouges dans le sang chez les habitants des hauts plateaux de 1'Amérique du Sud. *Comptes Rendus Hebdomaires des Seances de l'Académie des Sciences, Paris, 111*, 917–918.

Vincent, S., Wilson, R., Coelho, C., Affolter, M., and Leptin, M. (1998). The *Drosophila* protein Dof is specifically required for FGF signaling. *Mol Cell, 2*(4), 515–525.

Walgenbach, K. J., Gratas, C., Shestak, K. C., and Becker, D. (1995). Ischaemia-induced expression of bFGF in normal skeletal muscle: a potential paracrine mechanism for mediating angiogenesis in ischaemic skeletal muscle. *Nat Med, 1*(5), 453–459.

Wang, G. L., Jiang, B. H., Rue, E. A., and Semenza, G. L. (1995). Hypoxia-inducible factor 1 is a basic-helix-loop-helix-PAS heterodimer regulated by cellular O2 tension. *Proc Natl Acad Sci U S A, 92*(12), 5510–5514.

Wang, G. L. and Semenza, G. L. (1995). Purification and characterization of hypoxia-inducible factor 1. *J Biol Chem, 270*(3), 1230–1237.

Wang, J., Cao, Y., Chen, Y., Chen, Y., Gardner, P., and Steiner, D. F. (2006). Pancreatic beta cells lack a low glucose and O_2-inducible mitochondrial protein that augments cell survival. *Proc Natl Acad Sci U S A, 103*(28), 10636–10641.

Wang, Y., Wan, C., Deng, L., Liu, X., Cao, X., Gilbert, S. R., Bouxsein, M. L., Faugere, M., Guldberg, R. E., Gerstenfeld, L. C., Haase, V. H., Johnson, R. S., Schipani, E., and Clemens, T. L. (2007). The hypoxia-inducible factor alpha pathway couples angiogenesis to osteogenesis during skeletal development. *J Clin Invest, 117*(6), 1616–1626.

Warburg, O. (1956). On respiratory impairment in cancer cells. *Science, 124*(3215), 269–270.

Webster, K. A. (1987). Regulation of glycolytic enzyme RNA transcriptional rates by oxygen availability in skeletal muscle cells. *Mol Cell Biochem, 77*(1), 19–28.

Webster, K. A. (2003). Evolution of the coordinate regulation of glycolytic enzyme genes by hypoxia. *J Exp Biol, 206*(Pt 17), 2911–2922.

Wei, W., Jin, J., Schlisio, S., Harper, J. W., and Kaelin, W. G. J. (2005). The v-Jun point mutation allows c-Jun to escape GSK3-dependent recognition and destruction by the Fbw7 ubiquitin ligase. *Cancer Cell, 8*(1), 25–33.

Weidemann, A. and Johnson, R. S. (2008). Biology of HIF-1alpha. *Cell Death Differ, 15*(4), 621–627.

Welcker, M. and Clurman, B. E. (2008). FBW7 ubiquitin ligase: a tumour suppressor at the crossroads of cell division, growth and differentiation. *Nat Rev Cancer, 8*(2), 83–93.

Welcker, M., Orian, A., Grim, J. E., Eisenman, R. N., and Clurman, B. E. (2004a). A nucleolar isoform of the Fbw7 ubiquitin ligase regulates c-Myc and cell size. *Curr Biol, 14*(20), 1852–1857.

Welcker, M., Orian, A., Jin, J., Grim, J. E., Harper, J. W., Eisenman, R. N., and Clurman, B. E. (2004b). The Fbw7 tumor suppressor regulates glycogen synthase kinase 3 phosphorylation-dependent c-Myc protein degradation. *Proc Natl Acad Sci U S A, 101*(24), 9085–9090.

Welcker, M., Singer, J., Loeb, K. R., Grim, J., Bloecher, A., Gurien-West, M., Clurman, B. E., and Roberts, J. M. (2003). Multisite phosphorylation by Cdk2 and GSK3 controls cyclin E degradation. *Mol Cell, 12*(2), 381–392.

Welm, B. E., Freeman, K. W., Chen, M., Contreras, A., Spencer, D. M., and Rosen, J. M. (2002). Inducible dimerization of FGFR1: development of a mouse model to analyze progressive transformation of the mammary gland. *J Cell Biol, 157*(4), 703–714.

Wigglesworth, V. B. (1930). A Theory of Tracheal Respiration in Insects. *Proceedings of the Royal Society of London. Series B, Containing Papers of a Biological Character, 106*(743), 229–250.

Wigglesworth, V. B. (1954). Growth and regeneration in the tracheal system of an insect, *Rhodinus prolixus* (Hemiptera). *Quarterly Journal of Microscopical Science, 95*, 115–137.

Wigglesworth, V. B. (1983). The physiology of insect tracheoles. *Adv Insect Physiol, 17*, 86–148.

Wilk, R., Weizman, I., and Shilo, B. Z. (1996). *trachealess* encodes a bHLH-PAS protein that is an inducer of tracheal cell fates in *Drosophila*. *Genes Dev, 10*(1), 93–102.

Wingrove, J. A. and O'Farrell, P. H. (1999). Nitric oxide contributes to behavioral, cellular, and developmental responses to low oxygen in *Drosophila*. *Cell, 98*(1), 105–114.

Winter, S. F., Acevedo, V. D., Gangula, R. D., Freeman, K. W., Spencer, D. M., and Greenberg, N. M. (2007). Conditional activation of FGFR1 in the prostate epithelium induces angiogenesis with concomitant differential regulation of Ang-1 and Ang-2. *Oncogene, 26*(34), 4897–4907.

Wolf, C. and Schuh, R. (2000). Single mesodermal cells guide outgrowth of ectodermal tubular structures in *Drosophila*. *Genes Dev, 14*(17), 2140–2145.

Wu, G., Lyapina, S., Das, I., Li, J., Gurney, M., Pauley, A., Chui, I., Deshaies, R. J., and Kitajewski, J. (2001). SEL-10 is an inhibitor of notch signaling that targets notch for ubiquitin-mediated protein degradation. *Mol Cell Biol, 21*(21), 7403–7415.

Wu, R., Feng, Q., Lonard, D. M., and O'Malley, B. W. (2007). SRC-3 coactivator functional lifetime is regulated by a phospho-dependent ubiquitin time clock. *Cell, 129*(6), 1125–1140.

Yada, M., Hatakeyama, S., Kamura, T., Nishiyama, M., Tsunematsu, R., Imaki, H., Ishida, N., Okumura, F., Nakayama, K., and Nakayama, K. I. (2004). Phosphorylation-dependent degradation of c-Myc is mediated by the F-box protein Fbw7. *EMBO J, 23*(10), 2116–2125.

Yan, Q., Bartz, S., Mao, M., Li, L., and Kaelin, W. G. J. (2007). The hypoxia-inducible factor 2alpha N-terminal and C-terminal transactivation domains cooperate to promote renal tumorigenesis in vivo. *Mol Cell Biol, 27*(6), 2092–2102.

Ye, X., Nalepa, G., Welcker, M., Kessler, B. M., Spooner, E., Qin, J., Elledge, S. J., Clurman, B. E., and Harper, J. W. (2004). Recognition of phosphodegron motifs in human cyclin E by the SCF(Fbw7) ubiquitin ligase. *J Biol Chem, 279*(48), 50110–50119.

Yeh, E., Cunningham, M., Arnold, H., Chasse, D., Monteith, T., Ivaldi, G., Hahn, W. C., Stukenberg, P. T., Shenolikar, S., Uchida, T., Counter, C. M., Nevins, J. R., Means, A. R., and Sears, R. (2004). A signalling pathway controlling c-Myc degradation that impacts oncogenic transformation of human cells. *Nat Cell Biol, 6*(4), 308–318.

Zagzag, D., Zhong, H., Scalzitti, J. M., Laughner, E., Simons, J. W., and Semenza, G. L. (2000). Expression of hypoxia-inducible factor 1alpha in brain tumors: association with angiogenesis, invasion, and progression. *Cancer, 88*(11), 2606–2618.

Zelzer, E. and Shilo, B. Z. (2000). Cell fate choices in *Drosophila* tracheal morphogenesis. *Bioessays, 22*(3), 219–226.

Zelzer, E., Wappner, P., and Shilo, B. Z. (1997). The PAS domain confers target gene specificity of *Drosophila* bHLH/PAS proteins. *Genes Dev, 11*(16), 2079–2089.

Zhou, D., Xue, J., Lai, J. C. K., Schork, N. J., White, K. P., and Haddad, G. G. (2008). Mechanisms underlying hypoxia tolerance in *Drosophila* melanogaster: *hairy* as a metabolic switch. *PLoS Genet, 4*(10), e1000221.

Zhou, J., Schmid, T., Schnitzer, S., and Brune, B. (2006). Tumor hypoxia and cancer progression. *Cancer Lett, 237*(1), 10–21.

Zhou, Y. D., Barnard, M., Tian, H., Li, X., Ring, H. Z., Francke, U., Shelton, J., Richardson, J., Russell, D. W., and McKnight, S. L. (1997). Molecular characterization of two mammalian bHLH-PAS domain proteins selectively expressed in the central nervous system. *Proc Natl Acad Sci U S A, 94*(2), 713–718.